A STUDY OF EARLY AND INTERMEDIATE TYPE STARS AT THE GALACTIC POLES

A. D. McFadzean

A Thesis Submitted for the Degree of PhD
at the
University of St Andrews

1985

A Study of Early and Intermediate Type Stars at the Galactic Poles

A.D.McFadzean

A Thesis submitted to the University of St.Andrews
in application for the degree of Doctor of Philosophy

June 1984

Abstract

A catalogue of faint blue stars at the North Galactic Pole, compiled from the literature, is presented. Spectral classifications for catalogue stars within 3° of the pole have been obtained from U.K.S.T. objective prism and St.Andrews grism plates.

Photometric data on the uvbyβ system is presented for 572 O-F8 stars at the South Galactic Pole, with radial velocities being given for 161 of these stars.

From this South Galactic Pole data the interstellar reddening towards the Pole is shown to be negligible, in agreement with the findings of other authors. A number of photometrically odd stars are isolated, including several intermediate Population II, Population II and Am stars.

From available data at both Poles the relative proportions of various population groups as a function of height are discussed. There is an apparent excess of PI A over iPII stars out to 1kpc., relative to the numbers expected on the basis of the 'thick disk' of iPII stars reported by Gilmore and Reid (1983).

The w-velocity distributions of Pop.I A and F stars within 200pc. of both Poles are shown to be well fitted by gaussians and these gaussians are shown to be the

same for both Poles. The Pop.I A stars are shown to have a mean w-velocity of 0.6 kms^{-1} (rms 11.1 kms^{-1}) and the corresponding F stars to have a mean w-velocity of -2.9 kms^{-1} (rms 10.9 kms^{-1}), implying negligible net streaming through the galactic plane.

I, Alan Donald McFadzean, hereby certify that this thesis which is approximately 55,000 words in length has been written by me, that it is the record of work carried out by me, and that it has not been submitted in any previous application for a higher degree.

I was admitted as a research student under Ordinance #12 on 1st. October 1981; the higher study of which this is a record was carried out in the University of St.Andrews between 1980 and 1983.

date: 30th June 1984

A.D.McFadzean

I certify that A.D.McFadzean has fulfilled the conditions of the Resolution and Regulations appropriate to the degree of Ph.D. of the University of St.Andrews and that he is qualified to submit this thesis in application for that degree.

date: 1984 June 30

R.W.Hilditch

Contents

Acknowledgments

I would like to thank my supervisor, Dr.R.W.Hilditch for all of the obvious reasons, but particularly for his patience and guidance throughout the course of this research.

I am grateful to Prof.D.W.N.Stibbs and all the staff for the facilities made available at the University Observatory. In particular I thank Mr.J.R.Stapleton, for assistance with computers, FORTH and micro-densitometers, Dr.R.P.Edwin, for assistance with grisms and telescopes, Dr.W.Tobin for practical assistance with photometry and walnut shells, and the Technical Staff for keeping the telescopes working and the darkrooms supplied.

I thank my fellow research students, past and present, for discussions and suggestions. In particular, B.J.Mclean and A.C.Davenhall for their aid in making FORTH go, and A.Bridger (for GIPSY), C.S.Jeffery, G.J.Malcolm, J.K.Worrell and P.Starkey.

I would also like to thank Drs.D.C.B.Whittet and I.Butchart for their assistance in the production of this thesis.

I gratefully acknowledge the financial support of The Carnegie Trust for the Universities of Scotland.

Finally I would like to thank my parents, without whom none of this would have been possible, and my wife, Anita, for typing the tables and digging the garden while I finished this work.

Chapter 1

Introduction

'In order to see clearly, it is necessary to walk in the dark, with both eyes shut'

St.John of the Cross

1: Introduction

1.1 Aims

1.1.1 Galactic Structure towards the Galactic Poles

The importance of the galactic poles in the study of galactic structure has long been recognised, and much work has been done in this area since Kapteyn's (1922) pioneering study of Kz, the force law perpendicular to the plane. This importance is due mainly to the vertical segregation of the various components of the galaxy: the transition between dominant groups is more pronounced in this direction than in any other. In addition the dust which produces interstellar extinction is strongly concentrated towards the galactic plane and is therefore of less consequence along lines of sight towards the poles. This is of particular importance to photometric studies. Furthermore a radial velocity observed towards either pole is effectively a velocity, W, perpendicular to the plane. Therefore the w-velocity distribution (relative to the galactic plane, as opposed to the sun) of a group of objects observed near the poles may be studied without knowledge of their proper motions.

Thus, from photometric and spectroscopic observations of stars lying close to the poles different stellar groups may be identified and their space and velocity distributions determined as a function of z, the perpendicular distance from the plane. These distributions may then be used to determine Kz over the distance range observed, leading to an estimate of the local mass density, ρ_o. In general some model for the space and velocity distributions is first adopted. The observed distributions impose severe constraints on this model which must also satisfy all other known galactic structure parameters. These distributions are also of general use in the selection of realistic galaxy models for other applications.

1.1.2 Aims of the Present Work

Since the time of Kapteyn (1922) there have been many attempts to determine Kz and ρ_o from the observed space and velocity distributions of stars at the galactic poles. All of these have suffered to some extent from limitations in the available data or the model used. In order to determine the space distribution, for example, a well-calibrated photometric system is required. This must be capable of identifying and correcting for interstellar extinction (albeit a small amount at the poles), of segregating different stellar population groups on the basis of metallicity and evolutionary state, since each group may have a distinctive distribution, and of providing good estimates of absolute magnitudes (and hence distances) for objects within these groups. Finally, if tne observing program is to be feasible the system must be such that a large number of (faint) stars may be observed with a moderate sized telescope. Such a photometric system has rarely been applied to the study of the poles. The observed velocity distributions have also suffered from this deficiency as the distribution of each distinct population group may be quite different, and hence segregation is again necessary. In addition the lack of velocity data at the poles has led to the use of non-homogoneous samples culled from many sources, leading to serious systematic errors.

Hill, Hilditch and Barnes (1979, and references therein) have attempted to overcome these observational limitations with a large scale study of the O-F8 stars within 15° of the galactic poles. They have used the uvbyβ photometric system which permits accurate reddening corrections, stellar classifications and distance determinations to be made, with the aim of obtaining homogeneous photometric and radial velocity samples covering all such stars brighter than 15th magnitude at both poles. For the NGP stars photometry of over 1000 stars has been published (Hill et al 1982d). Radial velocities for 300 of the brightest of these stars have also been published (Hill et al 1976) and velocities for the rest of the NGP stars should be available by early 1985.

This published photometry has been used to investigate the distribution of interstellar reddening in the survey area. This was found to be insignificant between 100 and 1000 pc. from the plane, with significant reddening (E(b-y)$\sim$0.008) covering half the field within 100pc. and a small dense patch (E(b-y)$\sim$0.024 identified with an HI cloud and associated dust at $\sim$120pc. The data have also been used to identify $\sim$100 intermediate population II (iPII) and population II (PII) stars as well as other rarer objects (eg. horizontal branch stars and white dwarfs), and to derive an intrinsic uvbyβ calibration for the B9-A3 main sequence stars (Hilditch et al 1983). Hill, et al (1979) have re-analysed older data for the NGP A-F stars, supplemented by their own data available at the time (principally photometric). This analysis is discussed in sections 1.2 and 1.3.

The work presented here was intended as an extension of this survey to a magnitude limit of 17m within 3° of the North Galactic Pole. This was to be done by identifying the appropriate objects on photographic plates taken with the 1m James Gregory Cassegrian-Schmidt Telescope at St.Andrews, using the newly commissioned grating-prism (grism) to obtain spectra of the stars at dispersions of 800-1200 A°/mm. on IIIaJ plates, each covering a field of radius 2°. The grism and its performance are described in Appendix II.

Once identified, uvbyβ photometry and radial velocities would be obtained for these objects and the NGP data sample would thus be extended to a greater distance from the plane. This, it was hoped, would establish the reality, or otherwise, of the apparent increase in velocity dispersion with z distance found for Population I (PI) A and F stars in the analysis of Hill et al (1979). The expanded sample would provide data on Kz out to a greater distance and allow a refined value of the dynamical local mass density to be determined. It was also expected that this sample would contain a large number of iPII and PII stars, which would allow a preliminary study of their distributions to be undertaken. In addition the interstellar reddening could be studied out to a much greater distance than before. Although it was unlikely that this extension could be completed in the time available it was hoped that a substantial amount of data would be collected and a preliminary analysis performed.

However the form of the work presented here is somewhat different from that outlined above. The grism's arrival, scheduled for December 1980, was delayed until April 1981, precluding its effective use in the 1980-1981 observing season at St.Andrews. To assist with the intended survey a catalogue of known and suspected blue objects of 14th-18th magnitude, lying within 15° of the pole was compiled from the literature. Objects in this catalogue which lay within 3° of the pole were classified from a single U.K.Schmidt Telescope objective prism plate. From this plate a provisional list of the 50 brightest O-F8 stars was compiled. An attempt to obtain uvbyβ photometry of these objects was frustrated by poor weather and inadequate equipment. The grism survey was performed, but the instrument's performance was disappointing.

Hill, Hilditch and Barnes had already obtained a quantity of raw photometric and spectroscopic data for the bright O-F8 HD stars within 15° of the SGP as an extension of their work to the southern hemisphere. These data were kindly made available for reduction, leading to the uvbyβ photometry of 572 stars and radial velocities for 161 stars which are presented here. More spectroscopic data was available, but could not be reduced due to a serious problem encountered with the computer controlled Joyce-Loebl microdensitometer at St.Andrews. Insufficient velocity data was obtained for a re-determination of Kz and ρ_o to be attempted.

The data presented here have been subjected to a preliminary analysis (Chapter 5). A full analysis must await the completion of the survey. Nevertheless, the photometric data presented here have permitted a study of the interstellar extinction to be made and, in combination with the published NGP data, have improved the determination of the proportions of different population groups within 400pc. of the plane. The velocity data have been combined with those from the NGP in order to determine the perpendicular velocity dispersions of A and F stars within 200pc.

1.2 The Distribution of Stars in the Galaxy

1.2.1 Introduction

In the most simplistic view the galaxy consists of three basic components: a thin disk of gas and young metal rich stars (Population I), a larger spheroidal distribution of older, metal poor stars (Population II), and a yet larger, probably spherical, corona of unidentified, optically dark material often referred to as Population III. (The latter should not be confused with the hypothesised first generation of extremely metal poor stars which are also often refered to as Population III. If they exist, such stars could account for some of the unseen coronal mass.) The existence of these three components is inferred from studies of external galaxies as well as our own. (See Bok, 1983 for a discussion.) Such studies have also indicated an expected degree of sub-structure within the disk and spheroid leading to the concept of the five basic stellar populations, each with its own distinctive space and velocity distributions suggested by Oort (1958) and summarised in Table 1.2.1.

Unfortunately the true picture of the galaxy is not so simple. The parameters which specify the various components in Table 1.2.1 are uncertain, and within a given population some sub-structure is evident. For example, Ichikawa (1981) and Mikama and Ishida (1981) have suggested that the K-M giants, nominally old Population I, form several subgroups each with a distinctive space and velocity distribution. To divide the stellar component of the galaxy into five populations rather than two (PopI,PopII) is still a simplification.

Traditionally the stellar distribution in the galaxy has been investigated by means of star counts which give the number density of stars of a specific spectral type and absolute magnitude range at a specified point in the galaxy. From these counts it is possible to find the luminosity function (the number density of stars of a given spectral type and absolute magnitude range in the solar neighbourhood) and the density function (which gives the variation in the luminosity function for non-solar neighbourhood stars). The determination of the luminosity and density functions from star count data is a complex problem and a description of the technique may be found in Mihalas and Binney (1981). The successful application of the technique requires the elimination of a number of error sources. For example the effect of interstellar absorption on the counts must be identified and corrected. It is important to ensure that all stars of the desired spectral type in the field studied, which are brighter than a pre-specified absolute magnitude limit, have been selected otherwise a biased sample will result, leading to an incorrect analysis of the stellar distribution. For this reason an absolute magnitude limited sample is required, whereas the sample has traditionally been selected by kinematical considerations, and then 'converted' to an (incomplete) absolute magnitude limited sample.

The most recent applications of star count data to the study of galactic structure (eg. Gilmore and Reid (1983) have tended to use automatic measuring machines to detect and photometrically measure stellar images on photographic plates. The method of photometric parallax is used to determine the distances of these stars, based on a photometric population classification, and an absolute magnitude limited sample is defined within a certain distance limit.

A major problem with the stellar distribution as determined from star count analysis is that such data only provide information on the density distribution. As noted by Gilmore (1984) many quite incompatible models of the galactic density distribution give equally good fits to the best available star count data. In order to define uniquely the basic parameters of galactic structure, kinematical and chemical abundance data are required. Furthermore, these wide-band photometric methods are incapable of detecting small differences between the various subgroups of the basic populations, which may all have distinctive space distributions. With this in mind it can be seen that a potentially fruitful approach to the problem would be to perform a detailed photometric and spectroscopic survey of a distinctive type of star in a field of special interest. Obviously such a survey could not encompass the vast number of objects (>10,000) found in the best machine measured, absolute magnitude limited samples. However the problem of a (relatively) small sample of 1-2,000 stars would be compensated for by the wealth of detail on individual stars obtained by using intermediate band photometric systems capable of accurately classifying the sample into population subgroups. For the early type stars such a sytem is the uvbyβ sytem, with the complementary DDO system being ideal for the late type stars.

The galactic pole O-F8 star survey begun by Hill, Hilditch and Barnes (1979), of which the present work forms a part, is an example of such an approach. Photometric measurements of individual stars lead to reddening corrected distances and detailed population segregation, resulting in a direct determination of the density distributions of the groups sampled. Combining these with radial velocity data, the velocity distributions of the samples can be determined as well. These space and velocity distributions are of great value in the assesment of galaxy models and are directly applicable to the determination of Kz and the local mass density, ρ_o.

1.2.2 The Stellar Distribution within 5kpc. of the Galactic Plane

There have been a number of recent studies of galactic structure at high galactic latitude, both through star count analysis and detailed observations of individual stars. The discussion below has been limited to those studies important to the understanding of galactic structure within 5 kpc. of the plane since this region is of most significance in the present work. The general star count analyses will be considered first.

The Basle RGU photometric system was designed to allow the segregation of disk and halo stars from photographic photometry, using an ultraviolet excess parameter to isolate the metal poor halo stars with which the survey was primarily concerned. The resulting survey, covering eight high galactic latitude fields, is described by Becker (1980). The data in the polar regions indicate a steep density decrease and small scale height for the halo stars within 5kpc. This is probably a result of contamination of the halo sample by disk stars due to the inadequacy of the UV excess parameter as a population discriminator (Bahcall, Schmidt and Soniera 1983). However there is some evidence for an excess of halo stars within 5 kpc, relative to those expected on the basis of the space density distribution for 5-8kpc (Gilmore 1984).

Yoshii (1982) has pointed out that the identification of evolved stars is difficult in the RGU system. He suggests that a large fraction of the Basle field halo stars are disk subgiants and believes that failure to recognise this would lead to the steep halo density gradient found by Becker (1980). He has re-analysed the RGU data for the field SA 57 (which lies close to the North Galactic Pole), by transforming the data onto the UBV system using well established transformation equations, and thus obtains star counts as a function of V magnitude and (B-V) colour, complete down to V=18. He allows for a mix of sub-giants, red giants and main-sequence stars in both the disk and the halo and assumes exponential density laws for both components. By adopting specific forms for the disk and halo luminosity functions, predicting star counts from these, and comparing with his data, he obtains values for the parameters of his density laws. Yoshii takes the disk luminosity function from McCuskey (1966) and considers three possible forms for the halo luminosity function: those of the globular cluster M92, the globular cluster M3 and the disk. His analysis rules out the possibility of a disk-type luminosity function for the halo but cannot choose between the other two. He finds a scale height of about 300 pc. for the disk and 1.9-2.4 kpc for the halo, the halo density gradient being much gentler than that found by Becker (1970). There is also a suggestion of a flattened distribution for the nearer halo stars.

Chiu (1980a,b) has derived proper motion data for objects down to V=20 in three high latitude fields including SA 57. Combining these proper motions with photographic UBV data he classifies the objects into different population groups (Population I main-sequence, Population I white dwarfs and Population II subdwarfs) and derives luminosity functions(for $3 \leqslant M_V \leqslant 12$) and space densities for each group. His derivation of the Pop.I main-sequence luminosity function requires a model for the chemical composition gradient in the line of sight, and a model of the density distribution chosen to be consistent with the data. He considers two power law models for the density distribution, one with a scale height of 300 pc. and no composition gradient, the other with a scale height of 500 pc. but a much more rapid density fall-off and a composition gradient. The second model is consistent with the Wielen (1974) main-sequence luminosity function and the available kinematic data. When applied to the white dwarfs this gives a space density in the solar neighbourhood which is in good agreement with other determinations (0.02 pc^{-3}). For the subdwarfs the best density law is a flattened spheroid with axial ratio 1:3 or 1:4. The derived luminosity function is different for each of the three fields but all are steeper than those of the globular clusters M92 and NGC 6397. The differences between the fields (all at different galactic latitudes) can be resolved to some extent by invoking a third population intermediate between the Pop.I main-sequence and the Pop.II subdwarfs. This population has kinematics intermediate between those of PI and PII stars and a flattened distribution of axial ratio 1:3 or 1:4 but does not extend to the same height as the true population II .

Pritchett (1983) has analysed star count data down to V=23 from three fields each covering 0.38 square degrees. He used a simple galaxy model fitted to the data to investigate various aspects of galactic structure. His analysis preferred the Wielen (1974) luminosity function to that of Luyten (1968) (although there is little difference between them until their faint limits) and showed that exponential disk models were to be preferred to the self-gravitating isothermal disks of Camm (1950, 1952). For this exponential disk he finds a scale height of about 350 pc. The halo component of the galaxy (based on a power law density model with luminosity function taken to be that of Wielen for $Mv<+4$, and for $Mv\geq+4$ the average of those for the globular clusters M3, M92 and M13) is found to have an axial ratio of 1:1 and a local contribution of 0.1%. He discusses the possible existence of an intermediate population 'thick disk' of scale height >1kpc., consisting of halo-type stars in a flattened distribution caused by their response to the gravitational field of the disk. He concludes that his data cannot exclude the possibility of its existence if it contributes less than 10% of the projected disk density. This is compared with the Sb spiral NGC 4565 which shows a thick disk component contributing about 5% of the surface density.

A fundamental flaw inherent in all the above analyses is the adoption of a pre-specified form for the density function or the luminosity function (or both) which severely limits the validity of the final analysis. In general, assumptions such as this are made in order to simplify the analysis, although they are sometimes required because of the limited sample available.

Reid (1982) has obtained photoelectric photometry of a complete sample of faint red dwarfs identified from objective prism plates. From this data he derives the PI main-sequence luminosity function for stars with $7 \leqslant Mv \leqslant 12$ lying within 50pc. of the sun and finds it to be consistent with both the Luyten (1968) and the Wielen (1974) functions. This absolute magnitude limit was extended to Mv=19 by Reid and Gilmore (1982) who, from UK Schmidt plates, obtained COSMOS measured photometry for a complete sample of stars brighter than I=17 (in the UBVRI system) in a field of 18 square degrees towards the South Galactic Pole. Photometric parallaxes were derived using their own well-calibrated Mv/(V-I) relation, and the sample includes all stars with $I \leqslant 17$, $Mv \leqslant 19$ lying within 30pc. of the sun. Gilmore and Reid (1983) have derived absolute magnitudes for the 12,500 stars in their sample with $V \leqslant 19$, $I \leqslant 18$ which do not lie within 100pc. of the sun. From the total sample they have derived the stellar luminosity function in absolute visual magnitude, bolometric magnitude and stellar mass in the solar neighbourhood for all stars with $M_v \leqslant 19$, the minimum mass for nuclear burning. The luminosity function obtained is consistent with both the Luyten and Wielen functions. In determining absolute magnitudes they have allowed for two possible forms for the metallicity gradient perpendicular to the plane, both constrained by available abundance data.

They have also derived (Gilmore and Reid 1983) density laws as a function of z distance for each absolute magnitude and, equivalently, the luminosity function at varying distances from the plane. In deriving these density laws they excluded all stars with $V \geqslant 18.5$, all K stars with $V \leqslant 14$ and all stars within 100pc. in order to minimise contamination of the sample by unidentified galaxies, distant G-K giants and young disk stars. For unevolved stars within 1kpc. of the plane the best fit to the data was obtained using an exponential distribution of scale height ~300pc, irrespective of the adopted metallicity gradient. From 1-5kpc. the data are equally well fitted by an exponential of scale height ~1350pc, and a power law spheroid of axial ratio 1:4. Again this result is independent of the assumed metallicity gradient. This second component of the stellar distribution, intermediate between the disk (old PI) and the true halo (extreme PII), has a steeper luminosity function and a mild metal deficiency relative to the old PI and is readily identified with the intermediate Population II. It dominates the stellar density distribution between 1 and 5kpc. from the plane and is presumably a local component of the spheroid whose kinematics and hence space distribution have been modified by the gravitational potential of the disk. About 2% of the solar neighbourhood stars belong to this population, which is within the limit of 10% imposed by Pritchett.

Traditionally the disk and spheroid stars can be crudely segregated on the basis of their velocity distributions. Disk stars tend to have higher rotational velocities but lower velocities perpendicular to the plane than do the spheroid stars. When a large number of stars are studied it is found that the disk stars have a smaller velocity dispersion as well. This can be seen in Table 1.2.1 in which the mean velocity, $\overline{w}$, increases with scale height, $\overline{z}$. The same is true of the velocity dispersions. Solar neighbourhood kinematics have recently been reviewed by Mihalas and Binney (1981). The old disk population can be represented by the metal rich RR Lyrae stars with a w-velocity dispersion of about $30 kms^{-1}$ and the spheroid by the metal poor RR Lyraes with a dispersion of about $90\ kms^{-1}$. There are several groups of stars with scale heights, mean w-velocities, velocity dispersions and metallicities intermediate between these extremes (Gilmore 1984). These are readily identified with the intermediate population II of Table 1.2.1.

Information concerning the structure of our galaxy can also be obtained from studies of external galaxies thought to be similar to ours. Burstein (1979) has found surface photometry of S0 galaxies to indicate the existence of thick disks intermediate between the disk and spheroid but found very few spirals to show this feature. However Van der Kruit and Searle (1982) have found, also from surface photometry, that many spirals do indeed show this thick disk. They identify this as the intermediate population II spheroid flattened by the gravitational field of the disk, and on this basis, expect it to have a velocity dispersion intermediate between that of disk and spheroid.

From the above it would appear that the old disk population is quite well represented by an exponential of scale height around 300-350pc. Suggestions of a component intermediate between disk and spheroid appear to be confirmed. This is apparently a very flattened component of the spheroid responding to the gravitational field of the disk. It is well represented by both a flattened spheroid of axial ratio 1:4 and an exponential of scale height around 1.5 kpc., and dominates the stellar distribution between 1 and 5 kpc. from the plane. That it is quite distinct from the disk is shown by the abrupt change in the stellar number density at 1.5 kpc. (Gilmore and Reid 1983). In both chemical composition and kinematics it would appear to be intermediate between the old disk and the outer spheroid. This thick disk contains around 2% of the stars in the solar neighbourhood and is readily identified with the intermediate population II. The outer spheroid represented by the extreme population II and the globular clusters probably dominates the distribution beyond 5 kpc. Observations of globular clusters and field RR Lyraes suggest that this component is roughly spherical with a power law density distribution of exponent -3.3 ± 0.1. This is consistent with the de Vaucouleurs law derived from surface photometry of external spirals. Beyond this the mass of the outer regions of the Galaxy is presumably dominated by the dark corona whose existence is suggested principally by the flat rotation curves of both our

Galaxy and external spiral galaxies.

Bahcall and Soniera (1980) have constructed a model for the disk and spheroid components of the Galaxy, based on the conventional thin exponential disk and De Vaucouleurs spheroid, with parameters based on observational data. The adopted luminosity function for the disk stars was based on the data of McCluskey (1976), Luyten (1968) and Wielen (1974) for the range $-6 \leqslant Mv \leqslant 16$. The disk scale height was, on the basis of observational evidence, taken to be a function of intrinsic luminosity and evolutionary stage, ranging from about 100pc for the brightest stars ($M4 < -4$) to about 300pc for the faintest (Mv about 16). The spheroid is taken to consist of a spherical distribution of PII stars, with a luminosity function identical to that of the disk over the range $4 \leqslant Mv \leqslant 12$, with a ratio of disk/spheroid components of 800:1.

This model was then used to predict stellar distributions projected into the sky and these were compared with the observed number counts of Kron (1978), ($20 \leqslant mv \leqslant 22$), Tyson and Jervis (1978) ($12.3 \leqslant mv \leqslant 22$) and Peterson et al (1979) ($17.3 \leqslant mv \leqslant 22$). The model makes no allowance for the existence of a component intermediate between disk and spheroid, and no evidence for such a component is forthcoming from the star count analysis. Bahcall et al (1983) did consider such a component and used the same star counts, and essentially the same model, to derive upper limits to the number density of stars belonging to it. These limits are dependent on the form of space density adopted for the component, but for an exponential disk of scale height 1kpc the local density of the intermediate population must be less than 13% of the disk density. Since most of these star counts are concerned with very faint stars in small high galactic latitude fields the bulk of the stars sampled will be either subdwarfs at distances of 10-20kpc from the plane, or red dwarfs less than 1kpc. from the plane. Thus the region in which the thick disk is expected to dominate will not be sampled.

The model's predicted counts for stars with $15 \leqslant V \leqslant 17$ bear no resemblance to the actual counts of Gilmore and Reid (1983) for the South Galactic Pole region. Gilmore and Reid attribute this failure to predict observed counts for brighter stars to the erroneous choice of spheroid luminosity function and the neglect of the intermediate component. As a result of these the Bahcall and Soniera model does not agree with the Gilmore and Reid data for z distances greater than about one kiloparsec.

Photographic surveys such as those discussed above are invaluable because of their ability to collect data on a vast number of stars in a short time, and they yield much important information concerning what might be termed 'gross' galactic structure. However all such surveys are essentially broad band photometric surveys and as such encounter problems with the segregation of the various evolutionary groups included in the sample (eg. main-sequence, subgiants, giants, horizontal branch, subdwarfs and white dwarfs) and in some cases even the separation of different population groups is inadequate. These problems can be reduced by the use of a suitable narrow or intermediate-band photometric system capable of identifying both evolutionary and metallicity differences in the sample. Unfortunately this requires precision photoelectric photometry and therefore data aquisition is much slower than for wide-band photometric surveys. In addition the apparent magnitude limit of the survey is much reduced. Consequently such surveys tend to be limited to small areas and specific types of object. The galactic caps are an obvious choice of region and the G-K giants and the F stars are suitable candidates for study. The F stars are readily detected at distances beyond 1 kpc. and are easily segregated into their various subgroups by uvbyβ photometry. They are also quite common, but not so numerous that an impossibly large sample is obtained. The G-K giants are detectable at much greater distances and are slightly harder to segregate (but see Hartkopf and Yoss (1982) for metallicity segregation using the DDO photometric system), but share the other advantages of the F stars.

A study of high latitude F stars is being made by Stromgren and others (Stromgren 1976), Blaauw 1978, Crawford et al 1979). Stars are classified as extreme Population II or intermediate population II on the basis of uvbyβ photometry. The local densities of these groups relative to the old disk were found to be 6% (iPII) and 0.02% (ePII). Towards the NGP these were found to have decreased by a factor of about 100 (iPII) and 3 (epII) at a height of 1 kpc. above the plane. For the ePII this corresponds to an exponential distribution of scale height 1 kpc. and is a much greater decrease than is expected for a spherical population following a de Vaucouleurs density law. Gilmore (1984) has identified these 'ePII' stars as part of the galactic thick disk component.

The galactic poles O-F star survey of Hill, Hilditch and Barnes has already been mentioned. Here the published results of this work will be considered (Hill et al 1979). Since their own survey was incomplete and their primary aim was the determination of the force law, they investigated the space distribution of the A-F stars using the Yale Catalogue (Hoffleit, 1964) and by re-analysing the star counts of Upgren (1962,1963). However, they were unable to divide these into population groups, but derived the density distribution on the assumption that all stars of the same spectral type have the same absolute magnitude regardless of luminosity or population group. The resulting density distribution for the F5-F8 (F) stars is well fitted out to 600 pc. by Camm's (1950, 1952) model for a self-gravitating disk in which the w-velocity dispersion increases with distance from the plane. For the A0-F4 (A) stars the same model fits well out to 300 pc. but seriously underestimates the observed distribution between 300 and 600 pc.

From their own homogeneous sample of around 400 NGP stars with known space motions, distances and intrinsic uvbyβ colours they have studied the velocity distributions of the population I main-sequence A and F stars. They found that the velocity dispersions were constant out to 200pc., but between 200 and 300pc. there was a real increase. For the A stars both the dispersion and its increase were larger than for the F stars (Table 1.2.2). Additional data were taken from the catalogue of Eggen (1961) for stars within 40 pc. of the sun and, with uvbyβ photometry from other sources, separated into A and F stars of PI, iPII and PII. The velocity dispersions for this sample are also shown in Table 1.2.2. The agreement with the Hill et al F stars within 200 pc. is good, but for the A stars those within 40 pc. give a smaller dispersion than those within 200 pc. There is no evidence that these two samples belong to different population groups, and the indication seems to be that the population I main-sequence A stars within 300 pc. have a velocity distribution in which the w-dispersion increases with distance from the plane. It is therefore possible that there are at least two distinct distributions of apparently identical A stars near the plane. However contamination of these velocity samples by other objects with slightly different velocity distributions (eg. unrecognised iPII) cannot be ruled out.

Increases in w-velocity dispersion with distance from the plane have been found by previous studies (eg.

Harding et al (1971) for the A0 stars and Jones (1972) for the M dwarfs) but the reliability of the population segregations and distance determinations for the objects studied are in doubt.

Hartkopf and Yoss (1982) have observed a sample of over 1000 G-K giants at both galactic poles using the DDO photometric system to study their metallicity distribution in these directions. Dividing the sample into metal poor stars ([Fe/H]<-0.5), taken to be PII, and metal rich ([Fe/H]>-0.5), stars taken to be PI, they found a surprisingly large proportion of metal rich stars out to 6kpc from the plane. The proportion of metal-poor to metal-rich stars initially showed a steep increase with z distance and they dominate the sample beyond 1.3kpc. However from 1.5-3kpc. this proportion levels off at about 70% and is still only 80% at 6kpc. There is therefore evidence for a substantial population of metal-rich G-K giants at a very large distance from the plane. Unfortunately, not having a complete sample over a given area they could not determine the density distribution of these objects. The dominance of metal-poor stars beyond 1.3 kpc. is of interest in comparison with the dominance of metal deficient iPII stars beyond about 1.4-1.5kpc. found by Gilmore and Reid (1983).

Hartkopf and Yoss obtained radial velocities for about one third of their sample. They find that for both metal rich and metal-poor stars the w-velocity dispersion shows a small increase with z distance out to 1.5kpc., then drops slightly to a constant value with some evidence for a further increase beyond 5 kpc. for the metal-poor stars (Table 1.2.2). It is not clear to what extent these findings are attributable to the very small data set beyond 1.5kpc. The mean dispersion for all metal-rich stars was found to be $22 km s^{-1}$, about half that for the metal-poor. For the metal rich stars between 1 and 1.5 kpc. from the plane the dispersion was found to be about $32 km s^{-1}$, suggestive of kinematics intermediate between those of Pop.I and Pop.II. In general for a given height above the plane, the velocity dispersion was found to increase with decreasing metallicity, down to [Fe/H]=-1.0, after which it levelled off. This is in keeping with the simple model of population structure described in 1.2.1. The G-K giant survey of Hartkopf and Yoss is, as yet, incomplete and these findings can only be regarded as preliminary.

From detailed studies of specific stellar groups in the vicinity of the poles two problems emerge:

i) There is evidence from PI main-sequence A-F stars and PI G-K giants for a small local (z<1kpc) increase in w-velocity dispersion with z distance for a given sub-group.

ii) There is evidence for a population of metal-rich (PI) G-K giants existing at large distances from the plane and forming a substantial proportion of all late type giants in the range 1-2kpc. Kinematically these stars appear to be intermediate between old disk and extreme halo.

Rodgers et al (1981) have found a number of metal-rich (PI) main-sequence A stars at the SGP with z distances of 1-4.5kpc, having kinematics intermediate between disk and halo populations (w-velocity dispersion about $66 kms^{-1}$). Stetson (1983) has found evidence of a number of solar neighbourhood PI main-sequence A stars with abnormally large space motions (w-velocity dispersion about $57 kms^{-1}$, transverse velocities > $80 kms^{-1}$) which he suggests are the local manifestation of the A star distribution found by Rodgers et al. Pier (1983) has confirmed the detection of main-sequence metal-rich A stars at the SGP with large velocity dispersions (about $60 kms^{-1}$) lying 1-3 kpc out of the plane, but finds no evidence for such stars beyond 3kpc. However he notes that the criteria used in selecting his sample will produce a bias against the selection of metal-rich objects. A number of authors (eg.House and Kilkenny 1978, Keenan and Dufton 1983) have reported finding high-velocity solar-metallicity unevolved OB stars at large z-distances. Several detailed studies of these objects (Tobin and Kilkenny (1981), Tobin and Kaufmann (1984), Keenan and Dufton 1983) have shown that these stars are spectroscopically indistinguishable from the PI OB stars in the disk.

There is therefore a considerable body of evidence to suggest the existence of a substantial number of unevolved OB stars, solar metallicity A dwarfs and G-K giants at distances of more than 1kpc. from the plane, with kinematics apparently intermediate between those of the old disk and the halo. No current model of the galactic formation, mass distribution or chemical evolution can account for the existence of these objects at such distances from the plane. The suggestion that they have formed in the plane is untenable as no feasible mechanism is capable of scattering them out of the plane in such numbers or, in the case of the OB stars, on a time scale less than the ages of the stars themselves (Tobin and Kilkenny 1981).

These stars are not the same as the metal-deficient intermediate population II thick disk of Gilmore and Reid (1983). They may have a similar distribution but their relationship to the iPII stars is unclear. Much more work is needed in this area of metallicity anomalies in the inner halo.

The apparent increases in velocity dispersion with distance from the plane for PI main-sequence A stars within 300pc. found by Hill et al (1979) do not really fit in with this picture of intermediate kinematic solar abundance stars at large z distances. It is possible however that the sample of Hill et al (1979) was contaminated by the tail of the space/velocity distribution of the A stars of Rodgers et al. leading to erroneous velocity dispersions. This would explain the effect but there is, as yet, no evidence to confirm it. Again much more work on the problem is required, and hopefully the completion of the galactic poles O-F star survey down to 17m will clarify the situation.

1.3 The Galactic Force Law and the Local Mass Density

1.3.1 Background

The galactic force law perpendicular to the plane is defined as

$$Kz = -\frac{dI}{dz}$$

where $I(r,\theta,z;t)$ is the potential function of the galactic system, (r,θ,z) defines a cylindrical co-ordinate system and t is time. For a steady state axially symmetric system with no net expansion or contraction, and in which the potential can be separated into radial and perpendicular components, $(I(r,z) = Ir(r)+Iz(z))$, the following equations are valid:

$$\frac{d}{dr}(v\overline{uw}) + \frac{d}{dz}(v\overline{w^2}) + \frac{v\overline{uw}}{r} = vKz \qquad 1.3.1$$

$$\frac{dKr}{dr} + \frac{Kr}{r} + \frac{dKz}{dz} = -4\pi G\rho(r,z) \qquad 1.3.2$$

where $Kr = -\frac{dIr}{dr}$,

$\rho(r,z)$ = mass density

u = velocity in radial direction

w = velocity in perpendicular direction

$v(r,z)$ = stellar number density

In principle, v, $\overline{w^2}$ and $\overline{uw}$ can all be determined observationally as functions of z for a specific sub-system of tracer stars. From these Kz is found, and from its slope at z=0 and the observed solar neighbourhood values of $\frac{dK_r}{r}$ and $\frac{K_r}{r}$ the local mass density, ρ_o, is found. The tracers chosen should be numerous, observable over a large range of z distances and should be such that accurate population segregations and distance determinations are possible. These requirements are met by the main-sequence A-F stars and the G-K giants. The latter are more numerous at z > 1kpc, but the former are more readily segregated into population groups. The fundamental assumption is that the chosen tracers all share a common stellar distribution function. If this is incorrect, then the analysis fails. It is commonly assumed that this distribution function is an even function in u and w and hence $\overline{uw}=0$ everywhere. (In fact $\overline{uw}$ is extremely difficult to determine out of the plane so this assumption has never really been tested. However Oort (1965) suggests that $\overline{uw}$ is almost zero in the plane, and small elsewhere.) Equation 1.3.2 then becomes:

$$K_z = \frac{1}{\nu}\frac{d}{dz}(\nu\overline{w^2}) \qquad 1.3.3.$$

It is difficult to determine the run of $\overline{w^2}$ with z over a sufficiently large distance from the plane and consequently a model is usually adopted for the velocity distribution. Most analyses have followed Oort

(1932) and taken the velocity distribution perpendicular to the plane to be a gaussian, in which case $\overline{w^2}$ is a constant and :

$$Kz = \overline{w^2} \frac{d}{dz}(\ln[v/v_o]) \quad 1.3.4$$

where v_o is the value at z=0.

The validity of this last assumption is uncertain. Evidence has been presented which supports an increase of velocity dispersion with distance from the plane for population I main-sequence A stars (Hill et al 1979) and G-K giants (Hartkopf and Yoss (1982). It is likely, however, that these apparent increases are due to contamination by kinematically distinct, but spectroscopically identical systems. The problem once again lies with the precise definition of a population sub-system.

If the velocity distribution of the chosen tracers is truly non-gaussian then it can generally be represented by a sum of gaussians and a modified form of equation 1.3.4 holds. In any case the force law is then found by observing the appropriate velocity dispersions and space densities and substituting in 1.3.4.

Once the force law is known, the local mass density is found from equation 1.3.2 using the (small) observed values for $\frac{dK_r}{r}$ and $\frac{K_r}{r}$ near the sun. In order to determine the mass density out of the plane these must be found from a suitable model of the galactic mass distribution. Such models will not be considered here but it is noted that the number and variety of available models reflect the uncertainties in the observationally imposed constraints. No mass model exists which allows for the existence of both the thick disk and the solar metallicity stars at large z distances. Were a suitable, accurate model available it could be used directly with equations 1.3.1 and 1.3.2 to determine the force law and mass density from the empirical stellar distributions.

Most work on the force law and local mass density has followed the basic method of Oort (1932) (Kuzmin (1952), Kuzmin (1955), Nahon(1957), Eelsalu (1958), Hill (1960), Oort (1960), Jones (1962), Upgren (1962), Perry (1969)) but there have been notable exceptions (Woolley and Stewart (1967), Turon-Lacarrieu (1971), Gould and Vandervoort (1972), Jones (1972)). Woolley and Stewart assumed a double-gaussian velocity distribution for their sample and using observed velocity dispersions and space densities obtained best-fit parameters for a model of the galactic potential from which the force law and mass density were derived. Turon-Lacarrieu (1971) attempted a radically different approach using King's (1965) dynamical 'psuedo-moments' to separate the variation of the space density and velocity dispersion in equation 1.3.3. thus eliminating the need for a velocity distribution model. Gould and Vandervoort (1972) described a new method of determining the force law based on the reformulation of the problem in terms of a set of virial equations describing the perpendicular structure of a sub-system. The method has to be adapted to the specific system used, but it is claimed that it can be applied to a sample in which many different sub-systems are represented.

In all derivations of the force law and mass density, regardless of technique used, the appropriate space density has been found from star counts within some catalogue. Considerable errors are present in such counts due to:

i) systematic and large random errors in apparent magnitudes and spectral types

ii) uncertainties in luminosity classes

iii) uncertainties in the absolute magnitude scales leading to errors in the distances

iv) lack of knowledge of population groups

v) incompleteness of sample within assumed distance limit

Exactly the same problems are encountered when determining the velocity distribution of the sample- distances and spectral types are uncertain, luminosity classes and population groups uncertain or unknown.

All of the determinations of the force law and mass density cited above suffer, to varying degrees, from these problems. In order to overcome them it is essential that a precise, distance limited, complete sample be defined and photometric and spectroscopic observations made in order to define accurately the sub-systems in the sample and determine their space and velocity distributions. The O-F8 stars survey of which the present work forms a part should meet these requirements. The preliminary analysis of the (incomplete) sample at the NGP (Hill et al 1979) combined the approach of Woolley and Stewart (1967) with the model of Camm (1950, 1952), the published data of Upgren (1962,1963) and the then available spectroscopic and photometric survey data (Hill et al

1976, Hilditch et al 1976) to determine the force law and the mass density. This analysis, which has been described in a previous section, obtains a best fit to the data by adopting a model in which the velocity dispersion of the sub-system increases with distance from the plane. This model is not a realistic representation of the sub-system and is only valid for an infinitely thin self-gravitating disk.

Once this survey is complete it should be possible to obtain an accurate form for the force law based on well determined space and velocity distributions. It will be interesting to compare the results obtained using several different techniques to find the force law, especially those of Turon-Lacarrieu (1971) and Gould and Vandervoort (1972).

1.3.2 The Local Missing Mass Problem

Since Oort's (1932) determination of the force law led to a value for the mass density in the solar neighbourhood there has appeared to be a discrepancy between this value, derived from dynamical data, and that found by summing the densities of all observed matter near the sun. The larger dynamical value was taken as evidence for the existence of an unseen mass component in the solar neighbourhood, the so-called 'local missing mass'. This should not be confused with the 'galactic missing mass' whose existence is inferred from the flat rotation curve of the Galaxy at large galacto-centric distances. However it is possible that the two 'missing masses', if real, are related.

Since the dynamical local mass density is found from the force law, or at the very least from the same observations, and the force law is not accurately known, it follows that the derived local mass density is extremely uncertain. In the past 30 years derived values of this dynamical density have covered the range 0.08-0.28 $M_\odot pc^{-3}$, with the most recent estimate of the visible mass density being 0.11 $M_\odot pc^{-3}$. This failure to determine the force law and dynamical mass density is attributable to the error sources discussed above. Joever and Einasto (1976) have discussed the problems with the derived dynamical mass densities and conclude that inadequate population segregation is responsible for much of the uncertainty. They claim that contamination of the sample by another population group will tend to increase the observed velocity dispersion of the sample, without adversely affecting the space densities, thus leading to an overestimate of the local mass density. The lower values of the dynamical mass density are therefore to be preferred, and considering the errors inherent in both dynamical and visible mass densities there is currently no real evidence either for or against the existence of an unseen mass distribution in the solar neighbourhood.

Most recently, Bahcall (1984) has taken the Galaxy model of Bahcall and Soneira (1980) and numerically solved the Poisson-Boltzmann equation to give the gravitational potential of this model. This potential as a function of z distance is then used to fit the F star distribution within 200pc., given by Hill et al (1979). Assuming their velocity distribution to be isothermal, and that any unobserved matter has a distribution proportional to that of the observed matter, the total mass density in the solar neighbourhood is found to be $0.185 \pm 0.02\ M_\odot\ pc^{-3}$, much greater than the observed mass density ($0.11\ M_\odot pc^{-3}$) and that calculated by Hill et al. ($0.14\ M_\odot pc^{-3}$). The unobserved disk material is at least as large as 50% of the total observed disk material.

Given the extreme sensitivity of the local mass density to uncertainties in the velocity dispersions of the tracer system used (cf Bahcall (1984)- an increase of 0.5 kms^{-1} in the dispersion of the PI F stars increases the mass density by ~14%, and Hill et al (1979)- a change of $\pm 1 kms^{-1}$ in the same dispersion alters the mass density by ~21%, different models being used in each case) any assessment of the true error in the derived mass density must take account of the uncertainties in the velocity dispersion of the tracer stars adopted. The basic conclusion that neither the dynamical nor the visible mass densities are well known still holds.

Table 1.2.1.

STELLAR POPULATIONS

	Extreme Pop I	Older Pop I	Disc Pop II	Interm. Pop II	Halo Pop II
Examples	Gas/dust Supergiants OB stars T Tauri stars Cepheids Spiral Arms	Sun A stars Me dwarfs Strong-line stars White dwarfs Late-type giants Main sequence	Planetary nebulae Galactic nucleus Novae RR Lyrae stars ($P < 0\overset{d}{.}4$) White dwarfs	High-veloc. stars Long-period var. ($P < 250^d$)	Globular clusters Extremely metal- - poor subdwarfs RR Lyrae stars ($P > 0.^d4$)
$\overline{\lvert z \rvert}$ (pc)	120	160	400	700	2000
$\overline{\lvert W \rvert}$ ($km.s^{-1}$)	8	10	17	25	75
Axial ratio	100	50	20	5	2
Z/H (mass)	0.03	0.02	0.01	0.004	0.001
~ Age (10^9 yr)	<0.1	0.1 - 1.5	1.5 - 5	5-6	6+
~ Mass ($10^9 M_\odot$)	2	5	40	40	16
~Brightest M_V	-8	-8	-3	-3	-3
Distribution	very patchy (spiral arms)	patchy	smooth	smooth	smooth

Table 1.2.2.

Hill et al (1979)

z(pc.)	PI A stars $\overline{W}$	PI A stars $(\overline{W^2})^{1/2}$	PI A stars n	PI F stars $\overline{W}$	PI F stars $(\overline{W^2})^{1/2}$	PI F stars n	source
0- 40	-6.5	7.6	153	-6.4	10.6	195	Eggen
0-200	-6.0	9.7	84	-4.1	10.5	109	Hill et al
200-300	-7.5	14.0	24	-7.1	12.6	15	Hill et al

Hartkopf and Yoss (1982)

z(pc.)	'PI' (metal-rich) $(\overline{W^2})^{1/2}$	'PI' (metal-rich) n	'PII' (metal-poor) $(\overline{W^2})^{1/2}$	'PII' (metal-poor) n
0-500	21.2	181	40.5	16
500-1000	23.1	46	43.8	18
1000-1500	33.3	12	46.3	19
1500-3000	22.2	12	39.7	21
3000-5000	----	--	40.5	10

Chapter 2

Selection of North Galactic Pole Stars

'I do not consider spectral classification to be a goal in itself'

Th.Schmidt-Kaler

2: Selection of North Galactic Pole Stars

2.1 Identification

2.1.1 Introduction

The first step in the expansion of the available sample of O-F8 stars at the North Galactic Pole was the identification of the 13m-17m O-F8 stars in the region. A survey area of radius 3° centred on the pole was chosen. A larger radius would have required an excessive number of survey plates and would have produced a sample too large to study in the time available. In addition, since a circle on the Celestial Sphere defines a conical volume of space and fainter stars are in general more distant, a small survey area was chosen to restrict the sample to stars lying close to the sun-pole line. Having determined that the identification of the sample would be based on wide field, low dispersion slitless spectroscopy, using a grism on the James Gregory Telescope, some consideration had to be given to the problem of classifying stars from the plate material.

2.1.2 Direct Visual Classification

The simplest way to classify the objects on an objective prism or grism plate is to look at each individual spectrum under high magnification and assign a spectral type on the basis of the features and structure seen. Guidelines for such classification have been given by Krug et al (1980), for unwidened spectra, and Kelly et al (1982), for widened spectra, obtained with the old objective prism of the U.K.Schmidt Telescope, at a dispersion of about 2480A°/mm at Hγ. A description of this prism may be found in Nandy et al (1977). Both Krug et al and Kelly et al give classification criteria for B to M stars based on studies of U.K.S.T objective prism spectra of a large number of objects of known spectral type. Kelly et al are concerned primarily with classification from microdensitometer scans, but the criteria given are applicable to direct classification. Both sets of criteria are based on the presence and strength of various spectral features (eg. Hydrogen lines, G-band, Balmer Jump , as well as continuum strengths).

This classification process is simplified if the plate material is obtained using Kodak IIIaJ emulsions, as this emulsion has a sharp 'red-end cut-off' at about 5380A°. Knowing the approximate dispersion of the plate the position of important spectral features may be calculated relative to this cut-off, thus allowing for their rapid identification.

Prior to the commencement of the St.Andrews grism survey a number of widened and unwidened U.K.S.T. objective prism plates (dispersion - 2480Å/mm) were obtained for the purpose of practising the techniques of spectral classification from such material, using the criteria of Krug et al and Kelly et al. One of these plates (UJ4530P) was that used by Kelly et al in establishing their classification criteria, and thus provided a set of spectral standards against which these test classifications could be checked until proficiency was obtained.

2.1.3 Classification from Microdensitometer Scans

Many of the problems and uncertainties inherent in direct visual classification may be removed if the classification is made from a microdensitometer scan of the spectrum. In principle this scan is converted to intensity units and displayed on a V.D.U., a spectral type being assigned using the criteria given by Kelly et al (1982). The method has the advantage of being much less tiring than direct visual classification using a magnifying eyepiece, thus reducing one major source of classification error- fatigue. In addition this enables a classification to be made using all the information stored in the spectrum, notably the shape of the continuum, and allows for objective measures of feature strength etc as opposed to highly subjective naked eye estimates. With the direct method problems are often encountered when working near the plate limit as such faint spectra show little structure. Working from microdensitometer scans the problem is reduced and by normalising the spectra faint objects may be compared with bright standards, which is extremely difficult to do using the direct method.

During April-May 1981 a number of test plates were obtained with the grism on the St.Andrews James Gregory Telescope, at a dispersion of about 1100Å/mm at Hγ. One of these was a 100 minute exposure of a field near the North Galactic Pole, taken in dark of moon (01/5/81) on an unbaked IIIaJ emulsion. The plate limit for direct visual classification was estimated to be about 14m, with objects brighter than about 11m being too over-exposed to be classifiable. This plate contained a large number of spectra and was consequently used to test various ideas on classification from microdensitometer scans of grism plates.

The entire plate was scanned by the University Observatory's computer controlled Joyce-Loebl microdensitometer. FORTH routines to control the scans were prepared by Mr.J.R.Stapleton. When scanning the plate is searched until a region is found in which the photographic density is higher than a previously specified background level. The Joyce-Loebl then centres on this region and takes a single scan through its centre, storing the scan and its plate position on disk. Once the plate has been properly aligned on the Joyce-Loebl and the minimum detection density set this process is automatic. It is, however, slow and inefficient, up to 48 hours being required to scan a single plate, with many spurious plate features (notably the zero order and second and higher order images on the grism plate) being detected and scanned. A typical example of a spectral scan is shown in Figure 2.1.1.

A selection of the stellar spectra obtained in this way were classified directly from the scan using the criteria of Kelly et al. No intensity calibration was available for this plate, and none was needed, implying that the classification does not depend to a great extent on the image exposure. These spectra were all normalised to unity before classification, and this appeared to be sufficient to allow the classification of extremely faint images. (Intuitively one would expect that a good density/intensity calibration would be required since the classification is largely based on the shape of the true spectrum. For the small range in magnitude covered by the spectra obtained here this does not seem to be the case.) The same spectra were classified directly from the plate and both sets of classifications are shown in Table 2.1.1. The agreement is satisfactory. A number of spectra which were too faint for direct classification were easily classified from the normalised scans. These were estimated to be as faint as 14m.5 (compared with the limit of about 14m for direct classification).

There are two major problems with the technique as described above:-

i) It is necessary to identify scans of overlapped spectra and non-first order spectra on the plates. The latter may be easily identified from the scans themselves and the former by checking the position of the scanned objects against a print of the original plate.

ii) It is not generally possible to scan continuously for 48 hours with the St.Andrews Joyce-Loebl due to demands by other users for both

Joyce-Loebl and computer time. The simplest solution to this particular problem is to have two-dimensional scans of the plates made elsewhere using a faster specialised machine (eg. COSMOS or the APM). A modified form of the Joyce-Loebl search/scan routines could then be used to extract the spectra from this data. With more sophisticated software many of the spurious scans could be rejected at this stage if they failed to show specific features (eg. the red-end cut-off, only seen in the first-order grism images). The time elapsed between obtaining the plates and classifying the spectra would be much greater than that taken to classify directly from the plate, but the astronomer would spend less time on each plate and could use the material more effectively.

2.2 The North Galactic Pole Catalogue

Since the work of Humason and Zwicky (1947) many surveys have been performed with the intention of detecting high latitude faint blue objects, generally through the medium of wide-field, wide-band two or three colour photographic photometry. To simplify the process of detection and classification in the present work a catalogue of North Galactic Pole blue stars was compiled, based on these surveys. The literature from 1947-1981 was searched for lists of high galactic latitude blue stars. From these a basic catalogue was prepared containing all suspected blue stars within 5d of the pole, in the magnitude range 13m-17m. Extensive cross-checking was required to ensure that there was no duplication of objects. (One of the remarkable features of these surveys is how little duplication there is between different surveys of the same field, possibly an indication of the problems inherent in classification from crude photographic photometry.)

Two main problems were encountered when compiling this catalogue:-

i) The various surveys tend to use different photometric systems and the quoted photometry frequently had to be converted to a common system before inclusion in the catalogue. The UBV system was chosen as standard and wherever possible magnitudes and colours were converted to V and (B-V). In some cases this was not possible due to the lack of colour data (in general such transformations require at least two colour indices to be known). Some of the surveys included in the catalogue give only a subjective measurement of colour (eg. 'blue', 'quite blue' and 'very blue') rather than an actual colour index. Objects with no measured colour indices are indicated in the catalogue.

ii) many of the earlier surveys give only estimates of magnitudes and colours, based on visual inspection of the plates. The errors in these estimates (when compared with modern measurements) are often very large, especially for the colour indices (up to 1m in (B-V).

Having compiled the basic catalogue, the literature was again searched in an attempt to locate available photoelectric photometry and spectral classifications for these objects.This resulted in improved magnitudes and colours in many cases, as well as some MK spectral types. These were all incorporated into the catalogue. Any known QSO's or other non-stellar objects are indicated. The catalogue and the sources used in its compilation are given in Appendix I.

2.3 U.K.S.T. Prism Plates

2.3.1 Introduction

Due to the delay in the delivery of the St.Andrews grism the North Galactic Pole grism survey, originally scheduled for January-March 1981, had to be postponed for a year. In the interim period the North Galactic Pole blue star catalogue was prepared and experience gained in the techniques of classification from objective prism plates. A U.K.S.T. objective prism plate centred on the North Galactic Pole was then used to assign a spectral type to those catalogue objects in the region covered by this plate. Later, when the grism plates became available they were used to confirm the classifications of the brightest stars on this plate.

2.3.2 Classification

A film copy of U.K.S.T. objective prism plate UJ4081P was available. This unwidened 'B' quality plate is centred on the pole itself and was obtained on 05/April/1978 with a 60 minute exposure on Kodak IIIaJ emulsion. The plate covers an area of about 6° X 6°. For all the stars in the North Galactic Pole blue star catalogue, 1978 coordinates were calculated and used to predict the stars' positions on the plate, using the normal method of Plate Constants with 27 positional standards from the S.A.O. Catalogue. Each object in the field covered by the plate was then identified and a spectral type assigned using the criteria of Krug et al (1980) and Kelly at al (1982). To assist in future identification each spectrum was numbered on a large scale print of the plate. Ambiguities in identification were resolved using finding charts from the original surveys where these were available. On the few occasions that no object was found within two arcminutes of the predicted position, the object was indicated in the catalogue. In all such cases the missing object had been detected by only one of the surveys and is therefore attributable to mis-identification of a plate flaw or similar in the original plate material.

2.4 The St.Andrews Grism Survey

2.4.1 Introduction

A description of the St.Andrews grism and its performance may be found in Appendix II. Briefly, the grism is a dispersing element, contained within the telescope near the focal plane, and is capable of producing low dispersion spectra over a small field. It has been designed specifically for the James Gregory 1 metre Cassegrian-Schmidt Telescope at St.Andrews. The telescope has a useful field of about $2^{\circ}.5$ diameter and the grism produces useful spectra over a 2° field, the size of plate required being 10cmx10cm.

2.4.2. The North Galactic Pole Survey

In order to cover an area of 3° radius centred on the Pole fourteen survey fields were required, each centred on an 8-10th magnitude guide star selected from the S.A.O. catalogue. Details of these fields are given in Table 2.4.1.

The grism was positioned in the telescope such that it produced a dispersion of about 1100A$^{\circ}$/mm at Hγ. The plates were all obtained between 25 January and 16 February 1982, Kodak IIIaJ plates being used throughout Observations were only obtained on nights of grey moon as a result of poor weather conditions throughout the period. All plates had previously been hyper-sensitised by baking in nitrogen for four hours at 65°C. Baked plates were stored in a nitrogen atmosphere and kept refrigerated. They were used within one week of baking.

One plate was obtained per field, with exposure times of 40-50 minutes. Exposures longer than 50 minutes are not feasible with these hyper-sensitised plates as a small increase in exposure time produces a dramatic increase in plate background in this region of the response curve. The goal of one 50 minute exposure per field was not always attained due to the extremely poor weather conditions during the 1981/1982 observing season at St.Andrews. However the difference between the plate limits for 40 and 50 minute exposures is marginal. All plates were developed for 5 minutes in

D19 developer at 20°C, standard procedures being used at all times.

Since these plates were all obtained during grey moon the sky background is higher than on the previously discussed 100 minute non-baked plate obtained in May 1981. Consequently the plate limit is not as faint on the survey plates. The faintest spectra classifiable by direct inspection are estimated to be those of stars brighter than 14th magnitude, and the overall quality of the spectra is poorer than those obtained during the previous season. This latter point is probably attributable to the poorer weather (and consequently seeing) conditions in February/March 1982. As a result of the high sky background it proved impossible to scan these plates with the Joyce-Loebl as the background density was extremely close to the detection limit for faint spectra and the search/scan routines proved incapable of segregating spectra from localised background fluctuations. Consequently the time taken to scan a single plate was increased by a factor of about 3, a vast number of spurious objects being detected.

It was by this stage apparent that a single U.K.S.T. objective prism plate was capable of covering the entire area of the grism survey, with the available unwidened North Galactic Pole plate giving classifiable spectra in the required magnitude range of 13m- 17.5m. Although the grism plates were obtained at higher dispersion, comparison had indicated that the spectra on the U.K.S.T. plate showed more detail than the corresponding grism spectra (presumably a result of better conditions, optics and a more powerful telescope) and were thus much simpler to classify directly from the plate. Consequently the grism survey was abandoned, with the available plates only being used in conjunction with the U.K.S.T. plate to provide classifications for the brighter stars in the North Galactic Pole blue star catalogue.

2.5 North Galactic Pole Blue Stars

The final version of the North Galactic Pole blue star catalogue is presented in Appendix I. Direct visual classifications from U.K.S.T. plate UJ4081P, supplemented by available grism plate classifications, are given in the final column for stars within 3° of the pole. The catalogue covers stellar objects within 5° of the pole in the magnitude range $13 < m_v < 17.5$, which have been identified as blue stars by previous surveys. No claim is made for the completeness of this catalogue.

It is expected to be incomplete as very few high galactic latitude surveys have been centred on the pole, most concentrating on the field SA 57 which is offset from the pole. Uncertainties in the quoted magnitudes ensure that the survey does not include all stars brighter than 17.5m - some fainter stars will be included, some brighter ones excluded. However the catalogue does merge all these surveys and provides a starting point for future work on the blue stars at the North Galactic Pole.

Table 2.1.1.

Comparison of Grism Classifications
Direct Classification vs. Classification from J-L Scan
From 100 min. exposure plate of NGP region on IIIaJ
Taken on 1/5/1981

Object	Classification Direct	Classification Scan
1	F	F
2	A	early F
3	A	A
4	A-F	F
5	B	B
6	G	G
7	B	B
8	F	early F
9	A-F	late A
10	A	A
11	mid-F	late F
12	F	F
13	late A-F	early F
14	late F	late F
15	A-F	early F
16	early F	early F
17	early F	late A
18	F	late F
19	A	A
20	A	A
21	late B-A	A
22	early F	mid F
23	mid F	mid F
24	early F	mid F
25	mid-late F	G
26	A	mid A
27	late F	G
28	B	A
29	A	A-early F
30	F	late F
31	B-A	A

Note : A further 8 faint objects classified from scans could not be classified directly from the plate.

Table 2.4.1.

Grism Survey Fields

Field	R.A. (1950) h	m	s	Dec. d	m	s	SAO guide star	mv	Sp. Type	Exposure of plate
1	12	47	05	+26	29	41	082516	8.8	K0	45 min.
2	12	53	39	+26	17	32	082575	9.1	A7	45 min.
3	12	52	43	+28	02	17	082565	8.0	G5	45 min.
4	12	45	59	+28	03	23	082507	8.0	F8	45 min.
5	12	52	38	+24	40	27	082563	8.8	G5	50 min.
6	12	46	06	+25	02	10	082508	8.9	F5	50 min.
7	12	40	52	+25	01	47	082558	9.2	F8	50 min.
8	12	39	43	+26	38	02	082543	9.0	K0	50 min.
9	12	39	56	+28	13	11	082545	9.3	G0	50 min.
10	12	43	43	+28	57	18	082584	9.3	F8	50 min.
11	12	49	59	+29	06	41	082544	8.5	G5	50 min.
12	12	57	30	+28	54	03	082582	8.9	K0	50 min.
13	13	00	29	+26	39	33	082621	9.1	K0	50 min.
14	12	58	38	+24	35	09	082607	8.0	K0	50 min.

Figure 2.1.1.

Typical Grism Spectrum

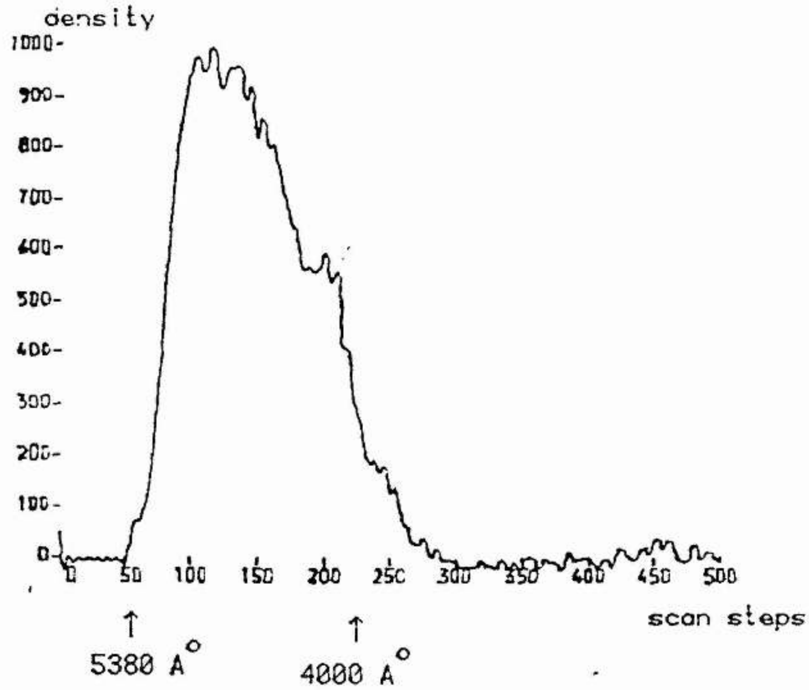

The wavelength scale is approximate.

Chapter 3

Photometry

'The life so short...'

3: Photometry

3.1. The uvby Photometric System

3.1.1 Introduction

The uvby system (Stromgren 1963,1966) was specifically designed for the study of A, F and G stars and has since been extended to cover the O and B stars. The system makes use of four intermediate band-pass filters (Table 3.1.1), the u filter being a glass filter while the others are interference filters.

The u band lies just shortward of the Balmer Jump, and the v band lies just longward of the Balmer Jump in a major line blanketing region for the F stars. The b band is centred on a less important blanketing region and is mainly used as a comparison point. The y band mimics, to a certain extent, the V band of the UBV system (Johnson and Morgan 1953) and the intensity in this band is used to determine the equivalent V magnitude, since,

$$V = y + \epsilon(b-y),$$

where ϵ is a constant, equal to 0.02.

The colour (b-y) is fairly insensitive to the number of lines in the stellar spectrum and is a basic indicator of effective temperature. The index c_1 = (u-v)-(v-b) is a measure of the strength of the Balmer Jump, and hence of the luminosity for a given temperature. In addition it is almost independent of chemical composition effects. The index m_1 = (v-b)-(b-y) measure of the line blanketing, and hence of the star's metallicity. All of these parameters (b-y), c_1 and m_1, as well as the V magnitude are affected by interstellar extinction and reddening.

Crawford and Barnes (1970) have given the primary standards for the system and have shown it to be (almost) totally filter defined. Once the effects of the Earth's atmosphere have been removed, the system is found to be independent of telescope, photometer and site. All of the filters have band passes located well within the transparent region of the atmosphere and thus none of the filter response curves have an atmospheric cut-off (cf. the UBV system in which the U band has an atmospheric cut-off).

3.1.2 Interstellar Extinction in the uvby System

All four band passes are affected by interstellar extinction, and thus the indices (b-y), c_1 and m_1 are all affected. The standard reddening relations between the indices have been given by Crawford (1975) as;

$$E(m_1) = -0.32\ E(b-y)$$
$$E(c_1) = 0.20\ E(b-y)$$
$$E(u-b) = 1.54\ E(b-y)$$

with,

$$E(b-y) = 0.74\ E(b-v)$$

From these relations it is possible to define indices $[c_1]$, $[m_1]$ and $[u-b]$ which are unaffected by interstellar reddening:

$$[c_1] = c_1 - 0.20(b-y)$$
$$[m_1] = m_1 + 0.32(b-y)$$
$$[u-b] = (u-b) - 1.84(b-y) = [c_1] + 2[m_1]$$

3.1.3 Intrinsic Colours and Two-Colour Diagrams

If the data for a large number of stars are plotted in the c_o vs. $(b-y)_o$ and m_o vs. $(b-y)_o$ planes, it is readily apparent that stars of a given type are grouped together. In addition there are well defined lower envelopes to the distribution of ZAMS population I stars. These envelopes are the intrinsic colour lines for ZAMS population I stars. A star's deviation from these envelopes is a measure of its difference from the ideal of the ZAMS population I object. Thus it is possible to infer a "spectroscopic" classification for a star on the basis of photometry alone. Photometric criteria for such classification from uvby photometry have been given by Hill, Barnes and Hilditch (1982d) based in part, on the photometric scheme of Kilkenny and Hill (1975).

Intrinsic colour lines for uvby photometry have been given by Crawford (1975,1978 and 1979) for the F, B and late A stars (A4-A9), and by Hilditch et al (1983) for the intermediate A stars (A0-A3). Hill, et al (1982d) give a provisional calibration for the Horizontal Branch stars. Hill (1982d) has pointed out a possible systematic error in the B star calibration which appears to be too red by approximately 0.006 magnitudes.

3.2 The Hβ Photometric System

3.2.1 Introduction

As a general rule the width of the Hydrogen Balmer lines in stellar spectra are dependent on the stellar atmospheric pressure and thus on the stellar surface gravity. Surface gravity is related to luminosity and therefore to absolute magnitude. There is therefore a correlation between the width of the Balmer lines and the star's absolute magnitude, Mv. A photometric parameter related to the line width, and showing this strong correlation with Mv would be extremely useful as a means of determining stellar distances. Such a parameter is the β index of the Hβ photometric system introduced by Stromgren (1956) and adapted by Crawford and Mander (1966). In its current form the system makes use of two interference filters, both centred on 4861Å (Hβ), one having a half-width of 30Å (the narrow filter) and the other a half-width of 150Å (the wide filter). The narrow filter is used to sample the intensity of the Hβ line and the wide filter measures the intensity of the line plus the surrounding continuum. The instrumental β index,

$$\beta = 2.5\,[\log(I_w/I_n)],$$

where I is transmitted intensity through the filter, is thus a measure of the strength of the Hβ line relative to the nearby continuum. It is obvious from the definition that $\beta \geqslant 2.5$. Since both filters have the same central wavelength and are reasonably narrow there are no extinction effects to be considered (either interstellar or atmospheric) and the transformation from the instrumental to the standard system is simple. For the same reasons the system is entirely filter defined.

However, the β index is a measure of the line broadening, which is not solely dependent on the surface gravity, but also on the temperature due to the effects of radiation pressure on line width. In general, radiation pressure opposes the surface gravity effect and reduces the pressure broadening. As a general rule the β index is a surface gravity parameter for B stars and a temperature parameter for A-F stars. The Hβ line may also be broadened by rotational effects, but if the filters used have a band-pass of 30A^{o} or more the β index will not be affected by this.

Since the system makes use of narrow filters the effective magnitude limit for Hβ photometry is about 2 magnitudes lower than that for uvby photometry with the same telescope and detectors.

3.2.2 Intrinsic Colour Lines and Photometric Classification

In conjunction with the uvby system Hβ photometry is used to produce plots of β vs. $(b-y)_o$ for a large number of stars, from which intrinsic colour lines are derived in the same way as for uvby photometry on its own. The use of the β index in photometric classification can remove ambiguities presented by the uvby photometry and is particularly helpful for identifying reddened objects, since β is not affected by the reddening. The classification criteria of Hill et al. (1982d) and the calibrations of Crawford (1975, 1978, 1979) and Hilditch et al. (1983) are all concerned with uvbyβ photometry.

3.3 uvbyB Photometry: SGP

3.3.1 Observations

All of the uvby photometry and 40% of the Hβ photometry presented here was obtained by R.W.Hilditch at SAAO in Octobers 1976 (no Hβ) , 1977 and 1978 with the 0.5m telescope with the People's Photometer and the 1.0m telescope with the St.Andrews Photometer. The 1976 and 1977 0.5m data were recorded using a charge integration system, all other data being acquired using a pulse counting system. Different Stromgren filters were used in 1976/1977 and 1978.The remaining 60% of the Hβ data were obtained by G.Hill at CTIO in October 1975 using the 0.4, 0.6 and 0.9m telescopes with single-channel photometers and pulse-counting systems.

On each night a large number of standard stars (~25) were observed. These were selected from the lists of Crawford and Mander (1966) for Hβ photometry and Crawford and Barnes (1970) for uvby photometry, with some secondary standards taken from Gronbech and Olsen (1976,1977). The V magnitudes were adopted from Iriarte et al (1965) and Johnson et al (1966).

A total of 580 stars were observed in uvby and 533 in Hβ by Hilditch. Hill observed 545 stars of which 460 were common to both Hill and Hilditch.

3.3.2 Reductions of Standard Stars

All of the 1975 Hβ data were fully reduced at DAO by G.Hill. All other standard star data were reduced by R.W.Hilditch at St.Andrews. Standard reduction techniques were followed in both cases, using programs developed by G.Hill to determine scale factors, zero points, extinction coefficients (uvby only) and colour terms (uvby only). For the Hβ photometry the zero points for B stars were determined separately from those for the AF stars. In every case the standard star residuals were checked for systematic variations dependent on time or (b-y) colour (uvby only). No time dependencies were found and the small colour terms present in the uvby data for a few nights were taken into account in the programme star reductions.

3.3.3 Reductions of Programme Star Data: uvby Photometry

All programme star data were reduced at St.Andrews using programs developed by G.Hill. Standard procedures were followed. A check was made for possible differences between the 1976 data (filter set 1), the 1977 data (filter set 1) and the 1978 data (filter set 2). Twenty stars common to all three years were used for this comparison, leading to the mean residuals and rms deviations given in Table 3.3.1. These differences were considered to be acceptably small, although the 1976 data appear to be of lower quality than the rest. However, few observations were actually obtained in this year.

Excluding stars with only one observation (41), the internal rms deviation of a single observation was found to be:

dV	d(b-y)	dm_1	dc_1
±0.011	±0.006	±0.012	±0.020

from 1516 observations of 535 stars.

To determine the external accuracy of the photometry the data were compared with five other sources with which there was sufficient overlap to justify such a comparison. The mean residuals in the sense (current-other) are given in Table 3.3.2, where n is the number of stars used in the comparison. In none of these cases do the individual residuals show any (b-y) dependence.

The agreement with Gronbech and Olsen, Stokes, and Phillip is good, and combining the data from these three sources gives:

$$\delta(b-y):-0.004;\delta V:-0.011;\delta m_1:+0.003;\delta c_1:+0.002$$

The relatively large difference in V between the current data and that of Gronbech and Olsen is odd, but not significant. There is no obvious reason for the large rms scatter which is present in the comparison with the photometry of Albrecht and Maitzen. However we note here that Albrecht and Maitzen have only one or two observations per star. The comparison with Knude (1982a, private communication) is given, despite the small overlap, because Knude has consistently found the interstellar reddening at the SGP to be higher than that found by other photometric surveys. The agreement is good, but not excellent. The explanation for Knude's large apparent reddenings must be sought elsewhere.

In conclusion, the excellent agreement with the photometry of Gronbech and Olsen, Stokes, and Phillip suggests that there are no serious discrepancies in the data presented here.

3.3.4 Reductions of Programme Star Data: Hβ Photometry

All of the 1975 data were reduced by G.Hill at DAO, the 1977/1978 data being reduced at St.Andrews. In both cases the reduction programs were developed by G.Hill, standard procedures being followed. The internal rms deviations for a single observation were found, from stars with two or more observations, to be:

1977/1978	$d\beta=$	± 0.009	(364 observations of 163 stars)
1976	$d\beta=$	± 0.011	(700 observations of 297 stars)

The 1975 data (from CTIO) were compared with the 1977/1978 data (from SAAO) giving an average difference, in the sense (SAAO-CTIO) of:

$$d\beta = 0.000 \pm 0.007$$

from the 460 stars in common. There thus appear to be no systematic differences between the two sets of observations and they were therefore combined, the final photometry having an internal rms deviation, from stars with two or more observations, of:

$d\beta = \pm 0.011$ (from 1692 observations of 566 stars)

This Hβ photometry was compared with that from four other sources with which a sufficient overlap existed. Differences were calculated in the sense (current-other), mean differences being given in Table 3.3.3. As for the four colour photometry, there is a large scatter present in the comparison with Albrecht and Maitzen's photometry. Again the agreement with Knude is not excellent, but is acceptable. However the agreement with both Gronbech and Olsen and Stokes is excellent, implying that there are no serious discrepancies in the Hβ photometry presented here.

3.3.5 Results

The final uvbyβ photometry for all 572 stars in the sample for which both uvby and Hβ data are available is given in Table 3.3.4. The columns are:

1) HD number. For visual pairs relative positions in the sky are indicated. Otherwise the brighter component is designated 'A'.

2)-5) Stromgren colour indices (b-y), m_1, c_1, and the V magnitude.

6) Number of individual four colour observations of each object.

7) β index

8) Number of individual Hβ observations of each object.

3.4 uvby Photometry: NGP

3.4.1 Observations

A total of 20 NGP BAF stars were observed with the 1.0m telescope at the OHP "Chiran" outstation in April 1982, using a single-channel photometer with a charge-integrating system, and uvby filters kindly supplied by KPNO. These stars were all of 13m-14m and had been selected from the NGP catalogue (chapter 2) after classification from UKSTU prism plates and, where available, JGT grism plates.

Observations were obtained on 4 nights only, out of 14 allocated. Due to the limited dynamic range of the available amplifier it was not possible to observe standard stars from the lists of Crawford and Barnes (1970). Consequently a list of secondary standards was compiled from the catalogue of Hauck and Mermilliod (1980), with final adopted colours being taken from the catalogue of Hill et al (1982d), whenever possible. These are listed in Table 3.4.1. With the equipment available it proved impossible to observe objects fainter than 14.5 magnitudes, and for brighter programme stars integration times of 60 seconds/filter were required, severely limiting the number of observations possible each night. Programme stars were observed in the sequence ybvu(star)-uvby(sky)-ybvu(star). For the standards the sequence ybvu(star)-uvby(sky) was employed. Between 11 and 14 standards were observed each night.

3.4.2 Reductions of Standard Stars

All reductions were performed at St.Andrews using the same programs and techniques employed for the SGP photometry. Due to the low number of standards observed, it proved impossible to accurately determine the extinction coefficients for each night.

Consequently, the standard values for KPNO (at the same altitude as Chiran) were adopted, namely:

Extinction Coefficients

(u-b)	:	0.4
(v-b)	:	0.12
(b-y)	:	0.06
V	:	0.15

Scale factors, zero points and colour terms were determined for each night individually. No (b-y) dependencies were found for any of the residuals, (taken in the sense (standard value - observed)) but there did appear to be an LST dependence in V on three nights (21/22,22/23 and 26/27), and in (u-b) on two nights (21/22 and 22/23). These terms were all taken into account in the final reductions.

The final standard stars residuals were found to be, on average:

(u-b)	:	± 0.030
(v-b)	:	± 0.015
(b-y)	:	± 0.015
V	:	± 0.015

from 54 observations of 21 stars.

These results are extremely poor for standard stars.

3.4.3 Reductions of Programme Stars

The programme star data were reduced in identical manner to the SGP data, the LST dependencies mentioned above being allowed for in the reductions. Excluding stars with only one observation (1) the internal rms deviation of a single observation was found to be:

d(u-b) : $\pm$0.015 ; d(v-b) : $\pm$0.08 ;
d(b-y) : $\pm$0.08 ; dV : $\pm$0.10 ,
from 62 observations of 19 stars.

The individual observations for each night are given in Table 3.4.2. From these, and the internal errors quoted above the poor quality of this data can be seen. No attempt was made to use the Stromgren indices to plot two-colour diagrams etc. using this data because of its low quality.Possible reasons for these poor results will now be considered.

Several possible sources of error can be discounted . The amplifier's stability was checked each night immediately before observing began, as it was known to be very susceptible to dampness in the air. On every occasion it was found to be stable. Both the power supply to the dome and the UHT supply to the photometer were monitored and remained constant throughout each night.

For each night an estimate was made of the Signal/Noise ratio of each observation through the 'y' filter.The noise level was defined on the basis of the spread of the signal about the means for both the star and the corresponding sky observation. A plot of S/N versus V magnitude was then prepared for each night, an example of such a plot being shown in Figure 3.4.1.The general trend is as expected: fainter stars have a smaller S/N ratio than brighter stars, with a greater spread about the mean curve for the programme stars than for the standards. However the S/N for a given magnitude is less than one would expect for a single-channel photometer on a 1m telescope at a good site. The mean curve for each night is similar in all four cases, suggesting that the sensitivity of the equipment did not vary over the observing period. Note that the S/N ratio for a given object varied considerably from night to night, though the overall trend remained the same. The low accuracy of the programme (and standard) star photometry is to be expected on the basis of such low S/N ratios.

The standard stars were chosen to have at least six individual observations by the same observers, with the same equipment, or failing that, three individual observations by the same observers with the same equipment, for at least three different observers. The final adopted colours were those of Hill et al (1982d), where possible in order to provide a consistent set of standards. Where no Hill et al observations were available, the adopted colours were weighted means of those from other sources, weighted by the number of observations and a quality parameter. The error present in these adopted colours is therefore expected to be small, certainly too small to explain the observed inaccuracy of the photometry.

Weather conditions during the observing period were extremely poor, with frequent low cloud and blizzards. On the four nights on which observations were obtained the sky appeared to be free of visible cloud or haze. However the (often systematic) slight variations in the chart recorder traces for both programme and standard stars suggest that high thin cloud may have been present at times, although none was visible.

There is no single obvious cause for the low quality of this photometry. However the scale of the S/N vs. magnitude curves mentioned above suggests that the sensitivity of the detection equipment was lower than anticipated. The chart recorder traces and the variations in S/N for a single star from night to night suggest the presence of a random element contributing to the inaccuracy, probably in the form of thin, obscuring cloud. The evidence available suggests that some combination of these two factors is responsible.

Table 3.1.1.

Central Wavelengths and Half-Widths of uvby Filters

filter	u	v	b	y
central L (Å)	3500	4110	4670	5470
half-width (Å)	300	190	180	230

Table 3.3.1.

SGP uvby Photometry- Comparison of Data Sets

δV	$\delta(b-y)$	δm_1	δc_1	
0.008	-0.007	0.011	0.009	
±0.020	±0.015	±0.026	±0.032	1977-1976
-0.010	0.004	-0.005	0.008	
±0.019	±0.015	±0.012	±0.022	1978-1977
0.009	0.003	0.012	-0.040	
±0.008	±0.019	±0.014	±0.063	1978-1976

Table 3.3.2.

SGP uvby Photometry- Comparison with other Photometry

δV	$\delta(b-y)$	δm_1	δc_1	n	source
-0.016	-0.003	0.004	0.001	30	Gronbech & Olsen
$\pm$0.012	$\pm$0.006	$\pm$0.012	$\pm$0.012		(1976)
-0.002	-0.003	0.009	0.000	12	Stokes
$\pm$0.019	$\pm$0.012	$\pm$0.018	$\pm$0.018		(1972)
-0.006	-0.006	-0.004	0.007	13	Phillip
$\pm$0.019	$\pm$0.009	$\pm$0.016	$\pm$0.028		(1972)
-0.080	-0.004	0.010	0.002	81	Albrecht & Maitzen
$\pm$0.052	$\pm$0.027	$\pm$0.022	$\pm$0.011		(1982)
-0.006	-0.013	0.010	-0.017	7	Knude
$\pm$0.006	$\pm$0.004	$\pm$0.015	$\pm$0.011		(1982a)

Table 3.3.3.

SGP Hβ Photometry- Comparison with other Photometry

dβ	n	source
-0.002 ±0.006	30	Gronbech & Olsen (1977)
-0.001 ±0.008	12	Stokes (1972)
-0.011 ±0.042	81	Albrecht & Maitzen (1982)
-0.022 ±0.018	8	Knude (1982a)

Table 3.3.4

HD no.	(b-y)	m1	c1	V	n	Beta	n
223352	-0.006	0.161	1.019	4.588	3	2.884	2
223466	0.048	0.226	0.974	6.413	3	2.854	4
223515	0.211	0.174	0.740	7.718	3	2.730	3
223654	0.098	0.180	1.028	6.231	3	2.812	3
223991	0.111	0.191	0.808	6.552	2	2.830	3
225202	-0.009	0.201	1.000	6.503	2	2.921	4
19	0.335	0.201	0.385	9.900	3	2.606	3
20	0.424	0.093	0.479	9.043	2	2.564	4
30	0.295	0.130	0.477	9.616	3	2.636	2
31	-0.031	0.144	0.878	6.303	3	2.825	10
50	0.160	0.215	0.636	9.714	3	2.810	3
90	0.326	0.163	0.546	9.646	3	2.625	3
91	0.216	0.170	0.574	9.909	3	2.752	3
117	0.363	0.147	0.404	9.004	3	2.640	3
140	0.264	0.153	0.528	9.825	3	2.675	3
141	-0.023	0.147	0.935	7.923	2	2.859	4
156	0.242	0.188	0.696	7.307	3	2.704	3
157	-0.036	0.175	0.921	10.681	1	2.836	4
171	0.259	0.167	0.409	9.346	3	2.676	3
189	0.335	0.171	0.471	8.554	2	2.638	4
203	0.243	0.171	0.522	6.137	2	2.676	3
225	0.327	0.154	0.471	8.244	3	2.627	3
235	0.031	0.166	1.018	8.670	2	2.904	5
241	0.315	0.175	0.345	10.254	3	2.629	3
243	0.250	0.156	0.495	8.410	4	2.672	3
255	0.073	0.169	1.070	6.204	2	2.820	3
256	0.295	0.132	0.421	10.001	3	2.612	3
266	0.300	0.150	0.420	7.045	2	2.646	4
306	0.046	0.171	0.953	9.462	3	2.847	3
319	0.077	0.166	1.047	5.922	1	2.845	3
343	0.189	0.177	0.680	9.762	3	2.681	3
392	0.312	0.176	0.515	7.585	2	2.637	3
394	0.302	0.185	0.468	9.505	3	2.661	3
427	0.298	0.150	0.499	7.875	4	2.651	3
428	0.296	0.141	0.468	8.643	3	2.652	3
464	0.343	0.186	0.444	9.321	2	2.645	3
465SE	0.256	0.141	0.533	10.235	3	2.651	2
466	0.262	0.157	0.612	7.779	3	2.687	3
484	0.300	0.156	0.388	9.369	3	2.642	2
493	0.267	0.178	0.605	5.381	1	2.670	3
506	0.264	0.153	0.500	9.792	3	2.674	2
511	0.325	0.160	0.391	8.919	3	2.637	5
535	0.167	0.166	0.777	9.807	1	2.746	3
536	0.282	0.156	0.509	8.354	3	2.660	3
562	0.071	0.193	0.966	7.648	2	2.846	3
574	0.268	0.182	0.465	10.048	3	2.664	3
575	0.337	0.163	0.435	9.460	3	2.600	3
590	0.249	0.164	0.498	9.924	3	2.665	3
605	0.289	0.171	0.427	10.313	1	2.641	3
704	0.071	0.169	1.050	8.449	2	2.870	3
718	0.297	0.166	0.431	8.484	3	2.646	3
719	0.213	0.191	0.769	9.410	2	2.762	3
732	0.349	0.181	0.493	7.855	2	2.629	3
739	0.289	0.151	0.445	5.235	3	2.654	4
768	0.236	0.160	0.520	7.910	2	2.698	3
781	0.301	0.155	0.468	9.114	1	2.655	3
798	0.282	0.164	0.461	8.251	2	2.677	3
824	0.296	0.136	0.442	9.125	3	2.642	3
836	0.315	0.158	0.450	8.731	3	2.647	3
867	0.309	0.165	0.451	9.541	3	2.642	3

Table 3.3.4

ID no.	(b-y)	m1	c1	V	n	beta	n
890	0.301	0.157	0.568	7.449	2	2.658	3
900	0.231	0.171	0.545	7.979	2	2.669	3
925	0.091	0.211	1.064	8.500	2	2.860	3
955	-0.081	0.104	0.349	7.372	3	2.669	3
1000	0.314	0.154	0.450	8.821	3	2.650	3
1001	0.276	0.156	0.521	9.245	2	2.663	3
1017	0.181	0.184	0.715	9.292	3	2.747	3
1052	0.296	0.160	0.516	9.469	3	2.660	3
1065	0.239	0.149	0.564	9.773	3	2.679	2
1078	0.279	0.155	0.495	8.008	2	2.668	3
1088	0.093	0.220	0.952	9.799	3	2.829	4
1097	0.240	0.339	0.464	9.077	3	2.732	3
1101	0.260	0.159	0.642	7.666	3	2.667	3
1104	0.300	0.148	0.420	9.398	3	2.642	3
1137	0.290	0.157	0.465	9.303	3	2.647	3
1232	0.305	0.150	0.465	8.563	3	2.629	3
1234	0.293	0.144	0.503	9.200	3	2.656	3
1244	0.313	0.165	0.447	9.725	2	2.632	3
1245	0.316	0.169	0.473	9.370	2	2.652	5
1250	-0.050	0.114	0.512	6.490	1	2.737	2
1265	0.266	0.164	0.498	9.645	3	2.647	2
1343	0.252	0.149	0.506	6.440	2	2.674	3
1431	0.001	0.118	0.720	6.705	2	2.778	3
1432	0.307	0.155	0.434	8.691	3	2.640	3
1433	0.288	0.151	0.443	9.458	3	2.637	3
1463	0.266	0.142	0.464	9.654	3	2.661	3
1464	0.319	0.143	0.468	9.305	3	2.582	4
1473	0.244	0.168	0.608	9.706	3	2.719	6
1482	0.282	0.150	0.471	9.256	3	2.658	4
1492	0.190	0.184	0.704	8.818	2	2.763	3
1493	0.283	0.145	0.426	9.700	3	2.650	2
1498	0.282	0.169	0.494	9.156	5	2.658	4
1524	0.292	0.159	0.505	8.764	2	2.668	4
1541	0.156	0.213	0.888	9.694	4	2.781	3
1557	0.305	0.156	0.468	9.152	3	2.633	3
1580	0.260	0.157	0.479	9.726	3	2.651	2
1595	0.329	0.148	0.395	9.435	3	2.620	3
1597	0.221	0.159	0.574	9.793	3	2.697	2
1616	0.207	0.246	0.676	8.620	3	2.757	4
1619	0.196	0.248	0.691	8.646	2	2.757	1
1666	0.327	0.182	0.485	8.160	2	2.638	3
1667	0.172	0.197	0.857	6.772	2	2.737	3
1683	0.325	0.149	0.488	7.130	3	2.634	3
1692	0.336	0.168	0.337	9.324	4	2.610	3
1738	0.296	0.153	0.434	9.281	3	2.642	3
1751	0.342	0.165	0.412	8.534	4	2.624	3
1776	0.310	0.149	0.427	8.986	3	2.657	3
1791	0.181	0.218	0.721	8.382	3	2.759	3
1797	0.268	0.174	0.508	8.417	2	2.672	3
1856	0.217	0.176	0.668	6.740	3	2.730	3
1857	0.308	0.173	0.470	9.479	3	2.639	3
1858	0.311	0.136	0.351	9.370	3	2.617	3
1909	-0.028	0.115	0.711	6.556	2	2.762	2
1938	0.322	0.155	0.440	9.991	3	2.631	3
1947	0.285	0.160	0.502	9.185	2	2.662	3
1980	0.311	0.152	0.418	7.413	3	2.618	4
1988	0.259	0.156	0.534	9.299	4	2.676	3
1999	-0.044	0.090	0.608	8.293	3	2.674	3
2007	0.089	0.236	0.969	9.475	3	2.833	4
2026	0.059	0.221	1.002	8.120	2	2.888	3

Table 3.3.4

HD no.	(b-y)	m1	c1	V	n	Beta	n
2057	0.184	0.121	0.790	8.352	2	2.735	3
2050	0.341	0.179	0.420	9.290	4	2.622	3
2052	0.293	0.135	0.449	9.165	4	2.657	3
2059	0.282	0.153	0.646	8.313	2	2.676	3
2066	0.276	0.152	0.505	8.466	2	2.664	3
2080	0.221	0.166	0.566	8.022	2	2.691	3
2131	0.335	0.143	0.350	8.845	3	2.611	3
2160	0.308	0.159	0.509	8.429	2	2.605	3
2161	0.347	0.166	0.503	7.702	2	2.630	3
2176	0.024	0.166	1.097	7.620	2	2.856	4
2200	0.262	0.140	0.506	10.221	3	2.661	3
2215	0.304	0.160	0.420	10.166	3	2.645	3
2240	0.240	0.166	0.591	10.125	3	2.663	3
2259	0.272	0.152	0.521	9.402	2	2.662	3
2279	0.329	0.173	0.419	9.057	3	2.636	3
2288	0.247	0.173	0.603	10.064	3	2.690	2
2318	0.262	0.166	0.658	8.447	2	2.680	3
2319	0.290	0.160	0.401	9.104	3	2.639	3
2320	0.152	0.166	0.706	6.933	5	2.739	3
2327	0.301	0.154	0.475	9.094	3	2.651	3
2337	0.301	0.145	0.414	9.332	2	2.616	3
2340	0.320	0.221	0.251	6.665	2	2.634	2
2362	0.277	0.166	0.466	9.520	3	2.660	3
2381	0.249	0.154	0.503	7.726	2	2.693	3
2395	0.145	0.200	0.833	6.778	2	2.792	3
2402	0.314	0.150	0.403	9.726	3	2.627	4
2415	-0.014	0.131	1.000	11.093	3	2.565	1
2425	0.342	0.134	0.420	8.451	2	2.642	3
2450	0.352	0.168	0.312	9.354	3	2.624	3
2465	0.309	0.192	0.359	9.157	3	2.603	3
2477	0.308	0.137	0.436	7.096	2	2.624	3
2527	0.188	0.170	0.936	7.116	2	2.735	3
2528	0.279	0.161	0.478	9.896	3	2.625	2
2554	0.240	0.165	0.642	9.838	5	2.682	4
2557	0.245	0.157	0.502	9.062	2	2.674	3
2571	0.347	0.174	0.445	9.886	3	2.595	4
2574	0.294	0.176	0.487	10.109	3	2.638	2
2613A	0.253	0.129	0.553	10.737	3	2.669	2
2613B	0.117	0.255	0.754	11.197	3	2.856	2
2615	0.301	0.127	0.435	7.619	2	2.626	3
2640	0.303	0.155	0.492	9.270	3	2.648	3
2641	0.050	0.208	0.993	9.518	3	2.895	3
2696	0.079	0.152	1.047	5.202	1	2.867	3
2719	0.328	0.146	0.471	7.538	2	2.638	3
2724	0.192	0.184	0.889	6.177	3	2.748	3
2783	0.238	0.183	0.652	8.403	2	2.689	3
2797	0.256	0.313	0.211	9.645	3	2.693	4
2799	0.015	0.166	1.280	10.985	3	2.865	3
2810	0.301	0.171	0.453	10.133	3	2.625	3
2846	0.207	0.165	0.711	10.522	3	2.706	2
2859	0.289	0.155	0.449	10.315	3	2.624	1
2860	0.245	0.162	0.628	9.983	3	2.696	2
2862	0.326	0.151	0.410	9.354	3	2.626	3
2870	0.404	0.205	0.427	9.517	3	2.592	2
2903	0.305	0.175	0.463	9.738	3	2.655	2
2916	0.247	0.160	0.544	7.305	2	2.691	3
2978	0.241	0.163	0.514	9.626	3	2.656	4
2980	0.215	0.167	0.726	8.941	3	2.717	4
2988	0.290	0.148	0.499	9.447	3	2.664	3
2998	0.342	0.187	0.449	10.083	3	2.629	1

Table 3.3.4

HD no.	(b-y)	m1	c1	V	N	Beta	n
3002	0.131	0.191	0.656	9.465	3	2.795	3
3017	0.323	0.169	0.340	9.561	3	2.609	2
3019	0.319	0.170	0.473	8.875	2	2.634	3
3020	0.303	0.173	0.425	10.100	3	2.642	2
3033	0.404	0.215	0.403	9.102	3	2.602	3
3050	0.269	0.141	0.469	9.304	3	2.669	3
3061	0.213	0.153	0.639	7.865	3	2.712	3
3065	-0.026	0.162	0.921	7.415	3	2.804	3
3092	0.291	0.163	0.421	8.223	4	2.650	3
3109	0.260	0.171	0.438	10.387	3	2.666	3
3110	0.263	0.161	0.470	10.003	3	2.675	3
3132	0.321	0.164	0.493	9.364	3	2.639	3
3135	0.214	0.255	0.672	9.672	3	2.738	3
3160	0.290	0.123	0.400	9.050	3	2.645	3
3166	0.277	0.054	0.613	9.041	3	2.663	4
3216	0.292	0.160	0.493	9.505	3	2.674	3
3217	0.278	0.156	0.406	8.363	3	2.656	3
3244	0.171	0.149	0.773	8.225	3	2.731	2
3257	0.244	0.145	0.607	8.620	3	2.690	3
3299	0.137	0.167	0.663	9.647	3	2.766	4
3300	0.266	0.162	0.428	10.280	3	2.603	2
3311	0.051	0.241	0.926	9.006	3	2.860	3
3314	0.335	0.161	0.351	9.793	3	2.616	1
3316	0.356	0.151	0.399	9.265	3	2.609	3
3326	0.165	0.230	0.723	8.046	3	2.767	4
3336	0.223	0.153	0.645	8.465	3	2.704	3
3337	0.265	0.164	0.426	7.864	2	2.660	3
3354	0.303	0.190	0.363	9.257	4	2.644	3
3391	0.265	0.166	0.466	10.071	3	2.658	2
3389	0.234	0.194	0.700	7.934	3	2.699	4
3387	0.316	0.141	0.382	10.046	3	2.632	3
3417	0.185	0.178	0.710	10.760	3	2.737	2
3423	0.256	0.160	0.494	10.239	3	2.679	3
3436	0.198	0.182	0.631	9.810	3	2.739	3
3437	0.314	0.186	0.474	10.096	3	2.638	2
3479	0.269	0.139	0.599	8.551	2	2.676	3
3506	0.284	0.157	0.537	8.378	3	2.662	3
3525	0.320	0.156	0.462	8.787	3	2.648	2
3559	0.116	0.201	0.908	8.533	3	2.832	3
3580	-0.070	0.125	0.490	6.721	2	2.716	3
3581	0.265	0.157	0.492	7.101	3	2.679	3
3596	0.315	0.167	0.509	8.946	2	2.645	3
3597	0.328	0.152	0.430	8.852	3	2.629	3
3604	-0.021	0.178	0.931	9.556	3	2.868	3
3621	0.373	0.134	0.398	8.317	4	2.607	4
3622	0.115	0.206	0.812	7.757	3	2.805	3
3696	0.278	0.165	0.494	10.029	3	2.668	2
3734	0.292	0.130	0.412	9.269	3	2.652	3
3735	0.340	0.130	0.382	6.673	2	2.613	4
3736	0.106	0.162	1.096	8.579	2	2.813	3
3762	0.132	0.195	0.884	8.033	3	2.573	3
3772	0.227	0.158	0.655	9.998	3	2.688	3
3785	0.343	0.150	0.455	8.694	2	2.619	3
3783	0.284	0.172	0.424	9.505	3	2.645	3
3813	0.290	0.163	0.432	10.179	3	2.648	2
3812	0.263	0.152	0.504	9.574	3	2.658	2
3835	0.343	0.144	0.405	8.356	3	2.625	3
3850	0.261	0.155	0.508	9.326	3	2.685	3
3864	0.267	0.155	0.560	9.108	3	2.649	3
3865	0.264	0.179	0.472	9.841	3	2.670	2

Table 3.3.4

HD no.	(b-y)	m1	c1	V	n	beta	n
3867	0.052	0.181	0.975	8.321	3	2.882	3
3876	0.267	0.161	0.527	10.119	3	2.679	3
3885	-0.060	0.102	0.865	9.759	3	2.764	4
3978	0.280	0.152	0.464	9.624	3	2.677	3
3999	0.040	0.219	0.987	9.520	3	2.868	3
4010	0.280	0.156	0.434	9.037	3	2.655	2
4011	0.217	0.140	0.650	9.570	3	2.703	3
4023	0.306	0.157	0.457	9.251	2	2.636	4
4035	0.324	0.161	0.417	8.724	3	2.626	3
4052	0.155	0.214	0.779	10.593	3	2.751	2
4065	-0.021	0.159	0.914	6.042	3	2.864	3
4072	0.265	0.148	0.530	10.221	3	2.652	3
4073	0.268	0.156	0.522	9.591	3	2.684	3
4110	0.209	0.171	0.689	10.282	3	2.726	3
4124	0.321	0.184	0.436	8.940	3	2.644	3
4143	0.311	0.128	0.382	8.921	2	2.640	3
4157	0.001	0.154	1.071	9.565	3	2.813	4
4158	0.223	0.095	0.744	9.539	3	2.674	4
4169	0.308	0.160	0.430	7.628	2	2.652	3
4189	0.339	0.174	0.342	9.031	2	2.620	3
4210	0.303	0.155	0.467	9.035	3	2.664	3
4247	0.230	0.137	0.533	5.222	2	2.705	4
4248	0.133	0.210	0.851	10.347	3	2.803	2
4259	0.223	0.151	0.632	8.925	2	2.699	3
4260	0.240	0.153	0.516	9.076	3	2.681	4
4274	0.355	0.158	0.402	8.715	3	2.607	3
4288	0.308	0.140	0.449	9.846	3	2.620	2
4289	0.253	0.166	0.500	8.934	3	2.632	3
4291	0.279	0.138	0.511	8.955	2	2.672	3
4327	0.077	0.188	1.059	9.506	3	2.842	4
4329	0.065	0.212	1.038	10.120	3	2.870	3
4336	0.183	0.189	0.806	6.466	2	2.750	3
4339	0.286	0.149	0.474	9.800	3	2.656	3
4375	0.290	0.150	0.527	7.261	3	2.653	3
4397	0.349	0.139	0.292	9.005	3	2.591	3
4399	0.158	0.195	0.806	9.646	3	2.774	3
4414	0.188	0.168	0.703	9.063	3	2.734	4
4417	0.310	0.180	0.423	9.861	3	2.622	2
4426	0.325	0.158	0.469	9.477	1	2.629	3
4455	0.300	0.151	0.431	8.958	3	2.641	3
4470	0.262	0.156	0.541	9.305	3	2.665	3
4485	0.051	0.179	0.952	10.516	3	2.855	2
4507	0.121	0.219	0.907	7.496	3	2.819	3
4530	0.331	0.166	0.405	9.055	3	2.625	3
4586	0.237	0.158	0.616	9.183	3	2.686	3
4596	0.296	0.152	0.539	9.117	3	2.644	3
4622	-0.031	0.142	0.960	5.562	2	2.842	4
4623	0.196	0.169	0.736	7.572	3	2.722	3
4642	0.356	0.193	0.316	9.252	2	2.605	3
4679	0.309	0.147	0.427	8.666	3	2.649	3
4689	0.255	0.165	0.489	9.424	3	2.642	3
4691	0.224	0.155	0.580	6.765	3	2.697	3
4731A	0.291	0.181	0.437	8.847	4	2.667	2
4731B	0.400	0.200	0.382	10.075	4	2.605	2
4735	0.318	0.151	0.417	8.973	3	2.615	3
4763	0.290	0.133	0.451	8.528	3	2.649	3
4772	0.067	0.165	1.193	6.268	2	2.832	4
4792	0.348	0.178	0.416	9.456	3	2.607	3
4876	0.212	0.226	0.618	9.430	3	2.675	3
4966	0.353	0.145	0.319	9.508	3	2.594	3

Table 3.3.4.

ID no.	(b-y)	m1	c1	V	n	Beta	n
4974	0.219	0.160	0.664	9.404	3	2.721	3
4975	0.367	0.164	0.355	7.133	3	2.617	3
4983	0.333	0.166	0.253	9.175	2	2.620	3
4999	0.257	0.158	0.516	9.023	3	2.677	3
5024	0.219	0.162	0.700	9.214	2	2.694	3
5057	0.305	0.152	0.452	7.621	3	2.655	3
5060	0.325	0.175	0.366	9.407	3	2.639	3
5081	0.012	0.140	1.109	8.629	3	2.866	3
5132	0.133	0.220	0.740	7.615	3	2.760	2
5134	0.359	0.172	0.302	9.092	3	2.614	3
5145	0.285	0.147	0.517	9.296	3	2.651	3
5156	0.288	0.143	0.522	6.437	3	2.655	4
5173	0.227	0.162	0.619	8.336	3	2.715	3
5204	0.318	0.174	0.414	9.666	3	2.633	3
5205	0.227	0.164	0.648	8.583	3	2.705	3
5228	0.280	0.156	0.471	8.979	3	2.657	3
5250	0.270	0.149	0.609	8.810	1	2.642	2
5251	0.271	0.159	0.500	8.962	2	2.645	3
5265	0.268	0.144	0.501	8.543	3	2.678	3
5270	0.335	0.160	0.455	10.059	1	2.627	2
5271	0.250	0.164	0.710	8.051	3	2.694	3
5288	0.301	0.123	0.464	9.304	3	2.650	3
5321	0.274	0.145	0.515	8.442	3	2.667	3
5339	0.342	0.172	0.453	8.282	3	2.643	3
5423	0.259	0.193	0.488	9.949	1	2.838	2
5444	0.335	0.153	0.359	8.176	3	2.615	3
5454	0.281	0.164	0.488	9.759	1	2.645	2
5466	0.303	0.148	0.456	8.958	3	2.640	3
5487	0.049	0.172	1.103	8.054	3	2.898	3
5496	-0.033	0.123	0.922	10.573	1	2.811	2
5497	0.102	0.213	0.842	9.049	3	2.836	4
5508	0.354	0.135	0.331	8.879	3	2.593	3
5524	0.056	0.189	1.043	7.199	3	2.897	3
5531	0.318	0.156	0.417	8.753	3	2.624	3
5546	0.122	0.177	0.974	10.226	1	2.811	2
5590	0.258	0.165	0.513	9.186	3	2.697	3
5617	0.042	0.168	1.037	6.916	3	2.893	3
5618	0.070	0.198	1.095	8.869	3	2.860	3
5630	0.202	0.200	0.704	9.991	1	2.732	2
5643	0.255	0.085	0.632	7.741	3	2.675	3
5669	0.286	0.166	0.491	8.870	3	2.664	3
5698	0.309	0.142	0.422	9.335	3	2.635	4
5737	-0.060	0.111	0.451	4.302	2	2.658	3
5745	0.323	0.145	0.456	9.051	3	2.632	3
5768	0.290	0.174	0.613	9.947	1	2.655	2
5769	0.106	0.206	0.909	9.307	3	2.868	3
5815	0.288	0.149	0.521	9.384	4	2.635	3
5816	0.166	0.199	0.818	9.303	3	2.755	3
5824	0.189	0.159	0.716	9.637	1	2.729	3
5836	0.331	0.163	0.500	9.518	3	2.638	3
5868	0.326	0.125	0.413	8.520	3	2.634	3
5865	0.438	0.191	0.363	9.742	1	2.582	2
5866	0.321	0.175	0.479	9.039	3	2.649	4
5910	0.261	0.151	0.479	8.350	3	2.668	4
5912	0.333	0.153	0.396	9.507	4	2.625	4
5921	0.295	0.155	0.507	9.043	3	2.662	3
5922	0.382	0.195	0.323	10.029	1	2.591	2
5932	0.227	0.156	0.658	7.871	3	2.710	3
5961	0.272	0.163	0.452	8.818	3	2.661	3
6002	0.239	0.143	0.682	9.940	1	2.698	2

Table 3.3.4.

ID no.	(b-y)	m1	c1	V	n	Beta	n
6056	0.251	0.152	0.502	9.010	4	2.672	3
6068	0.292	0.143	0.492	9.065	2	2.636	3
6069	0.200	0.173	0.535	8.912	4	2.720	3
6088	0.213	0.165	0.630	9.750	3	2.703	3
6139	0.322	0.163	0.444	8.003	3	2.625	3
6140	0.210	0.131	0.622	8.441	3	2.709	3
6170	0.041	0.107	1.009	5.494	2	2.896	3
6196	0.313	0.152	0.365	10.066	3	2.624	2
6219	0.329	0.149	0.449	9.132	4	2.618	3
6234	0.358	0.170	0.299	8.518	3	2.605	3
6244	0.203	0.134	0.433	8.600	3	2.651	3
6270	0.257	0.169	0.495	9.565	3	2.668	2
6292	0.429	0.183	0.518	10.150	1	2.577	2
6307	0.309	0.155	0.424	8.765	3	2.632	3
6322	-0.044	0.160	0.971	9.228	3	2.822	4
6339	0.316	0.175	0.511	9.871	3	2.651	2
6340	0.041	0.212	1.004	8.966	3	2.910	3
6352	0.144	0.192	0.637	10.529	3	2.811	2
6353	0.302	0.163	0.460	8.943	4	2.649	3
6354	0.076	0.206	1.021	7.026	3	2.852	3
6363	0.232	0.163	0.602	9.962	4	2.697	3
6364	0.172	0.203	0.734	9.622	3	2.769	3
6365	0.150	0.164	0.622	9.805	4	2.789	3
6366	0.332	0.166	0.457	9.311	3	2.639	3
6367	0.292	0.144	0.477	[illegible].278	3	2.664	3
6390	0.318	0.172	0.524	8.753	4	2.655	3
6402	0.333	0.140	0.434	8.230	3	2.639	3
6411	0.319	0.168	0.307	9.384	4	2.621	3
6412	0.305	0.148	0.536	7.479	3	2.636	3
6427	0.305	0.200	0.389	10.440	3	2.623	2
6451	0.116	0.257	0.885	8.563	3	2.843	3
6492	0.165	0.186	0.855	9.175	4	2.751	3
6493	0.264	0.146	0.486	7.172	3	2.670	3
6491	0.239	0.160	0.639	8.115	3	2.716	3
6504	0.314	0.163	0.449	8.277	3	2.655	4
6515	0.223	0.167	0.583	8.494	3	2.713	3
6516	0.236	0.142	0.527	9.219	4	2.696	2
6531	0.292	0.164	0.451	8.981	4	2.655	3
6532	0.080	0.233	0.851	8.427	3	2.884	3
6533	0.337	0.156	0.338	9.305	3	2.619	3
6547	0.172	0.201	0.719	9.060	4	2.763	3
6548	0.296	0.151	0.459	9.792	3	2.644	3
6594	0.374	0.179	0.406	8.111	3	2.617	3
6593	0.303	0.166	0.449	9.311	4	2.658	3
6619	0.056	0.238	1.013	6.605	2	2.880	3
6640	0.323	0.160	0.514	8.189	4	2.636	3
6653	0.339	0.182	0.347	10.016	3	2.609	2
6668	0.130	0.201	0.826	6.348	3	2.826	3
6670	0.213	0.150	0.652	9.375	2	2.718	3
6723	0.178	0.171	0.746	9.081	2	2.737	3
6724	0.253	0.145	0.619	9.303	2	2.683	3
6740	0.310	0.170	0.419	9.962	3	2.633	3
6790	0.350	0.204	0.340	9.353	3	2.602	3
6807	0.294	0.133	0.462	9.864	1	2.645	2
6806	0.351	0.161	0.366	8.206	3	2.606	3
6855	0.231	0.164	0.572	9.436	2	2.692	3
6868	0.313	0.154	0.431	8.186	3	2.640	3
6894	0.586	0.396	0.383	10.399	4	2.543	2
6958	0.050	0.219	0.933	8.407	3	2.884	3
6993	0.281	0.153	0.471	9.911	2	2.657	3

Table 3.3.4.

HD no.	(b-y)	m1	c1	V	n	beta	n
7037	0.345	0.169	0.430	9.616	2	2.627	2
7038	0.252	0.179	0.505	9.503	2	2.630	3
7058	0.340	0.166	0.437	10.171	3	2.625	3
7059	0.268	0.149	0.539	8.671	3	2.663	3
7079	0.205	0.157	0.599	10.212	3	2.665	3
7092	0.415	0.211	0.319	10.446	3	2.582	2
7135	0.263	0.153	0.540	9.708	2	2.602	3
7184	0.111	0.228	0.854	9.868	4	2.830	3
7209	0.271	0.153	0.462	9.672	2	2.678	3
7257	0.303	0.147	0.404	7.628	3	2.642	3
7259	0.305	0.155	0.512	6.508	2	2.660	3
7269	0.305	0.158	0.439	9.078	2	2.652	3
7281	0.310	0.157	0.454	9.567	3	2.628	3
7312	0.166	0.195	0.816	5.942	2	2.764	3
7323	0.066	0.163	1.055	7.802	3	2.859	2
7362	0.269	0.174	0.454	7.248	4	2.678	3
7399	0.299	0.167	0.428	8.847	2	2.644	3
7400	0.209	0.175	0.711	9.734	2	2.734	3
7413	0.310	0.176	0.471	9.513	2	2.655	3
7468	0.300	0.144	0.445	8.216	3	2.650	3
7487	0.327	0.183	0.141	8.788	2	2.630	3
7496	0.143	0.204	0.788	8.524	4	2.811	3
7553	0.199	0.171	0.658	9.568	2	2.711	3
7594	0.362	0.188	0.362	8.488	2	2.602	3
7606	0.266	0.175	0.390	8.692	3	2.659	3
7607	0.370	0.136	0.392	9.641	1	2.605	2
7629	0.184	0.179	0.755	7.127	3	2.742	4
7631	0.323	0.176	0.430	9.810	3	2.638	2
7642	0.286	0.148	0.453	8.864	2	2.652	3
7643	0.270	0.157	0.598	8.254	3	2.680	3
7676	0.085	0.280	0.715	8.375	3	2.830	3
7704	0.335	0.165	0.444	8.920	2	2.630	3
7729	0.344	0.144	0.388	8.759	3	2.625	3
7739	0.270	0.161	0.501	8.877	3	2.651	2
7751	0.250	0.153	0.580	8.291	4	2.688	3
7786	0.310	0.178	0.417	8.742	2	2.648	2
7817	0.343	0.160	0.342	8.186	3	2.617	3
7826	0.192	0.208	0.677	9.741	2	2.736	2
7827	0.289	0.145	0.496	10.023	2	2.660	2
7867	0.296	0.146	0.423	8.628	3	2.648	3
7875	0.165	0.239	0.832	9.712	4	2.739	3
7876	0.085	0.211	0.992	10.047	3	2.852	3
7898	0.158	0.182	0.821	7.729	3	2.762	3
7908	0.196	0.136	0.660	7.286	3	2.729	4
7932	0.297	0.177	0.390	9.894	3	2.635	3
7951	0.387	0.198	0.346	9.812	2	2.599	2
7954	0.203	0.189	0.777	8.734	3	2.738	3
7971	0.269	0.168	0.471	9.103	2	2.669	3
8033	0.179	0.205	0.645	9.188	4	2.733	3
8040	0.303	0.154	0.418	7.834	3	2.657	3
8072	0.355	0.184	0.402	9.285	2	2.619	3
8076	0.385	0.198	0.333	7.643	3	2.608	3
8104	0.333	0.161	0.446	9.452	2	2.623	3
8130	0.027	0.156	1.031	7.437	3	2.877	3
8145	0.192	0.196	0.779	8.438	3	2.750	3
8164	0.288	0.171	0.424	9.173	2	2.644	2
8279	0.299	0.160	0.413	9.512	2	2.638	3
8282	0.307	0.148	0.369	9.030	2	2.636	3
8304	0.342	0.157	0.408	9.768	1	2.616	4

Table 3.3.4.

HD no.	(b-y)	m1	c1	V	n	beta	n
8330	0.302	0.155	0.492	8.342	2	2.656	4
8351	0.141	0.203	0.907	6.701	3	2.762	4
8360	0.233	0.273	0.567	8.068	3	2.731	3
8400	0.291	0.157	0.459	8.291	3	2.664	3
8415	0.275	0.186	0.215	8.857	2	2.655	3
8430	0.320	0.166	0.437	9.411	1	2.640	3
8431	0.262	0.128	0.551	9.832	1	2.680	4
8471	0.315	0.170	0.421	9.446	1	2.640	3
8487	0.138	0.209	0.615	8.644	3	2.820	3
8603	0.077	0.200	0.995	8.600	3	2.866	3
8604	0.277	0.154	0.510	8.777	3	2.656	3
8616	0.273	0.146	0.468	9.261	1	2.653	3
8715	0.303	0.144	0.451	8.081	3	2.643	2
8716	0.132	0.197	0.929	8.919	3	2.790	3
8743	0.097	0.192	0.950	8.860	3	2.852	3
8795	0.278	0.156	0.529	9.742	1	2.652	3
8806	0.302	0.144	0.383	8.843	2	2.641	2
8866	0.059	0.223	1.013	8.919	3	2.875	3
8868	0.216	0.150	0.669	9.772	1	2.716	4
8895	0.266	0.151	0.533	8.892	3	2.656	3
8899	0.264	0.153	0.479	9.592	2	2.654	3
8924	0.178	0.176	0.765	10.014	2	2.757	3
8932	0.035	0.228	0.960	9.104	3	2.906	3
8933	0.278	0.171	0.519	8.531	3	2.692	3
8970	0.215	0.259	0.701	8.549	3	2.730	3
8983	0.073	0.231	0.961	8.703	3	2.869	3
8985	0.352	0.153	0.407	7.720	3	2.642	3
9019	0.277	0.152	0.535	8.752	1	2.660	3
9026	0.210	0.188	0.735	8.100	4	2.743	3
9027	0.063	0.212	0.967	9.354	3	2.877	3
9061	0.291	0.144	0.519	6.647	3	2.652	3
9063	0.133	0.194	0.869	7.030	3	2.800	3
9065	0.192	0.161	0.775	6.583	3	2.714	3
9084	0.355	0.169	0.358	8.844	3	2.626	3
9113	0.348	0.205	0.460	9.193	1	2.653	3
9131	0.303	0.162	0.374	9.154	1	2.639	3
9132	0.004	0.810	-0.208	5.124	4	2.889	3
9133	0.133	0.192	0.894	8.904	4	2.810	3
9134	0.315	0.178	0.353	9.052	2	2.634	3
9159	0.275	0.159	0.571	8.292	5	2.670	3
9205	0.232	0.160	0.605	9.319	2	2.698	3
9206	0.242	0.168	0.644	8.732	3	2.694	3
9245	0.369	0.188	0.403	9.153	2	2.606	3
9291	0.259	0.163	0.464	9.529	2	2.682	3
9292	0.214	0.162	0.691	8.032	3	2.713	3
9301	0.271	0.156	0.474	9.022	2	2.670	3
9310	0.306	0.157	0.458	9.333	2	2.638	3
9316	0.259	0.153	0.487	9.223	2	2.670	3
9317	0.289	0.155	0.467	8.465	3	2.645	3
9336	0.139	0.212	0.816	6.835	3	2.812	3
9400	0.093	0.177	1.014	9.409	3	2.821	3
9401	0.196	0.182	0.724	8.480	3	2.731	3
9411	0.166	0.195	0.759	7.243	3	2.761	3
9413	0.350	0.192	0.335	8.890	2	2.614	3
9422	0.299	0.178	0.435	9.840	2	2.639	3
9436	0.330	0.180	0.480	9.128	2	2.636	3
9451A	0.097	0.218	0.881	7.990	1	2.835	2
9451B	0.277	0.131	0.241	8.998	1	2.593	1
9475	0.195	0.218	0.748	8.715	2	2.729	3
9487	0.148	0.220	0.821	8.650	3	2.806	3

Table 3.3.4.

HD no.	(b-y)	m1	c1	V	n	beta	n
9515	0.340	0.189	0.409	9.668	2	2.626	2
9553	0.167	0.185	0.784	9.197	3	2.760	3
9577	0.299	0.156	0.426	8.263	3	2.650	3
9607	0.345	0.167	0.406	8.013	3	2.636	3
9651	0.267	0.142	0.632	9.723	1	2.666	2
9673	0.136	0.176	0.919	7.665	3	2.812	3
9693	0.268	0.154	0.470	9.558	2	2.674	2
9769	0.326	0.164	0.399	8.496	2	2.624	3
9793	0.364	0.128	0.372	9.713	1	2.594	3
9857	0.207	0.163	0.628	9.725	3	2.715	3
9906	0.209	0.181	0.696	5.666	2	2.731	4
9918SE	0.069	0.251	0.642	9.605	1	2.809	2
10001	0.296	0.151	0.537	8.232	3	2.647	4
10136	0.319	0.160	0.493	9.951	3	2.625	2
10140	0.210	0.170	0.813	5.567	2	2.719	3
10161	-0.033	0.119	0.867	6.667	2	2.779	3
10177	0.357	0.172	0.366	8.940	3	2.625	3
10176	0.306	0.191	0.415	8.964	3	2.628	3
10166	0.173	0.196	0.702	7.620	3	2.769	3
10209	0.196	0.185	0.719	7.427	3	2.726	3
10255	0.268	0.161	0.495	10.206	3	2.655	3
10412	0.230	0.166	0.638	8.410	3	2.706	3
10433	0.066	0.207	1.109	5.236	3	2.863	3
10510	0.266	0.169	0.603	7.715	3	2.667	3
10536	-0.013	0.170	1.046	5.669	2	2.877	5
10640	0.193	0.202	0.735	10.341	3	2.720	3
10691	0.104	0.181	1.011	6.625	4	2.862	4
11231	0.291	0.179	0.490	8.556	3	2.667	3
11369	0.291	0.155	0.523	8.973	2	2.646	1
11396	0.186	0.184	0.710	8.772	1	2.719	1
11573	0.122	0.207	0.850	8.022	3	2.813	3
11597	0.294	0.161	0.415	8.147	3	2.652	3
11808	0.086	0.242	0.867	8.525	3	2.863	3

Table 3.4.1.

Standard Stars for uvby Photometry at NGP

star	V	(b-y)	m_1	c_1	n
BD+25 2409	9.80	0.148	0.227	0.766	
BD+32 2188	10.76	0.014	0.065	0.924	3
BD+33 2171	10.61	0.201	0.110	0.691	4
BD+25 2478	10.65	-0.007	0.148	1.060	2
HD 107131	6.46	0.096	0.191	0.955	4
HD 107214	9.02	0.364	0.192	0.292	
BD+38 2330	10.90	0.329	0.183	0.306	
HD 108101	9.13	0.147	0.214	0.835	2
HD 108908	8.52	0.232	0.156	0.699	5
HD 109691	8.89	-0.002	0.139	1.045	3
HD 109762	8.59	0.166	0.227	0.784	4
BD+25 2534	10.53	-0.147	0.109	-0.159	2
HD 110166	8.76	-0.038	0.100	0.686	2
HD 110688	9.19	0.357	0.157	0.426	6
HD 110854	8.25	0.006	0.146	0.936	3
HD 112152	9.07	0.129	0.197	0.882	2
HD 112431	8.93	0.130	0.224	0.835	
HD 112487	9.66	0.076	0.173	1.061	
HD 115403	7.57	0.181	0.165	0.744	3
BD+25 2672	10.26	0.213	0.168	0.572	3
HD 120830	9.30	0.141	0.223	0.820	

NB: 'n' refers to no. of observations by Hill et al (1976)

Table 3.4.2.

uvby Photometry of NGP Stars

Star	V	(b-y)	m_1	c_1	n
LB 11274	13.57 ±0.08	0.312 ±0.050	0.115 ±0.066	0.483 ±0.243	4
LB 11302	13.80 ±0.10	0.134 ±0.070	0.021 ±0.090	1.183 ±0.028	3
TON 117	14.38 ±0.07	-0.018 ±0.100	0.103 ±0.099	1.343 ±0.460	3
LB 11355	14.28 ±0.08	0.475 ±0.077	-0.001 ±0.123	0.518 ±0.190	3
LB 11357	13.51 ±0.08	0.335 ±0.105	0.128 ±0.152	0.396 ±0.121	3
LB 11360	14.64 ±0.06	0.180 ±0.171	0.318 ±0.255	0.438 ±0.409	2
LB 11370	14.18 ±0.05	0.267 ±0.063	0.638 ±0.094	0.530 ±0.152	4
LB 11373	15.67 ±0.14	0.002 ±0.276	0.645 ±1.065	-0.973 ±1.723	2
LB 11374	13.63 ±0.03	0.052 ±0.045	0.154 ±0.077	1.116 ±0.213	4
TON 666	14.27 ±0.51	0.084 ±0.091	0.143 ±0.171	1.091 ±0.395	3
LB 11395	13.62 ±0.04	0.293 ±0.018	0.085 ±0.054	0.344 ±0.056	4
LB 11406	12.80 ±0.04	0.357 ±0.058	0.108 ±0.073	0.396 ±0.160	4
LB 11414	12.46 ±0.05	0.327 ±0.020	0.111 ±0.065	0.364 ±0.091	3
LB 11432	14.08 ±0.12	0.323 ±0.110	0.089 ±0.100	0.254 ±0.270	4
LB 11433	14.35 ----	0.519 -----	-0.030 -----	0.419 -----	1

Figure 3.4.1.

S/N "Chiran" 20/21 April 1982

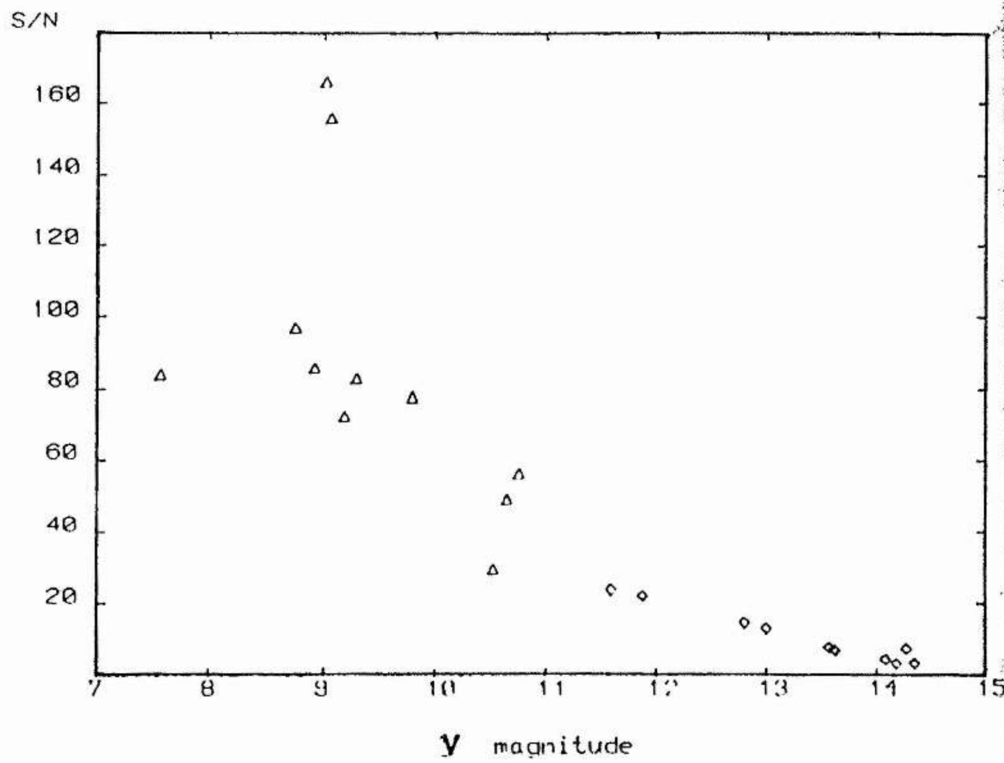

Diamonds represent programme stars. Triangles represent standard stars.

Chapter 4

South Galactic Pole Radial Velocities

'..the craft so long to learn'

Hippocrates

4: South Galactic Pole Radial Velocities

4.1 The Measurement of Stellar Radial Velocities

4.1.1 Introduction

Stellar radial velocity measurement has its basis in the well-known Doppler-Fizeau effect and the fundamental principles will not be discussed here. All radial velocities in this work have been measured using the D.A.O. REDUCE (Hill et al 1982c) and VCROSS (Hill 1982b) packages. These are fully described in the above mentioned works and only a brief outline of the relevant features will be given here. Both packages are written in FORTRAN and are designed for use on a VAX 11/780 computer such as that at St.Andrews.

4.1.2 REDUCE

REDUCE is designed to process microdensitometer scans of photographic spectra or spectrometric data from an IPCS or RETICON system stored on VAX disk in FITS format. FITS format is described by Wells et al (1981) and Greisen and Harten (1981) but is basically a standardised format for digital arrays held on magnetic tape for use in the transfer of such arrays between institutions with different data handling facilities. The package reduces these files to linearised stellar wavelength files which may if required be converted to intensity files and then continuum rectified. From these processed files the package can extract radial velocities, line positions, equivalent widths and rotational velocities using the subroutines VELMEAS (Hill, et al 1982a) and VLINE (Hill et al 1982b).

Within REDUCE the user is presented with a series of options (see REDUCE Manual) which are executed in the chosen sequence. This sequence of operations may be repeated indefinately on different data, and can be interrupted at any point to allow the user to change the sequence. Limitations on the possible sequences are described in the User Manual (Hill 1982c).

An important aspect of REDUCE is its file naming convention, more fully described in the Manual. The input FITS files have names of the form Snnnn.FTS (for the stellar spectrum) and Fnnnn.FTS (for the file containing the corresponding arc spectra), where nnnn is a number which identifies the particular observation. Once the arc spectra have been measured the resultant wavelength calibration is stored in a corresponding Snnnn.ARC file. If the stellar spectrum is noise-filtered details of the filter are stored in Snnnn.FLT with the filtered spectrum being Vnnnn.FTS.

The linearised stellar spectrum is stored in the file Wnnnn.FTS with the continuum rectified spectrum being Rnnnn.FTS.

In this work REDUCE has been used for two purposes:

- to measure stellar radial velocities using the VELMEAS subroutine
- to produce filtered, linearised and rectified stellar spectra for use with the cross-correlation package VCROSS

The features of REDUCE relevant to each application will be described seperately.

i) VELMEAS works from a standard plate of [X(mm).vs.λ(A)] (as described by Aitken, 1935), used to predict the positions of the comparison and stellar lines based on the known spectrograph constants (the package can handle the parameters of the grating equation, Hartmann constants or polynomial coefficients, whichever is appropriate to the spectrograph used). The actual line positions are then measured by fitting a parabola to the central region of each line profile. This simple parabolic fit is used for speed, rather than a slower more refined profile such as a gaussian. For saturated arc spectra a centroid is adopted. VELMEAS requires the position within the scan of a known reference wavelength near the centre of the scan. Using this line position and the standard plate the program predicts the position, in turn, of each new line in a predefined list. After each new measurement the predictor is updated and thus improved. Once the user is confident that the predictor is reliable (generally after 3-4 lines) VELMEAS may be switched to an automatic mode in which the remaining lines are located and measured without user interaction. When measuring stellar lines it is generally advisable to measure all lines in manual mode in order to ensure correct identification of the line and the line centre. This is especially true of lower dispersion spectra, such as those in this work, where lines lie close together in the scan and may appear blended.

An arc or stellar measurement consists of two cursor placements, the first on the line centre and the other on the wing. A parabola (with the above noted exception) is then fitted through all data in the window (2x¶centre-wing¶). It is possible to select only sections of a profile marred by eg. a plate scratch or another line.

Once the arc spectrum has been measured with reference to the standard plate and these measures checked, a polynomial is fitted through the data and correction values applied to the standard stellar positions. The heliocentric radial velocity correction is taken into account at this stage. Radial velocities are then derived from a comparison between the measured positions and the corrected rest positions of the stellar lines in a pre-defined list appropriate to the spectrograph dispersion and the spectral type of the star in question.

ii) In preparing spectra for the cross-correlation package VCROSS the wavelength calibration (including heliocentric velocity correction) is obtained using the VELMEAS subroutine as described above. The stellar spectrum is then noise-filtered, linearised and rectified as follows-

The observed stellar spectrum can be represented by $D(\lambda)$ where

$$D(\lambda) = F(\lambda) + N(\lambda) \quad , \lambda \text{ is wavelength}$$

Here $F(\lambda)$ is the true signal and $N(\lambda)$ is the random noise contaminating this signal. The Fourier transform of this specrum is

$$d(k) = f(k) + n(k) \text{ , k is frequency in the Fourier domain}$$

Here f(k) and N(k) are the transforms of F(λ) and N(λ). It can be shown (Gray 1976) that the higher frequency components of d(k) are mainly due to the noise signal and contain virtually no real data. By applying a filter, $\phi(k)$, it is possible to remove the high frequency noise component and thus recover the true signal.

The filtered, reconstructed data transform is defined to be

$$g(k) = [f(k) + n(k)].\phi(k)$$

The difference between f(k) and g(k) gives the error introduced by the filtering process. The optimum filter is defined such that the square of this error is minimised and can be shown to be (Brault and White 1971)

$$\phi(k) = \frac{1}{1 + [n(k)/f(k)]^2}$$

Note that the optimum filter depends on both the noise and the noise free signal, ie. the signal being measured and the noise which interferes with that measurement. However this is an optimum filter and small deviations from the true filter shape should only produce second order errors. Therefore it is usually sufficient to replace the actual complicated signal and noise power spectra by smooth, simple models involving only a few parameters. Let $f'(k\ a1, a2, \ldots)$ be a model of the signal power spectrum with parameters a1,a2,.... and $n'(k, b1, b2, \ldots)$ be a model of the noise power spectrum with parameters b1,b2,... , then these parameters may be adjusted until

$$d'(k) = f'(k) + n'(k)$$

is a good approximation to d(k), and then the filter is taken to be

$$\phi'(k) = \frac{1}{1 + [n'(k)/f'(k)]^2}$$

The choice of models for the power spectra depends on the type of data involved. In general the noise may be regarded as random and not correlated with the signal ("white noise") in which case

$$n'(k) = B \quad \text{, a constant}$$

Here B is the average of the observed noise power spectrum and may be determined from the noise dominated high frequency end of the observed signal power spectrum, d(k). The frequency beyond which d(k) is noise dominated is known as the "cut-off" frequency. Frequently (as with REDUCE) a gaussian model is chosen for the noise power spectrum, for example,

$$d'(k) = A.10^{-\alpha_0^2 k^2}$$

Here A is the amplitude and α_0 is a fitting parameter chosen such that d' (k) = 0.5 at the cut-off frequency. Combining these gives the filter:

$$\phi'(k) = \frac{1}{1 + \frac{B^2}{A}.10^{-2\alpha_0^2 k^2}}$$

where the parameters B, A and α_0 can be found from the power spectrum of the observed signal.

Within REDUCE a filter of the above kind is generated from the observed power spectrum. The power spectrum is displayed and the cursor used to define the cut-off frequency for the filter. This filter is defined in frequency space and the inverse transform of the selected box function tapered by an appropriate window function, a gaussian normally being adequate for photographic spectra. The filter thus defined is stored in real, as opposed to frequency, space in an Snnnn.FTS file. The actual filtering is performed in frequency space. The Fourier transforms of the spectrum (tapered at both ends by a cosine bell) and the filter are calculated and the inverse transform of their product is the filtered spectrum.

If spectra are to be compared by cross-correlation they must first be linearised (essentially, put on a common scale). This is also necessary if the spectra are to be added, subtracted, divided or multiplied in any way. Linearisation within REDUCE produces spectra on a linearised ln λ scale independent of the Earth's orbital velocity, stored as a Wnnnn.FTS file. Upper and lower wavelength limits are chosen for the linearisation, the rest of the spectrum being discarded. REDUCE recommends an optimum wavelength increment based on the sampling interval and spectrograph dispersion. The wavelength range and increment chosen must be consistent for all spectra which are to be compared using cross-correlation techniques, otherwise they will be incompatible.

The contribution of the wavelength dependent continuum to the shape of the stellar spectrum is removed by defining a background continuum for the spectrum, and normalising to it. Within REDUCE the spectrum is plotted and the cursor used to define the wavelengths and increments over which the continuum is measured and averaged. The rectification is completed by an interpolation between the average continua in these regions using the subroutine INTEP (Hill 1982a) which fits a smooth curve through these data. In averaging the continuum over each wavelength increment the user may define which of the data points in that segment are used in the calculation of this average. Generally the highest 66% of the data points are used, this percentage being controlled by a user defined variable. REDUCE stores the rectified, linearised, filtered stellar spectra in Rnnnn.FTS files. It is these files which are used by the cross-correlation package VCROSS.

4.1.3 VCROSS

The package VCROSS is designed to measure the radial velocity of a programme spectrum relative to that of a comparison spectrum by cross-correlating the two. The package uses the rectified, linearised files produced by REDUCE, as described above.

The determination of radial velocities by cross-correlation techniques has beeen discussed by Simkin (1974) and the method has been used extensively in recent years. It has the advantage that the entire recorded spectrum is used to measure the velocity thus overcoming some of the problems encountered with the line profile fitting method (as used by VELMEAS) in which a limited subset of the data is used.

In order to determine an object's radial velocity from its spectrum, the spectrum must, at least loosely, satisfy the following requirements:

i) The star must have a well defined spectral type.

ii) It must be possible to generate this spectrum from a known 'comparison' spectrum of the same mean spectral type by Doppler shifting the 'comparison' spectrum.

From this the principle of velocity determination by cross-correlation is easily deduced. By taking two stars of similar spectral type and Doppler shifting the spectrum of one relative to the other, their relative velocity may be found. If one of the stars has a known radial velocity, that of the other is thus determined. Consider the Doppler formula:

$$\Delta\lambda = (\lambda_1 - \lambda_0)/\lambda_0 = v/c$$

where λ_1 is the observed wavelength

λ_0 is the rest wavelength

v is the stellar radial velocity

c is the speed of light.

Then, taking logarithms,

$$\Delta \ln\lambda = \ln(1 + v/c) = z \text{ , the Doppler shift.}$$

The Doppler shift is thus a function of velocity only.

Let the programme spectrum be D(x) and the comparison be T(x), where $x=\ln\lambda$, then the cross-correlation function (ccf.) between these is,

$$C(z) = a\int_{-\infty}^{\infty} T(x)D(x-z)dx$$

Here a is a scaling factor dependent on T(x) and D(x). This cross-correlation function will have a maximum value when the comparison spectrum T(x) has been shifted by an amount z such that it coincides with the observed spectrum D(x).

For observational data these continuous functions become N discrete points sampled at equal intervals x and the ccf. is expressed as

$$C(z) = \sum T(x).D(x-z)/[N\sigma_t.\sigma_d]$$

$$\text{where } \sigma_t = \frac{\sum T^2(x)}{N}\ ,\ \sigma_d = \frac{\sum D^2(x)}{N}$$

The ccf. is usually calculated by using Fast Fourier Transforms. Let d(k) and t(k) be the discrete Fourier transforms of the spectra such that

$$d(k) = \sum D(x).\exp[-2i\pi kx/N]$$

$$t(k) = \sum T(x).\exp[-2i\pi kx/N]$$

then the Fourier transform of C(z) is

$$c(k) = \frac{d(k).t^{*}(k)}{N\sigma_t \sigma_d}$$

where $t^{*}(k)$ is the complex conjugate of t(k).

The inverse transform of this is then,

$$C(z) = \frac{1}{N\sigma_t \sigma_d} = \sum d(k).t(-k).\exp[2i\pi kx/N]$$

Thus the procedure is to compute the Fourier transforms of both spectra, take the complex conjugate of the comparison's transform, and the inverse transform of their product is the ccf. The position of the maximum of the ccf. gives the relative shift of the two spectra, from which their relative velocity may be found.

Unfortunately the use of the Fast Fourier Transform introduces some complications as the spectral segments become periodic when expressed in terms of a Fourier series and the last few terms of one spectrum will enter the cross-correlation sum as products with the first few terms of the other. Since the true spectra are not periodic this overlap distorts the maximum in the ccf. and can lead to significant errors in the measurement of the redshift, z, when this exceeds 10-20% of the array length. This overlap distortion is eliminated by setting the mean of each array to zero and then expanding the arrays to twice their length with terms of zero value (Simkin 1974).

To measure radial velocities with VCROSS the user must first define the initial velocity range over which the ccf. is to be displayed, and a number of wavelength intervals defining the spectral regions to be used in calculating the ccf. This latter feature enables parts of the spectrum to be omitted from the comparison, for example the broad, strong hydrogen lines in the spectrum of an early type star which can dominate the ccf. and produce an erroneous velocity measure.

The programme and comparison star spectra are then read in (the end points of the data being tapered by a cosine-bell function), averaged and zeros added to ensure that the ccf. is as 'clean' as possible (Bernat and Piersol 1971). The ccf. is then calculated as described above and displayed on a VDU. The position of the maximum is found by delimiting a region with the cursor through which a parabola is fitted. This gives the relative velocity of the two spectra. From the known velocity of the comparison spectrum, the actual programme spectrum's velocity is found.

4.2 Observations and Reductions

4.2.1 Observational Material

PDS scans of 576 stellar spectrograms were made available by G.Hill of D.A.O. These data were obtained by G.C.L.Aikman in October 1975 using the 0.6m telescope and Mt.Kobau spectrograph at Las Campanas Observatory, giving a dispersion of 82 Å/mm. An iron/argon comparison spectrum was used to provide a wavelength standard for each spectrum. These spectra had been scanned by W.A.Fisher at D.A.O. using a PDS microdensitometer with a step size of 2 μm. The scans were converted to FITS format and stored on magnetic tape for transit. All subsequent reductions were performed with the St.Andrew's University VAX 11/780 computer using the REDUCE and VCROSS reduction packages.

4.2.2 Rest Wavelengths for REDUCE

The rest wavelengths adopted for the stellar lines were those given by Hill et al (1976). These are listed in Table 4.2.1.

4.2.3 Radial Velocity Standards

Observations of thirteen standard stars were interspersed between programme star observations. These velocity standards are listed in Table 4.2.2 along with their accepted velocity, the source of this velocity and any relevant comments. At least one of these stars is a spectroscopic binary with known orbit (HD 27962) and one other shows signs of a velocity variation (HD 204867). Neither of these were actually used as comparison stars in these velocity reductions. The standard star observations were used to check the velocity system of the spectrograph, to check for differences between velocity measures made with REDUCE and VCROSS and as comparison stars for use with VCROSS.

Seven standard star spectra were measured using REDUCE and VCROSS (for VCROSS each spectrum was cross-correlated with those of several other standards of similar spectral type and the mean of these measures adopted). Table 4.2.3. gives the velocities obtained using REDUCE and VCROSS as well as the generally accepted values. REDUCE and VCROSS measures agree well with each other and with the standard velocities, with three exceptions (plates no. 452, 505, 654). Of these 505 and 654 are both spectra of HD 33904, which is a B star and is therefore not expected to give good results with VCROSS. Plate 452 is of HD 693, whose accepted velocity agrees well with the VCROSS velocity,but not with that obtained using REDUCE. Ignoring these three plates, the mean velocity difference and rms scatter, in the sense (REDUCE-VCROSS), are 0.6 ± 4.2 kms^{-1} from four plates.

VCROSS measures of standard stars were used to provide a more rigorous check on the velocity system. Each standard was cross-correlated against 3-4 compatible standard spectra (which had themselves been checked against the original seven comparison spectra of Table 4.2.3) and the mean taken. This confirmed the agreement with the standard system, with the above noted exceptions. Individual velocities for HD 27962 and HD 204867 are given in table 4.2.4.

A number of program stars were also measured with both VCROSS and REDUCE, and velocities for these are compared in Table 4.2.5. From these fourteen spectra the mean difference and rms scatter, in the sense (REDUCE-VCROSS) is 1.0 ± 5.9 kms^{-1}. Three plates (438, 442, 450) show large, uneplained, differences between VCROSS and REDUCE measures. Excluding these the mean difference and rms scatter are -1.7 ± 2.9 kms^{-1} from 11 plates. The agreement between VCROSS and REDUCE measurements is confirmed.

4.2.4 Reductions and Results

On the basis of the above tests velocities were measured using VCROSS for stars of type A0 and later, and REDUCE for the B stars (B stars do not give good results with cross-correlation techniques due to the generally smooth nature of the continuum in their spectra).

In order to measure the velocity of a programme star using VCROSS a spectral type must be assigned to it, as a compatible comparison spectrum is required. For those stars for which uvbyβ photometry was available equivalent MK spectral types were deduced from this (see Chapter 5). For others the MK type was taken from volumes 2 and 3 of the Michigan Spectral Catalogue (Houk and Cowley, 1982), or failing that, the HD classification was used.

Reductions proceeded smoothly with up to 70 spectra being measured in a single seven hour session, due largely to the computational speed of the VAX, the only delay being introduced by the actual plotting of the spectra. Individual velocities are given in Table 4.2.6. Seven spectra (all of different objects) showed apparent emission features, all of which were probably spurious. These spectra are indicated in the Table. All such apparent emission features were removed before cross-correlation.

The final velocities for individual objects are given in Table 4.2.7. The columns give :

i) HD number or other name

ii) Mk type

iii) radial velocity (kms^{-1})

vi) standard error (kms^{-1})

v) number of observations

A number of the stars in the sample are close optical pairs which may not have been resolved spectroscopically. These and the MK types of the two objects are indicated in the relevant table, as are all the objects designated 'odd' on the basis of uvbyβ photometry (chapter 5).

4.2.5 Comparison with Other Works

A number of the stars in the current sample have had velocities determined by Wayman (1961). For the purposes of a comparison between the two data sets the following criteria were used to select a common sample:

i) Only stars whose velocities, in both samples, were based on three or more observations were considered.

ii) Stars designated 'probable' variables in the present work (chapter 5) were excluded.

iii) Stars designated 'possible' variables in the current work (chapter 5) which had been designated 'variable' by Wayman were excluded.

Using these criteria only nine stars were available for the comparison. Of these five had been designated 'possible' variables in the present work. Differences were taken in the sense (this work - Wayman), the mean difference and rms scatter from all nine stars being:

$$\Delta v = 1.5 \pm 5.9 \text{ kms}^{-1}$$

The agreement is poor, given the large rms scatter in the mean. This can be explained in terms of the intrinsic errors in the velocities in this samples. For the nine stars used in the comparison, the average of their standard errors is $\pm 6.6 \text{kms}^{-1}$, with the corresponding value for Wayman's data being $\pm 2.6 \text{kms}^{-1}$. Treating these as mean errors in the velocities used in the comparison the error in the mean difference may be estimated as $\pm 7 \text{kms}^{-1}$, which is sufficient to explain both the systematic difference of 1.6kms^{-1} and the scatter of

$\pm 5.9 kms^{-1}$ found above. Excluding the five 'possible variables, the corresponding mean difference and rms scatter is:

$$\Delta v = -2.1 \pm 5.4 \ kms^{-1}$$

with the average standard error of the remaining four stars being $\pm 3.9 kms^{-1}$. Combining this with the mean standard error in Wayman's data, the error in the difference is estimated to be $\pm 5 kms^{-1}$, again sufficient to explain both the systematic difference and the rms scatter found above. Combining the error estimates with the extremely small sample size, it would be extremely rash to draw any conclusions from these comparisons.

It will be shown later (Chapter 5) that the radial velocity data for South Galactic Pole Stars presented here is consistent with that of Hill et al (1976) for North Galactic Pole stars.

Table 4.2.1.

Adopted Rest Wavelengths for REDUCE
from Hill et al (1976)

A0-F4 Stars		F5-M Stars	
Wavelength(A°)	I.D.	Wavelength(A°)	I.D.
3734.490	H13	3727.570	Fe blend
3750.154	H12	3758.380	Fe blend
3770.632	H11	3763.670	Fe
3797.900	H10	3767.140	Fe
3835.386	H9	3794.890	Fe blend
3872.670	FeI	3820.440	Fe
3889.051	H8	3850.040	Fe blend
3933.684	CaII	3952.680	Fe blend
3956.679	FeI	3968.490	Ca
4005.530	FeI	4005.590	Fe
4030.648	FeI	4045.610	Fe
4045.590	FeI	4063.550	Fe
4063.360	FeI	4071.690	Fe blend
4071.560	FeI	4101.690	H blend
4101.750	H-delta	4143.500	Fe
4132.310	FeI	4187.370	Fe
4215.600	FeI	4226.640	Ca blend
4226.730	FeI	4260.440	Fe blend
4233.312	FeI	4271.630	Fe blend
4250.510	FeI	4340.320	H blend
4271.562	FeI	4383.820	Fe
4340.427	H-gamma	4404.740	Fe blend
4481.241	FeI	4461.670	Fe blend
4549.460	FeII		

Table 4.2.1.

B0-B9 Stars

Wavelength(A°)	I.D.
3933.664	CaII
3964.727	HeI
3970.074	H-epsilon
3994.996	NII
4026.140	blend
4101.738	H-delta
4128.051	SiII
4130.876	SiII
4267.167	CII
4340.468	H-gamma
4387.928	HeI
4471.325	HeI
4481.228	MgII
4861.416	H-beta

Table 4.2.2.

Radial Velocity Standards

Star	Vel. ($km s^{-1}$)	Sp.	source and comments	
HD 693	14.7	F6	1	
HD 22484	27.9	F8	1	
HD 27962	35.0	A2	2	Spectroscopic Binary
HD 33673	24.7	F0	1	
HD 33904	28.0	B9	2	
HD 36079	-13.5	G5	1	
HD 45348	20.5	F0	1	
HD 154417	-17.4	F8	1	
HD 186791	-2.1	K3	1	
HD 204867	6.7	G0	1	Variable?
HD 222368	5.3	F7	1	
HD 222603	12.0	A7	2	

1: Astronomical Almanac
2: Yale Bright Star Catalogue (Hoffleit 1964)

Table 4.2.3.

Comparison of REDUCE and VCROSS Velocities for Standard Stars

Plate No.	Object	Spec.	REDUCE	VCROSS	Accepted
452	HD 693	F6	21.2±2.2	14.1±1.5	14.1
593	HD 27962	A2	36.6±3.5	39.0±7.3	35.0 (1)
444	HD 33673	F0	28.4±1.4	26.1±1.0	24.7
505	HD 33904	B9	28.0±8.5	17.2±3.0	28.0
654	HD 33904	B9	33.4±2.5	24.6±7.5	28.0
460	HD 204867	G0	20.1±2.9	20.3±0.4	6.7 (2)
461	HD 222603	A7	13.7±4.5	11.0±1.0	12.0

Notes:
1) Spectroscopic Binary
2) Suspected Variable

All velocities in kms^{-1}.

Table 4.2.4.

VCROSS Velocities for HD 27962 and HD 204867

HD 27962

Plate No.	J.D.	Velocity ($km s^{-1}$)
522	42717.867	40.1±3.2
545	42718.868	16.7±2.0
593	42721.867	33.8±5.9

HD 204867

Plate No.	J.D.	Velocity ($km s^{-1}$)
460	42715.498	20.3±0.4
507	42717.498	4.4±1.8
594	42722.498	10.8±1.7

Table 4.2.5.

Comparison of REDUCE and VCROSS Velocities
from Programme Stars

Plate No.	Object	Spec.	REDUCE ($km s^{-1}$)	VCROSS
449	HD 739	F5	-12.5±2.7	-12.0±0.4
455B	HD 1101	F3	-10.6±2.3	-4.9±0.7
448	HD 1909	B9	18.9±3.4	21.8±6.7
456	HD 2719	F7	-4.5±2.2	-4.0±0.6
450	HD 2724	F0	15.4±5.0	6.7±1.6
457	HD 5487	A2	30.2±4.3	35.6±5.0
458	HD 5932	F1	11.4±1.8	11.5±0.7
439	HD 9411	A8	-13.1±2.5	-9.3±0.6
438	HD 9673	A7	13.1±4.4	-0.4±4.0
459	HD 10186	A8	-6.6±2.6	-2.2±1.9
440	HD 10830	F0	12.7±3.1	9.6±1.0
442	HD 10863	F2	25.3±1.9	14.6±3.1
441	HD 111000	F5	13.7±4.7	15.4±3.2
453	HD 224763	F5	9.9±0.7	6.6±0.1

Table 4.2.6.

HD number	Julian Date	vel(kms^{-1})
141	42699.613	3.8
	42719.625	-7.3
156	42701.551	8.8
	42723.531	15.8
	42730.542	16.3
203	42695.677	8.0
	42699.628	8.0
	42718.606	27.2
235	42711.613	28.3
	42717.741	-11.6
256	42701.562	-12.5
	42723.505	3.8
	42730.552	14.2
268	42695.694	14.0
	42695.704	18.7
	42699.638	15.2
	42728.621	11.3
	42731.563	15.3
319	42699.646	-20.3
	42712.748	21.2
	42718.528	-2.8
	42727.516	-22.3
	42728.631	-17.3
	42731.572	-4.8
	42733.558	-3.8
392	42699.660	1.5
	42719.531	-1.0
	42728.644	-7.8
	42731.583	-4.7
427	42715.764	-23.1
	42721.607	-14.1
493	42699.674	9.5
	42718.617	0.1
	42731.596	8.0
562	42699.688	6.1
	42719.646	3.4
732	42702.678	-13.7
	42719.672	-9.4
	42728.675	-7.6
739	42713.709	-12.2
	42721.623	7.5

Table 4.2.6.

HD number	Julian Date	vel(kms^{-1})
899	42699.707	19.1
	42719.699	17.0
	42708.704	24.8
900	42702.700	20.6
	42719.727	11.3
	42728.735	20.5
955	42716.522	-5.1
	42723.515	-4.9
	42726.550	-10.2
	42730.565	-6.3
	42733.525	-12.0
1000	42699.719	-18.8
	42719.755	-17.8
	42725.539	-10.1
	42731.603	-5.8
1101	42714.756	-5.1
	42720.567	42.4
	42726.570	4.7
1256	42712.755	-5.6
	42718.624	-14.7
	42718.635	11.2
	42722.503	10.6
	42727.522	-11.1
	42731.611	12.0
	42733.564	69.9
1343	42701.571	4.4
	42723.567	-7.5
	42730.575	5.2
1431	42718.643	10.6
	42725.549	27.7
	42727.529	17.9
	42731.617	21.7
	42733.569	40.5
1667	42702.714	10.9
	42718.659	13.2
	42725.557	16.7
	42731.624	5.4
	42733.576	26.6
1683	42710.723	-0.03
	42716.646	7.8
	42724.539	8.9
	42733.654	-5.4

Table 4.2.6.

HD number	Julian Date	vel(kms^{-1})
1856	42716.658	4.1
	42724.556	10.5
	42724.854	17.3
	42725.869	32.5
	42732.612	4.2
1909	42713.695	22.8
	42721.627	-2.6
	42727.807	38.4
	42732.622	16.6
	42733.667	20.4
1980	42701.585	5.3
1999	42717.783	-24.6
	42729.584	-17.1
2026	42702.735	-9.8
	42722.524	-6.6
2037	42702.769	20.4
	42722.564	4.1
	42725.578	14.5
2718	42722.594	32.0
2381	42711.646	22.7
	42721.644	17.6
2394	42701.610	19.2
	42723.580	16.2
	42730.590	23.0
2395	42718.673	11.9
	42722.607	21.1
	42728.762	9.4
	42731.633	2.0
	42733.585	21.4
2477	42722.621	-23.2
	42725.600	-16.7
	42731.646	31.4
2527	42702.808	-19.5
	42722.635	9.3
2630	42701.621	5.1
	42730.602	16.4
2696	42700.693	5.7
	42712.760	22.2
	42731.654	-2.3
2719	42714.779	-2.6
	42720.605	-5.3
	42726.591	-4.9

Table 4.2.6.

HD number	Julian Date	vel(kms^{-1})
2724	42710.734	-5.8
	42713.720	6.6
	42724.567	-6.5
	42732.631	-8.4
2916	42715.529	-7.6
	42722.651	-19.5
	42725.613	-2.1
3085	42710.744	-35.5
	42717.809	3.3
	42724.579	11.6
3244	42715.554	1.4
	42722.678	-4.5
3326	42700.696	10.4
	42718.697	5.7
3580	42700.700	-4.5
	42712.768	13.9
	42725.746	7.7
3581	42702.824	16.3
	42718.709	6.3
	42725.755	4.9
	42731.662	7.2
3622	42715.584	7.5
	42722.707	-1.0
3735	42716.732	-24.8
4065	42713.732	-1.4
	42724.591	20.1E
	42732.714	1.1
	42733.673	-11.8
	42733.693	1.2
4247	42700.704	7.1
	42712.763	16.8
4338	42701.677	4.2
	42701.686	-8.1
	42723.592	12.3
	42726.605	5.3
	42730.609	6.1
4375	42701.696	10.1
	42723.605	16.8

Table 4.2.6.

HD number	Julian Date	vel(kms^{-1})
4507	42715.604	-7.4
	42718.726	-8.6
	42725.773	-11.4
	42731.680	-13.2
4622	42709.708	23.5
	42712.772	15.5
4623	42715.619	0.8
	42718.747	0.8
4691	42700.714	6.8
	42712.778	3.5
	42725.792	-11.9
	42731.693	3.2
4772	42700.720	6.4
	42712.785	-7.8
	42722.721	-8.1
	42728.772	-6.8
	42731.772	-2.9
	42733.591	-1.0
4975	42721.666	13.5
	42724.603	21.3
5057	42715.638	16.7
	42722.740	1.9
5132	42701.715	6.8
5156	42700.727	-12.3
	42711.773	-35.6
	42731.710	-4.8
5487	42714.803	30.5
	42723.629	39.3
5524	42711.787	5.6
	42718.766	9.9
5616	42698.690	15.3
	42701.739	4.5
	42723.655	2.5
5617	42701.726	-4.2
5659S	42698.711	6.1
	42701.760	-4.1
	42723.683	2.2
	42723.714	-5.6
5659N	42698.732	-1.3
5737	42699.724	-24.3
5932	42714.832	14.3
	42723.748	9.1

Table 4.2.6.

HD number	Julian Date	vel(kms^{-1})
6178	42700.733	-30.3
	42724.615	-10.4
	42732.719	-7.1
	42733.679	-23.0
6354	42711.664	-12.1
	42717.830	-8.9
	42721.703	-16.2
	42732.732	-10.5
6367	42711.681	10.6
	42721.687	11.7
	42729.635	22.1
6412	42699.738	-6.1
	42725.630	-1.0
6491	42715.661	0.6
	42725.651	-4.8
6493	42715.783	2.6
	42717.849	2.8
	42724.626	17.6
	42732.752	13.7
6532	42699.767	0.3
	42715.691	-15.6
6619	42700.737	13.7
6668	42715.707	7.2
	42725.668	29.6
	42728.780	-24.8
	42731.718	-15.6
	42733.596	-1.1
6723	42722.785	-2.5
6767	42711.693	12.6
	42717.863	10.2
	42724.636	-0.1
	42732.766	15.3
	42733.683	6.8
7257	42699.799	2.6
	42725.683	9.1
7259	42700.742	12.1
	42724.642	19.5
	42732.775	13.4

Table 4.2.6.

HD number	Julian Date	vel(kms^{-1})
7312	42700.748	27.1
	42724.653	18.7
	42732.788	12.9
	42733.689	14.1
7323	42716.676	9.0
7382	42716.694	4.6
	42724.664	15.4
7495	42698.789	-8.6
	42715.718	-1.0
	42723.779	-1.9
	42726.663	0.7
7629	42711.813	-6.4
	42718.784	-6.5
7676	42716.758	4.0
	42726.632	9.2
7751	42698.813	-5.6
	42726.690	-4.1
7898	42721.724	6.5
7908	42711.840	13.4
	42718.802	17.1
8040	42721.754	21.0
8076	42724.692	-2.9
8130	42700.764	12.9
	42724.716	-12.1
	42732.807	1.3
8350	42698.834	-10.7
	42726.716	-11.1
	42730.739	-0.9
8351	42700.755	-20.0
	42724.728	15.3
	42732.831	16.7
8487	42718.820	-15.3
8895	42699.818	19.1
	42719.821	19.8
	42725.806	12.0
	42731.729	13.5
8957	42698.845	22.3
	42723.804	24.0
	42726.764	16.6
	42730.751	20.8

Table 4.2.6.

HD number	Julian Date	vel(kms^{-1})
8985	42715.863	30.0
	42722.830	28.1
9026	42711.713	22.8
	42721.786	16.9
9061	42698.857	2.8
	42720.755	-4.2
	42726.768	-9.3
	42730.764	16.6
9063	42699.833	7.9
	42718.838	4.4
9065	42700.772	-33.4E
9132	42711.853	9.3
	42725.814	7.3
	42728.851	3.9
	42730.793	-1.4
	42733.776	-46.0
9336	42698.867	-4.4
	42723.823	-3.6
9411	42699.849	-2.3
	42712.824	-11.4
	42722.860	-59.8
	42730.782	-13.5
9451	42716715	25.0
	42725.705	17.3
9672	42698.874	8.3
	42726.776	18.8
	42730.772	20.1
	42733.534	15.7
9673	42712.801	-0.9
	42725.729	-47.2
	42728.803	-51.2
	42731.781	31.8
9895	42710.771	7.3
	42716.780	8.6
	42726.783	16.8
	42733.703	8.6
9906	42700.777	-17.9
	42721.858	14.2

Table 4.2.6.

HD number	Julian Date	vel(kms^{-1})
10148	42711.857	17.0
	42718.853	18.6
	42725.859	16.1
	42731.807	22.0
	42733.779	17.1
10161	42718.861	31.7
	42725.864	23.4E
	42731.817	31.9
10186	42714.859	-5.6
	42723.849	10.3
10209	42699.868	-2.4
	42719.840	-1.8
	42728.834	3.8
	42731.836	12.6
10481	42724.835	19.5
10538	42700.787	-13.3
	42721.863	-34.4
	42724.842	34.7
	42729.807	10.3
	42732.844	-46.4
	42733.709	-39.1
10798	42710.791	-24.9
	42716.792	-11.7
	42729.792	-2.5
10830	42712.835	6.8
	42719.854	14.0
10863	42712.860	8.5
	42733.796	-0.6
11100	42710.864	4.3
	42712.846	1.4
	42719.865	7.3
11137	42700.798	6.4
	42729.656	25.8
11262	42716.805	17.2
	42727.834	25.2
11379	42710.814	3.4
	42716.816	14.1
	42729.675	28.3

Table 4.2.6.

HD number	Julian Date	vel(kms^{-1})
11459	42716.836	-14.5
	42729.693	1.5
	42733.723	-3.2
11481	42710.839	35.7
	42716.861	23.7
11535	42711.749	2.3
	42721.821	3.3
	42729.717	-2.7
11573	42715.803	-12.2
	42724.753	-13.7
11597	42715.832	-0.6
	42729.755	5.2
51250	42699.881	16.2
223561	42699.520	6.5
	42715.513	51.0
	42725.525	16.8
	42731.524	6.1E
223655	42710.561	8.0
	42717.515	4.4
	42727.544	-2.4
	42732.534	9.6
223884	42702.509	-17.6
	42715.504	-3.5
	42719.511	0.6
	42731.512	-7.9
	42733.539	11.1
223957	42710.591	9.1
	42717.542	14.9
	42727.575	17.4
223991AB	42699.534	21.2
	42702.524	26.1
	42725.513	23.0
	42728.517	24.0
	42731.538	13.3
224096	42710.629	24.0
	42717.575	27.5
	42727.606	24.0

Table 4.2.6.

HD number	Julian Date	vel(kms^{-1})
224112	42716.541	24.1
	42724.521	9.3
	42727.626	22.2
	42733.603	11.7
224113	42716.532	-20.4
	42724.509	66.5
	42727.633	39.5
	42733.608	-54.2
224410	42717.601	-8.0
	42727.642	-1.2
224514	42699.552	6.5
	42702.541	13.1
	42728.538	-0.6
224529	42717.626	12.6
	42727.668	14.7
224641	42702.571	24.1
	42718.565	18.9
	42728.570	22.9
224642	42717.656	6.5
	42727.701	13.0
224763	42714.534	3.3
	42723.552	24.4
	42726.532	3.6
224820	42710.684	27.6
	42717.696	-2.8
	42727.735	-3.7
224914	42716.553	-9.0
	42721.554	-6.3
	42732.567	-10.0
224990	42710.714	2.0
	42713.685	15.2
	42717.501	12.3
	42721.520	12.9
	42724.528	15.5
	42727.506	16.9
	42732.511	-0.5E
	42733.610	22.3
225045	42695.642	-0.4
	42702.592	1.8
	42702.601	0.4
	42731.546	-4.5
	42733.546	-4.0

Table 4.2.6.

HD number	Julian Date	vel(km s^{-1})
225119	42702.615	24.2
	42719.563	26.7
	42728.600	37.2
225120	42711.525	44.3
	42715.739	-17.9
	42721.577	-11.6
	42733.624	-23.3
225132	42701.540	-24.4
	42720.510	21.4
	42723.498	30.1
	42726.520	9.3
	42730.533	16.7
225187	42716.576	15.4
	42721.527	16.7
	42732.599	26.6E
	42733.641	-3.4
225200	42695.663	10.3
	42699.577	5.2
	42702.628	-8.9
	42727.511	18.2
	42728.511	8.9
	42731.552	14.5E
	42733.553	13.6
225206	42699.591	-21.1
	42702.639	-16.5
225264	42702.656	21.0
	42719.597	29.3
225282	42711.572	20.4
	42716.598	12.9
	42729.525	49.0
225297	42729.557	2.1

E: apparent (spurious) emission feature in spectrum

Table 4.2.7.

HD number	radial veloc.	std. error	n	MK type	notes
141	-1.8	5.6	2	B9	
156	13.6	3.4	3	F2	
203	14.4	9.1	3	F3	P1
235	8.4	20.0	2	A1	
256	1.8	11.0	3	A4	
268	14.9	2.4	5	F5	
319	-7.2	13.9	7	A4	
392	-3.0	3.6	4	F6	
427	-18.6	4.5	2	F5	
493	5.9	4.1	3	F3	
562	4.8	1.4	2	A3	
732	-10.2	2.5	3	F8	
739	-2.4	9.9	2	F5	
899	20.3	3.3	3	F5	P6
900	17.5	4.3	3	F1	
955	-7.7	2.9	5	B5	
1000	-13.1	5.4	4	F6	
1101	14.0	20.5	3	F3	
1256	10.3	26.5	7	B8	
1343	0.7	5.8	3	F3	
1431	23.7	10.1	5	A0	P5,7
1667	14.6	7.1	5	A8	
1683	2.8	5.9	4	F7	
1856	13.7	10.6	5	F1	
1909	19.1	13.2	5	B9	
1980	5.3		1	F6	
1999	-20.9	3.8	2	B8	
2026	-8.6	1.6	2	A2	Am,P7
2037	13.0	6.8	3	A5	iPII
2178	32.0		1	A1	P1
2381	20.2	2.6	2	F2	
2394	19.5	2.8	3	F8	
2395	13.2	7.3	5	A7	
2477	-23.8	6.1	3	F5	iPII
2527	-5.1	14.4	2	F0	ePI
2630	10.8	5.7	2	F2	
2696	8.5	10.2	3	A4	
2719	-4.3	1.2	3	F7	
2724	-3.5	5.9	4	F0	Am?
2916	-9.7	7.3	3	F2	P3,7
3085	-6.9	20.5	3	B9	
3244	-1.6	3.0	2	A8	
3326	8.1	2.3	2	A8	
3580	5.7	6.2	3	B6	
3581	8.7	4.5	4	F3	

Table 4.2.7.

HD number	radial veloc.	std. error	n	MK type	notes
3622	3.3	4.3	2	A5	
3735	-24.8		1	F7	iPII
4065	1.8	10.3	5	B9	
4247	12.0	4.9	2	F1	
4338	4.0	6.6	5	A9	
4375	13.5	3.4	2	F5	
4507	-10.2	2.3	4	A6	
4622	19.5	4.0	2	B9	
4623	0.8	0.0	2	F0	
4691	0.4	7.3	4	F1	
4772	-3.4	5.1	6	A2	HB,P7
4975	17.4	3.9	2	F8	
5057	8.9	7.2	2	F5	P6
5132	6.8		1	F0	
5156	-17.6	13.1	3	F5	
5487	34.9	4.4	2	A2	
5524	7.8	2.2	2	A2	
5616	7.4	5.6	3	F0	
5617	-4.2		1	A2	
5659S	-0.4	4.8	4	F5	
5659N	-1.3		1	F5	
5737	-24.3		1	B7	P5,7
5932	11.7	2.6	2	F2	
6178	-17.7	9.4	4	A1	
6354	-13.4	3.1	4	A4	
6367	14.8	5.2	3	F5	
6412	-3.6	2.5	2	F5	
6491	-2.1	2.7	2	F2	
6493	9.2	6.7	4	F3	
6532	-7.7	7.9	2	A4	Am
6619	13.7		1	A2	
6668	-0.9	18.9	5	A6	
6723	-2.5		1	A9	
6767	9.0	5.4	5	A3	
7257	5.9	3.3	2	F6	
7259	15.0	3.3	3	F6	
7312	18.2	5.6	4	A8+F	
7323	9.0		1	A2	
7382	10.0	5.4	2	F3	
7495	-2.7	3.6	4	F8	
7629	-6.5	0.1	2	A9	
7676	6.6	2.6	2	A4	P1 3,5
7751	-4.9	0.8	2	F3	
7898	6.5		1	A8	
7908	15.3	1.5	2	F0	

Table 4.2.7.

HD number	radial veloc.	std. error	n	MK type	notes
8040	21.0		1	F6	
8076	-2.9		1	G0	
8130	0.7	10.2	3	A0	
8350	-7.6	4.7	3	F6	
8351	4.0	16.7	3	A7	Am
8487	-15.3		1	A6	
8895	16.1	3.4	4	F4	
8957	20.9	2.8	4	F0	
8985	29.1	0.9	2	F4	
9026	19.9	3.0	2	F1	
9061	1.5	9.7	4	F6	
9063	6.2	1.8	2	A6	
9065	-33.4		1	F0	
9132	-5.4	20.6	5	A0	P2 4 6,7
9336	-4.0	0.5	2	A7	
9411	-21.8	22.3	4	A8	
9451	21.1	4.0	2	A5+F	PII,P7
9672	15.7	4.6	4	A2	
9673	-16.9	34.7	4	A7	
9895	10.3	3.8	4	F2	
9906	-1.9	16.1	2	F0	
10148	18.2	2.1	5	F0	Am/ePI?
10161	29.0	4.0	3	B9	
10186	2.4	7.9	3	A9	
10209	3.1	6.1	4	F0	
10481	19.5		1	F3	
10538	-14.7	29.0	6	B9	
10798	-13.0	9.2	3	A8+F	
10830	10.4	3.6	2	F0	
10863	4.0	4.5	2	F2	
11100	4.4	2.4	3	F5	
11137	16.1	9.7	2	F3	
11262	21.2	4.1	2	F6	
11374	15.3	10.2	3	F5	
11459	-5.4	6.7	3	F6	
11481	29.7	6.0	2	A2	
11535	1.0	2.6	3	F3	
11573	-13.0	0.8	2	A5	
11597	2.3	2.9	2	F5	
51250	16.2		1	G5+A2	
223561	20.1	18.6	4	A2	
223655	4.9	4.6	4	F1	
223884	-3.5	9.5	5	A5	
223957	13.8	3.5	3	G2	
223991AB	21.6	4.3	5	A5+F	

Table 4.2.7.

HD number	radial veloc.	std. error	n	MK type	notes
224096	25.2	1.6	3	F5	
224112	16.8	6.4	4	A7	
224113	7.9	47.6	4	B5/8	
224410	-4.6	3.4	2	F6	
224514	6.3	5.6	3	A2	
224529	13.7	1.1	2	F5	
224641	22.0	2.2	3	F0+F0	
224642	9.8	3.3	2	F2	
224763	10.4	9.9	3	F5	
224870	7.0	14.5	3	A0	
224914	-8.4	1.6	3	F5	
224990	12.1	7.2	8	B3/5	
225045	-1.4	2.7	5	F8	
225101	11.8	10.0	4	F2	
225119	29.4	5.6	3	Ap	
225120	-2.1	27.1	4	F8	
225132	10.6	18.8	5	A0	
225187	13.8	10.9	4	B8	
225200	8.8	8.3	7	A1	
225206	-18.8	2.3	2	B8/9	
225264	25.1	4.2	2	A0	
225282	11.0	8.5	3	A0	
225297	2.1		1	G0	

Table 4.2.7.

Notes

"P" : denotes star selected as "odd" on basis of uvbyB photometry.
"P1": E(b-y) < -0.03
"P2": E(b-y) > 0.1
"P3": dc1 < -0.05
"P4": dB > 0.28
"P5": Unknown Spectral Type
"P6": Photometric Variable?
"P7": Yale Catalogue Variable
iPII: Intermediate Pop. II
pII : Pop. II
epI : Evolved Pop. I
HB : Horizontal Branch Stars

Chapter 5

Analysis of South Galactic Pole Data

'The great tragedy of science- the slaying of a beautiful hypothesis by an ugly fact.'

T.H.Huxley

5: Analysis of South Galactic Pole Data

5.1 Interstellar Reddening at the South Galactic Pole

5.1.1 Introduction

It has been known for many years that the total visual extinction is extremely low in the region of the galactic poles. The identification of fields with negligible amounts of interstellar material is of great importance to many areas of astronomy, since objects observed in such fields will display their true intrinsic colours and apparent magnitudes. This allows the determination of photometric calibrations and distance indicators for stars which are rare in the solar neighbourhood notably evolved halo population II stars such as long-period RR Lyraes. Systematic errors in the colours and magnitudes of galaxies will produce errors in the observed distribution of galaxies, of great importance in many cosmological studies. Such errors will also adversely effect the study of individual galaxies. These problems may be avoided by observing in areas known to have little interstellar extinction. The study of such areas is also important in investigations of the relationship between dust (reddening) and HI gas distributions in the Galaxy. As discussed in Chapter 3 the uvbyβ photometric system can be used to study the distribution of interstellar reddening, and consequently the data presented in Table 3.3.4 have been used in a study of the interstellar extinction within 15° of the South Galactic Pole.

5.1.2. Interstellar Reddening

Using the intrinsic colour lines of Crawford (1975, 1978, 1979) for the F, B and A3-A9 stars, and Hilditch et al (1983) for the intermediate A stars, values of E(b-y) have been calculated for all normal, unevolved Population I objects in the sample, ($-0.05 \leq dm_1 \leq 0.05$; $dc_1 \leq 0.28$), not known to be binaries and whose colours lie within the range of the calibrations. All stars classified as "odd" (section 5.2) were excluded from this analysis.

The procedure used by Hilditch et al (1976) was adopted here. That is, mean reddening values were calculated in (l,b) sectors for $b \leq -75°$ and distance zones, any areas of similar reddening being combined. In the whole volume covered by the sample there is no significant reddening out to 400pc. The mean reddening from the 415 stars within this volume is, formally, $E(b-y)=-0.004\pm0.003$. Those zones in this region for which there are no data are shown in Figure 5.1.1. Beyond 400pc. the sample is too incomplete to continue the reddening survey. However, the 23 stars observed in this region show no evidence of reddening.

Maps of the HI column density at both galactic poles have been published by Heiles (1976) and more recently discussed by Burstein and Heiles (1982). Although their SGP map is only complete for $25^{\circ} \leqslant l \leqslant 215^{\circ}$; $60^{\circ} \leqslant b \leqslant 90^{\circ}$, it shows that the reddening within 15° of the pole in the sample region is insignificant (HI column density $\leqslant 2.87 \times 10^{20}$ atoms cm^{-2}, giving $E(b-y) \leqslant 0.007$ using their calibration. The accuracy of the method is approximately ± 0.007 in E(b-y).) The zero point of the SGP uvbyβ photometry presented here is therefore in good agreement with the HI/galaxy count method of Burstein and Heiles (1982). The same is true of the NGP survey photometry (Hilditch et al 1982).

Perry and Johnston (1982) have projected the observed E(b-y) values for 1436 A2-F0 southern hemisphere stars into the z-direction and find the mean reddening within 200pc. of the plane to be $E(b-y) = -0.005 \pm 0.005$ in good agreement with the value derived here for the direction of the South Galactic Pole.

These results do not agree with those of Knude

(1977), Albrecht and Maitzen (1980) or Nicolet (1982). Knude found the average E(b-y) to be 0.040±0.001 from uvbyβ photometry of 110 AF stars in 11 Selected Areas around the SGP. Albrecht and Maitzen found E(b-y)=0.019 (no quoted error) from uvbyβ photometry of 90 BAF stars within 10° of the pole. Knude used a now obsolete calibration for the Late A stars (Crawford 1973), as did Albrecht and Maitzen, who in addition extrapolated this to give a calibration for the Early A stars. In both cases this would appear to redden these objects by about 0.006 in E(b-y), which still cannot explain the large differences. Nicolet has found E(b-y)=0.030 (no quoted error) for both poles from 129 B and Early A stars observed in the Geneva photometric system, the reddening being determined by the "photometric box" method. In all three of these cases Burstein and Heiles attribute the large apparent reddenings to real differences in the colour zero point of the photometry.

More recently Knude (1982b) has quoted $\langle E(b-y)\rangle \sim 0.02$ for three Selected Areas near the SGP. For the eight stars observed by Knude which lie in the present sample, our analysis of Knude's own data gives $\langle E(b-y)\rangle \sim 0.036$ in agreement with his value of $\langle E(b-y)\rangle \sim 0.035$. However analysis of the present photometry of these stars gives $\langle E(b-y)\rangle \sim 0.000$. This suggests that any differences between the reddenings presented here and those of Knude are due to small differences in the photometry rather than a fundamental difference in the calibrations used. However any deductions based on the comparison of only eight stars must be treated with caution.

Although there are areas of zero reddening at both poles it cannot be over-emphasised that there are areas of significant reddening ($E(b-y)>0.1$) at high galactic latitudes. Consequently it is difficult to make general statements regarding the average reddening over large areas of sky. Maps of the HI column density give a good indication of the distribution of interstellar matter and show the extreme patchiness of this material. Photometric reddening determinations seem to be valid only if they are based on well-defined samples of stars with large numbers per unit area of sky.

5.2 Photometric Classification of SGP Stars

5.2.1 Objects with Unusual Colours

The photometric data presented here has been used to plot two colour diagrams for all 572 stars in the sample. The c_1 vs. (b-y), m_1 vs. (b-y) and β vs. (b-y) diagrams are shown in Figures 5.2.1, 5.2.2. and 5.2.3.

Since there is no significant reddening affecting these stars the observed colour indices have been plotted. The intrinsic colour lines of Crawford (1975, 1978, 1979) and Hilditch et al (1982) are also shown. Several stars with unusual colours are present in the sample and these are listed in Table 5.2.2. These have been classified using the criteria given by Hill et al (1982) (see Table 5.2.1) and the photometric scheme of Kilkenny and Hill (1975). Some stars do not fit into this classification scheme and are designated 'unknown' in Table 5.2.2. The list also includes several apparently normal stars which give large positive or negative values of E(b-y) [E(b-y)>0.1 or E(b-y)<-0.03], and stars for which there is a suggestion of photometric variability. Those stars which are known (or suspected) to be velocity variables are marked as such. Table 5.2.2 gives the name, δc_1 (or $\delta\beta$ if asterisked), and δm_1 for all of these unusual objects.

5.2.2 Photometric Classification and Comparison with the MK system

Using the intrinsic colour lines of Crawford (1975, 1978, 1979) and Hilditch et al (1983) equivalent MK spectral types were assigned to all 572 SGP stars in the photometry sample with an accuracy estimated to be

±2-3 subclasses. Where possible spectral types obtained in this way were compared with MK types from the Michigan Spectral Catalogue. Both classifications are shown in Table 6.2.1. from which it can be seen that the agreement is generally within 2 subclasses for stars without unusual colours, which is well within the error margin. There are only four exceptions to this- HD 117 (MK:F2V, uvbyβ:F9), HD 5270 (MK:G2/3, uvbyβ:F7), HD 6365 (MK:A3III, uvbyβ:A7) and HD 223991 (MK:A2V+F, uvbyβ:A5). This last object is an optical pair, unresolved by the photometry, which may explain the discrepancy in spectral types. The other three discrepancies are unexplained.

5.3 Relative Proportions of Population Groups

The photometric data presented in chapter 3 has been used to study the relative proportions of various population groups as a function of distance from the plane. On the basis of the uvbyβ photometric classifications decribed above the stars in the photometric sample were separated into groups of B, A0-F4 and F5-F9 stars. Each group was then divided into separate samples of PI, ePI (evolved population I), iPII, PII, horzontal branch, Am and 'unknown' stars. (There were no Fm stars in the sample.) The 'unknown' stars were excluded from all subsequent analysis, as were the ePI stars for which no absolute magnitude calibration (and hence distance scale) was available. Distances for all other objects were determined by photometric parallax. For the Am, iPII and PII stars the adopted absolute magnitudes were those of the equivalent PI stars. For the horizontal branch stars Mv=+0.6 was adopted.

From these samples the proportions of Am, iPII, and PII stars relative to PI stars were determined for both the A and F stars as a function of distance from the plane. These are shown in Table 5.3.1 for stars within 400pc., the samples being too incomplete beyond this for any comparison to be attempted. Also shown are the proportions of horizontal branch stars relative to PI B stars and the relative proportions of PI B and A stars, and A and F stars. These are based on samples which are small and incomplete, and consequently should be regarded only as estimates of the true proportions. The relative proportions of PI, IPII and PII A and F stars within 1000pc. derived from the combined North and South pole samples have been presented by Hilditch et al (1984) and are shown in Table 5.3.1 for comparison purposes.

From the combined data it can be seen that the proportions are essentially constant out to about 400 pc. after which the numbers of iPII and PII stars start to increase, presumably reflecting the scale height of the disk. The proportion of iPII F stars to PI F stars is seen to be much higher than that for the A stars at all distances from the plane. At 1kpc. from the plane the number of PI F stars is only slightly greater than the number of iPII F stars, but for the A stars the PI stars dominate even at this distance. If the Gilmore and Reid (1983) 'thick' disk (of scale height about 1.4kpc.) is identified with all iPII stars as defined by uvbyβ photometry, then at about 1kpc. from the plane the proportion of iPII to PI stars should be about 0.4-0.5 as is found for the F stars. Relative to the expectations for an iPII 'thick disk' there is therefore an excess of apparent PI A stars out to at least 1kpc. from the plane. Presumably these are the stars reported by, eg., Rodgers et al (1981), although this excess may be due to contamination by photometrically similar HB stars at large z distances.

It must be stressed that these stars have been identified as PI A stars solely on the basis of uvbyβ photometry. Detailed spectroscopic analysis of individual objects is required to confirm this. Consequently all apparently PI objects from the South Galactic Pole photometry sample which lie beyond 500pc. have been collected in Table 5.3.2 which gives HD numbers, equivalent MK spectral types from the photometry and distances determined on the assumption that they are PI objects.

5.4 Detection of Variable Velocity Stars

Hill et al (1976) have described a method for identifying those stars in a sample which have a variable radial velocity. The traditional technique has been to compare a chi-square frequency distribution with the frequency distribution (histogram) of the observational data. Different values of the mean variance for constant velocity are then tried until the best match between theoretical and observed distributions is obtained for the region just before the maximum of the observed frequency distribution. In other words it is assumed that the observed histogram is composed of a central chi-square distribution, representing the observation of constant velocity stars, with the addition of several non-central chi-square distributions of different mean variances, representing the variable stars. Unfortunately histograms are subject to considerable distortion by sampling errors, especially if the data sample is fairly small, as is usually true of radial velocity samples.

Any technique intended to identify the variable velocity stars in a sample is useful only if the data are homogeneous. The stars considered must all belong to the same stellar group (in this case A stars or F stars), must all have been observed with the same spectrograph and must all have a velocity based on at least three observations with the same equipment. For such a sample the sum of squared residuals (S2) is computed for each star from the first three independent observations of the star (successive observations are not considered to be independent).

The method of Hill et al (1976) compares the cumulative distribution function of the observational data with the expected cumulative distribution function of a central chi-square random variable with (n-1) degrees of freedom, where n is the number of spectra of each star used in computing S^2 (ie n = 3 here). The cumulative distribution function of the observational data is a plot of the proportion, f_{obs}, of the total number of stars versus $S^2/\overline{\sigma^2}$, where $\overline{\sigma^2}$ is an adopted mean variance for constant velocity stars. The expected cumulative distribution gives, for any value of $S^2/\overline{\sigma^2}$ the proportion of a random sample from a chi-square distribution with (n-1) degrees of freedom which would have a value less than or equal to $S^2/\overline{\sigma^2}$. Then for each value of $S^2/\overline{\sigma^2}$ derived from the observed radial velocities there corresponds a certain proportion, f_{obs}, of the total number of stars observed and a theoretical proportion, f_{theo}, expected from the chi-square distribution of unit variance. A plot of f_{obs} vs f_{theo} will be a straight line for the region of the diagram occupied by constant velocity stars provided that the mean variance has been correctly chosen. If the value chosen is too small then the fraction observed will be less than expected and the relation will be curved convexly towards the f_{theo} axis. If the value chosen is too large then f_{obs} will exceed the expected fraction and the relation will be curved concavely towards the f_{theo} axis. Beyond the region of the diagram occupied by constant velocity stars the relation will deviate from a straight line by an amount dependent on the proportion of variable velocity stars in the sample. Thus, in principle, the identification of variable velocity stars in a sample may be made by picking an initial $\overline{\sigma^2}$, calculating f_{obs} and f_{theo}, comparing them, adjusting, and repeating the procedure until a value of $\overline{\sigma^2}$ is found which gives the most linear f_{obs} vs f_{theo} relation. Then any star in the sample for which the standard deviation from the mean velocity exceeds $\overline{\sigma^2}$ is likely to be a variable velocity star.

In practice those stars for which $\bar{\sigma} \leqslant \sigma < 2\bar{\sigma}$ are assigned 'possible' variable status and those for which $\sigma \geqslant 2\bar{\sigma}$ are described as 'probable' variables. A problem may arise with the A stars as the lower rotational velocities and larger number of measurable spectral lines of the Am and Ap stars compared with normal A stars results in a much lower mean variance for the Am and Ap types. Thus the Am/Ap stars must be considered separately. In this case the only stars observed in sufficient numbers for such an analysis were the Pop.I A and F stars.

Those stars in the velocity sample with velocities based on three or more independent spectra were divided into groups of A stars (A0-F4) and F stars (F5-F6) and the sum of the squared residuals found from the first three independent observations for each star. There were no known Am or Ap stars in the A star sample. Had there been their presence would have been betrayed by discontinuities in the plot of f_{obs} vs f_{theo}. No such discontinuities were noted. The finally adopted values of $\overline{\sigma^2}$ for the A and F stars, along with the number of stars present in each sample are given in Table 5.4.1 as are the percentages of the total samples designated possible and probable variables. For both the A and F star samples the total percentage of (possible + probable) stars is about 49% (in each case 33% possible and 16% probable). This can be compared with the results of Hill et al (1976) for their North Galactic Pole sample. From a much larger F star sample they deduced that about 45% were variable and from an A star sample slightly smaller than that presented here they found about 40% to be variable.

The possible and probable variables in the present sample are given in Table 5.4.2. None of these could be identified in the General Catalogue of Variable Stars (Kukarkin et al 1976).

5.5 The w-Velocity Distribution of the A-F stars at the South Galactic Pole

5.5.1 Selection of Sample

In order to study the w-velocity distributions of the A-F stars at the South Galactic Pole the radial velocity sample presented in chapter 4 was first separated into its constituent sub-systems on the basis of uvbyβ photometric data as described above. Where possible the photometry was taken from the sample of chapter 3, with nine stars having uvbyβ indices taken from the catalogue of Hauck and Mermilliod (1980). Those stars for which no photometry was available could not be segregated into sub-systems and were excluded from the subsequent analysis. It was decided not to expand this velocity sample using velocities from other sources, since no other source provided sufficient overlap for its intrinsic velocity system to be checked against that of the sample presented here.

The radial velocity sample was first divided into groups of B, A0-A5, A6-F4, F5-F6 and F7-F9 stars. The radial velocities of the B stars are not well known and they were dropped from the analysis at this stage. Each group was then split into sets of PI, Am, iPII, PII, and horizontal branch stars. 'Unknowns' were rejected at this stage.There are no Fm stars or white dwarfs in the sample. In principle the study of the velocity distributions should be based on an homogeneous sample of constant radial velocity stars, each velocity being based on at least three independent observations. Due to the limited sample available stars with velocites based on only two observations were included in the analysis, although they were initially kept separate from the sample of stars with three or more observations. Stars with 3+ observations which were indicated as 'probable' variables by the analysis of section 5.4 were excluded from subsequent analysis as were those with only two observations which satisfied the same criteria. As a consequence of these various segregations within the initially small sample the final samples were in many cases too small to be studied. Only unevolved PI stars were available in sufficient numbers and the rest of this discussion refers to them.

5.5.2 w-Velocity Distribution for Unevolved A-F Stars

It is assumed hereafter that the observed radial velocities of stars within 15° of the pole are equivalent to velocities perpendicular to the plane, the actual correction being small. For a star at the South Galactic Pole the observed stellar velocity, relative to the sun, in the standard frame of reference in which velocity increases towards the North Galactic Pole is given by $W = -v_r$, where v_r = radial velocity.

The samples of PI A and F stars were divided into groups of stars with 3+ observations and those with 2 observations, the A0-F4 stars being considered as one group and the F5-F9 stars as another (all the A stars and all the F stars were combined as a result of the small sample sizes). The Smirnov test (Conover 1971) was used to establish, with 95% confidence, that the distributions of stars with 3+ and 2+ observations within 300pc. for the A stars and 200pc. for the F stars (the effective limits of the samples) were the same. Consequently all samples of stars with 3+ and 2 observations were combined and the A0-A5, A6-F4, F5-F6 and F7-F9 stars considered separately. For each of these four groups the distributions of stars within different distance bands were studied and mean and rms velocities determined. The Cramer-von Mises Goodness of Fit test (Conover 1971) was used to establish at the 95% confidence level that each distribution in each distance band is gaussian. The Smirnov test was then used to establish that, for each distance band the distributions of A0-A5 and A6-F4 stars were the same, and the distributions of F5-F6 and F7-F9 stars were the same , at the 95% confidence level. The Cramer-Von Mises Goddness of Fit test was used at the 95% level to confirm that these combined distributions were gaussian.

The combined A stars samples in different distance bands were shown to have the same gaussian distribution, as were the combined F star samples in different distance bands. Again the Cramer-von Mises and Smirnov tests were used at the 95% level. Consequently all the A stars were combined into a single sample for which the mean and rms velocity were calculated. This was also done for the F stars. The results of these tests and combinations are summarised in Table 5.5.1. The samples in some cases were too small for any significant test to be performed and consequently the mean and rms are excluded from the table. On the basis of this small sample there is no evidence for a non-gaussian velocity distribution within 200pc. of the plane for the PI A or F stars.

5.5.3 Comparison with the North Galactic Pole

Hill et al (1979) have studied the velocity distributions of a large sample of A and F stars at the North Galactic Pole. They found the velocity distributions of PI A and F stars to be in reasonable agreement with the model of Camm (1950,1952), which requires an increase of velocity dispersion with distance from the plane. By comparison of their velocity data with that of Eggen (1961) for stars within 40pc of the sun (of which there were none in their sample) they found possible evidence of an increase in rms velocity with distance from the plane for stars within 200pc. The mean and rms velocities of their sample of PI A and F stars within 200pc. are shown in Table 5.5.1. The agreement with the values derived here is excellent considering the much smaller samples available in the present work.

Not all of the Hill et al NGP velocity data has yet been published, but using the selection procedures described above their published velocity data (Hill et al 1976) was used in conjunction with their published photometry (Hill et al 1982) to produce samples of PI A and F stars within 200pc. of the plane. These are slightly different from the samples used by Hill et al 1979. Mean and rms velocities were calculated (see Table 5.5.1) and the Cramer von-Mises test used to establish (at the 95% level) that the distributions are gaussian.

From these reduced samples the mean and rms velocities for the A stars are about 1.7kms^{-1} larger than those found by Hill et al (1976) and those from the SGP sample. However the Smirnov test confirms at the 95% level that these distributions are the same as those of the equivalent SGP stars. Consequently NGP and SGP samples were combined and the resultant distributions shown to be gaussian (Cramer-von Mises at 95% level) The mean and rms velocities for the combined NGP and SGP samples are shown in Table 5.5.1.

The sun's motion towards the NGP is generally taken to be $w_{\odot}$ =7$\pm$1 kms^{-1}. The velocity of an object towards the NGP is given by-

$$w = W + w_{\odot}$$

where W is the objects velocity relative to the sun. The mean w velocities for the A and F stars are given in Table 5.5.2. Taking account of the errors in these means, it appears that there is no net motion of the A stars in the perpendicular direction, but possibly a small streaming motion of the F stars at a few kms^{1} towards the NGP.

5.6 Velocity and Population

The Stromgren index δm_1 is a metallicity indicator and the iPII and PII stars are known to be metal deficient relative to the PI stars. They are also expected to have higher mean and rms velocities. Consequently a plot of δm_1 vs W for a large sample of stars may show specific groupings of PI, iPII and PII stars. To test this such a plot was made, using data on SGP stars with photometry and velocities based on two or more observations. Only 2 iPII and no PII stars satisfied these criteria, and the sample was augmented by the 13 iPII stars from the NGP sample which did. No suitable PII stars were found in the NGP sample. The resultant plot is shown in Figure 5.6.1. The iPII stars are easily identified by their low metallicity, and clearly show a much larger range of W velocities than the PI stars. For the samples used in plotting the diagram the mean and rms W velocities are:

	$\overline{W}$ (kms^{-1})	$(\overline{W^2})^{1/2}$	no.stars
PI	-5.6	11.6	82
iPII	-5.9	26.5	15

It must be stressed that the samples (especially of iPII stars) are small, but it is clear that, in addition to their low metallicities, iPII stars are distinguished from PI stars by their W-velocity dispersion, which is roughly twice that of the PI stars. Note also that the $\overline{W}$ velocities of these two samples are essentially the same, and imply minimal net motion perpendicular to the plane for both the iPII stars and the PI stars.

5.7 Limitations of the Velocity Distributions

5.7.1 The Non-Unique Nature of The Gaussians

In a preceding section the W velocity distributions of the PI A and F stars were discussed in an analysis of combined samples of NGP and SGP velocity data. It was shown that both the A and F stars have velocity distributions which are well fitted by gaussians with mean and dispersion of -6.4 and 11.0 kms^{-1} for the A stars, and -4.1 and 10.9 kms^{-1} for the F stars. Given the crucial role of the dispersion in the determination of the local mass density it is important to consider any other solutions which the data may permit. Consequently attempts were made to fit other gaussians to both the A and F star data, the Cramer Von Mises Goodness of Fit test being used at the 95% confidence level to determine whether or not such fits were compatible with the data.

It was found that , although the gaussians given above produced by far the best fits, there were alternatives. The results of these tests may be summarised as follows: For the A stars, with the mean taken at -6.4kms^{-1}, the allowable dispersions lay in the range $11 \pm 4 kms^{-1}$. For the F stars with the mean taken at $-4.1kms^{-1}$, the allowable dispersions lay in the range $10.9 \pm 3kms^{-1}$. By holding the dispersions constant at $11.0kms^{-1}$ and $10.9kms^{-1}$ respectively the allowable ranges in the means were $\pm 2kms^{-1}$ for the A stars and $\pm 1kms^{-1}$ for the F stars. (From the nature of a gaussian it is to be expected that only a small range in the mean would be acceptable.) These small ranges in acceptable means are comparable with the errors in the means of the observed distributions.

The allowable variations in the dispersions are of most significance here, and the effect of such variation must be considered. For a distribution with constant dispersion,

$$Kz = \overline{w_i^2} \frac{d}{dz} (\ln (v/v_0)_i)$$

where the subscripted variables refer to the ith mass component of the Galactic system being considered. From this Kz, the system force law, is found, and the local mass density is obtained by inserting solar neighbourhood values into,

$$\frac{dKr}{dr} + \frac{Kr}{r} + \frac{dKz}{dz} = -4\pi G\rho$$

In the solar neighbourhood, since $\overline{w_i^2}$ is constant in the case considered,

$$\frac{dKz}{dz} = \overline{w_i^2} A, \quad A = [\frac{d^2}{dz^2} (\ln (v/v_0)_i)]_0$$

and

$$[\frac{dKz}{dz}]_0 \gg [\frac{dKr}{dr} + \frac{Kr}{r}]_0$$

Thus $\rho_o = \overline{w_i^2} A$,where A is a constant.

If the dispersion of the appropriate sub-system is ~11kms^{-1}, a variation of ±1kms^{-1} in this dispersion will change the resultant mass density by ~20%. (cf Hill et al, 1979, who found, using a modified model due to Camm (1950, 1952), that a change of ±1kms^{-1} in the dispersion of their PI F star sample would require a change of ~25-30% in the mass density. However, such a change in dispersion, was not allowed by their data. A similar dependence of mass density on dispersion is shown in Bahcall (1984), where a different model is applied to the Hill et al data.) For the combined NGP and SGP data used here a dispersion change of ±4kms^{-1} would alter ρ_o by ~100%.

It is apparent from the above that the current velocity data is too ambiguous to be used in the determination of po, as it cannot be demonstrated that the adopted velocity distributions are unique, and small uncertainties in the adopted dispersions produce significant uncertainties in ρ_d.

5.7.2 The Existence of Contaminants

The presence of 'contaminants' in the observed PI velocity distributions has been discussed in Chapter 1, with reference to both the apparent velocity dispersion increase with z distance found by Hill et al (1979), and the presence of apparently normal PI stars at large distances from the galactic plane. By fitting composite gaussians to the available data, attempts were made to impose limits on the possible proportions of such contaminants in the data samples, the Cramer Von Mises Goodness of Fit test being used at the 95% level to test if these fits were compatible with the observed distributions.

Two possible contaminants were considered, the first having a dispersion of 30kms^{-1}, comparable with that for the 'classical' PII stars, and the second a dispersion of 60kms^{-1}, comparable with that found for the PI A stars at large z distances by, for example, Pier (1983). The former case is of particular interest as Bahcall (1984) has managed to obtain a good fit to the F star density distribution of Hill et al (1979) out to 500pc. by adding a 5% contaminant with this dispersion to the 'normal' PI distribution.

For the first case (dispersion 30kms^{-1}), it is found that the A star data will allow a contaminant of up to 35%, and the F star data permits a contaminant of up to 25%. For the second case (dispersion 60kms^{-1}) the A star data permits a contaminant of up to 25%, and the F star data up to 20%.

The implications of these results are that the available velocity data do not permit the identification of small gaussian contaminants with the quoted dispersions. In fact, as found in the preceding section, the data do not define a unique gaussian distribution, but can be quite well fitted by a number of different gaussians and sums of gaussians. Thus these contaminants may well exist, but the present data can not identify their presence.

5.8. Space Density Distribution and Galaxy Models

5.8.1 Observed Space Density Distribution

From photometric data such as that presented here it is, in principle, possible to determine the space density distributions of the various stellar groups observed. For an accurate determination of the space density the stellar sample must include all stars of the required type in a given volume of space ie a volume limited sample. For example if all A stars in a cone of known angle, out to a specified distance have been observed then the sample is complete within the volume defined by the cone. Obviously a large sample is required. The numbers of stars within given distance bands are counted and, the volumes of space associated with each distance band being known, the space density as a function of distance is obtained out to the limit of the sample. The space density distribution as a function of z distance is normally given relative to the value in the solar vicinity. It must be stressed that in order to do this the sample must satisfy the following requirements-

1/ It must be complete, ie all stars of the desired type within a defined volume must have been observed, and their distances known accurately.
2/ It must be large. (cf Hill et al (1979) who derived the distribution of all F stars within 500pc. of the plane with more than 2500 stars per distance band.)
3/ The space density at the sun must be well known if the results are to be expressed relative to it.

The photometry presented here gives data on $\sim$600 stars of spectral types B-F8, brighter than $\sim$10m, within $\sim 11^{\circ}$ of the SGP. Hill et al (1982d) have presented similar data for $\sim$1000 B-F5 stars brighter than $\sim$11.5m within 15° of the NGP. By combining these samples the A and F star space density distribution as a function of height, z, from the galactic plane may be estimated for illustrative purposes. Note that these estimates are not based on complete volume limited samples and require the (as yet unproven) assumption that the stellar distributions are symmetrical about the plane. Hill et al (1979) have used the data of Upgren (1962, 1963) and the Yale Catalogue (Hoffleit 1964) to obtain the z distribution of all A and F stars (PI, ipII and PII) out to ~600pc. (the F stars being defined as those of type F5-F8). For comparison purposes the combined PI, iPII and PII data are used here to give composite space density distributions for the A and F stars, determined solely from uvbyβ data at the NGP and SGP, the space densities in the plane being found from the photometry of Olsen (E.H. Olsen, 1983, Astr. and Ap. Supp. 54, 134). Olsen gives uvbyβ photometry for ~15,000 A5-G0 stars brighter than 8.3m, selected from the HD catalogue. To obtain space densities at the sun from this data requires the assumptions that all A stars have the same Mv as do all F stars. The numbers within 50pc, of the sun are then estimated from the photometry to give the number densities. Since Olsen's A star sample is incomplete for stars earlier than A5, the final A star distribution was renormalised to the plane by averaging the number counts for stars within 50pc. of the plane from the galactic pole data.

The resultant density distributions are shown in Figures 5.8.1 and 5.8.2, along with the distributions determined by Hill et al (1979). The inadequacies of the new distributions are obvious and to be expected in view of the incomplete nature of the samples (including Olsen's) used in their determination.

5.8.2. Comparison with Galaxy Models

Two current galaxy models will be considered here, namely that of Hill et al (1979) (hereafter the HHB model), and that of Bahcall (1984) (hereafter the Bahcall model). The general distributions of matter in the two models are quite similar , but their approaches are different. Both require as input the relative proportions and velocity dispersions in the plane of the observed components from which the model is constructed. From these the model computes a potential from a solution of the Poisson-Boltzmann equation and uses this to obtain a fit to the observed F star distribution of Hill et al (1979). The best fitting model is then used to predict the local mass density, ρ_o. Hill et al (1979) used Camm's (1950,1952) analytical solution of the Poisson-Boltzmann equation whereas Bahcall solved it numerically.

In this work the HHB model is used to predict the A and F star distributions for three values of the local mass density (0.10,0.14 and 0.185 $M_{\odot}pc^{-3}$),using the velocity dispersions and relative proportions in the plane adopted by Hill et al (1979) for the PI, iPII and PII stars. (Namely PI:iPII:PII is 0.96:0.04:0.0 for the A stars and 0.87:0.12:0.01 for the F stars, with the following dispersions- A stars: PI 7.3kms^{-1}; iPII 13.2kms^{-1}, F stars:

PI $10.4 kms^{-1}$; iPII $13.2 kms^{-1}$; PII $30.0 kms^{-1}$.) This illustrates the effect of a variation of ρ_o on the space density distribution or, conversely, the effect of a variation in space density distribution on the derived local mass density. The value of $0.14 M_\odot pc^{-3}$ for ρ_o is that obtained by Hill et al (1979) by fitting their model to the observed F star distribution. Bahcall (1984) obtained the value of 0.185 by fitting his model to the same data. The predicted and observed distributions are shown in Figures 5.8.3 (A stars) and 5.8.4 (F stars).

The observed A star distribution cuts across the predicted distributions out to $\sim$250pc. after which it fits the $\rho_o = 0.185 M_\odot pc^{-3}$ distribution, although not very well. The observed F star distribution bears no resemblence to any of the predictions, including that for $\rho_o = 0.14 M_\odot pc^{-3}$, which gave the best fit to the Hill et al (1979) F stars. The comparisons are compatible with the known incompleteness of the observed distributions, which will tend to underestimate the true distributions, the discrepancy increasing with z distance.

Bahcall (1984) has used his model to produce three forms of the Kz law corresponding to the cases of i) a galaxy with massive halo (his best-fit model to the HHB data) giving $\rho_o = 0.185 M_\odot pc^{-3}$, ii) a galaxy without a massive halo, giving $\rho_0 = 0.24 M_\odot pc^{-3}$ and iii) a galaxy with all unseen matter distributed in the same way as the interstellar medium, giving $\rho_0 = 0.245 M_\odot pc^{-3}$. These force laws have been used to predict the z distributions of the A and F stars, with the dispersions and proportions in the plane given by Hill et al (1979). They have also been used to predict the A star distributions for the case where PI A stars have the higher dispersion found here ($\sim 11 kms^{-1}$). Predicted and observed distributions are shown in Figures 5.8.5a, 5.8.5b (A stars) and 5.8.6 (F stars).

Figure 5.8.5a shows the observed A star distribution with the predictions of Bahcall's model assuming a PI A star velocity disperson of $7.3 kms^{-1}$, while Figure 5.8.5b shows the predictions for a PI A star dispersion of $\sim 11 kms^{-1}$. The observed A star distribution of Hill et al (1979) is also shown. In the first case the model underestimates the observed space densities beyond about 200 pc, and in the second case it overestimates it for all distances. For the F stars the observed distribution from the galactic poles photometry, does not fit any of the models,but the distribution of Hill et al (1979) does fit the models for $\rho_0 = 0.185$ and $0.24 M_\odot pc^{-3}$ out to ~ 300pc, after which the observed distribution is underestimated. Because of the known incompleteness of the photometric samples used to derive the density distributions given here, the failure of the models to fit these distributions is not surprising. However, for the distributions of Hill et al (1979) both the Bahcall models with ρ_0=0.185 and 0.24$M_\odot pc^{-3}$ and the HHB model with ρ_0=0.14$M_\odot pc^{-3}$ fit the F star distributions (to 300pc for the Bahcall models and 500pc. for the HHB model.) However, for the A star distribution of Hill et al only one of Bahcall's models fits the observations at all (that for an interstellar medium-like distribution of unseen matter and an adopted PI velocity dispersion lower than that found from the galactic poles velocity data) and this only fits to 200pc. Similarly, the best of the HHB models only fits the observations out to ~240pc. The implication is that there is something unusual about the A star distribution when compared with that of the corresponding F stars. Possibly the sample is contaminated in some way (eg by large velocity dispersion PI stars or mis-identified HB stars), or the A star distribution may be intrinsically odd. It appears in any case that the A stars are not suitable as a tracer for the determination of Kz and $\rho_\odot$ until their space and velocity distributions are better understood.

These are the only recent models which are specifically concerned with the stellar distribution perpendicular to the plane. They have been used to obtain the most recent determinations of the local mass density, based on the same observed distribution of F stars at the NGP. In view of the large discrepancy in the values of the local mass density obtained these determinations of ρ_o merit more attention.

The HHB model makes use of Camm's (1950,1952) solutions for a self-gravitating disk in which the velocity dispersion increases with distance from the plane. The available evidence for such an increase has been discussed in Chapter 1, and its assumption by Hill et al (1979) is reasonable, given the available data. However Camm's solutions are valid only for a self-gravitating (one-component) disk in which the potential felt by the mass whose distribution the model predicts is the potential due to that mass. It is not valid if applied to a multi-component galaxy and used to predict the distribution of one component, as each component responds to the potential due to all the components. Thus, although it provides a remarkably good fit to the observed F star distribution, it cannot be regarded as a valid model of the galaxy (Bahcall 1984).

Bahcall (1984) obtained a value of $\rho_o=0.185\pm0.002 M_\odot pc^{-3}$ by fitting his model to the F star distribution of Hill et al (1979). The fit is excellent out to $\sim$200pc. However he appears to have made no allowances for the fact that this F star distribution is a composite of three distinct components with different space/velocity distributions. Instead he adopts the PI F star velocity dispersion for the sample and makes the assumption that the velocity distribution is isothermal out to at least 200pc. (Beyond 200pc. the Hill et al data hints at an increase in velocity dispersion.) Bahcall obtains a better fit to the F star data out to ~600pc. (and a higher value of ρ_o) by assuminga 5% contaminant with a dispersion of $30kms^{-1}$ in his adopted F star distribution. Since the sample itself contains ~12% iPII stars with dispersion of $13.2kms^{-1}$ (or possibly as much as $27kms^{-1}$ - see section 5.6) and ~1% PII with dispersion of ~$30kms^{-1}$, this better fit obtained by adding higher dispersion contaminants is to be expected since the data do indeed contain such contaminants. Note however that allowing for contaminants gave Bahcall a better fit to the F star distribution, but also a higher value of ρ_o, increasing the discrepancy between his and previous determinations of the local mass density.

Table 5.2.1.

Photometric Classification Criteria

Type	Criterion
metallic?	$-0.08 < \delta m_1 \leqslant -0.05$
metallic	$\delta m_1 \leqslant -0.08$
Evolved Pop.I	$\delta c_1 > 0.28$
Horizontal Branch	$c_o > 1.12$
	$(b-y)_o > -0.01$
Intermediate Pop.II	Not Horizontal Branch
	$0.05 \leqslant \delta m_1 < 0.08$
Pop.II	Not Horizontal Branch
	$\delta m_1 \geqslant 0.08$

Table 5.2.2.

Photometrically Odd Stars

HD No.	δc_1	δm_1	comments
19	6	1	a normal?
20	20	11	iPII
50	-10	-1	c normal?/Am?
91	-11	1	c normal?
203	7	0	a normal?
258	11	4	a normal?
306	9	4	a normal?
343	21	-1	a d normal?
465SE	14	4	a normal?
590	7	1	a normal?
605	6	1	a normal?
719	6	-1	Am
899	16	1	d normal?
1086	12	-1	Am
1097	-17	-16	c Am?
1431	19*	-1	Unknown VAR
1464	20	8	d iPII
1482	6	2	d normal
1498	8	1	d normal
1541	15	-2	Am
1580	9	2	a normal
1616	-2	-6	Am
1619	0	-6	Am VAR
1858	3	6	iPII
2026	0	-8	Am VAR
2037	15	6	iPII
2080	8	1	a normal
2131	4	6	iPII
2178	22	4	a normal
2240	17	1	a normal
2337	9	5	a normal
2348	-11	-4	a c d normal?
2415	312*	-4	unknown
2477	10	6	iPII
2527	29	1	ePI
2528	14	3	a normal
2554	17	1	d normal
2613A	12	4	d normal
2613B	-13	-5	Am?-low c_1
2615	9	6	iPII
2641	-1	-7	Am
2724	21	0	Am?
2797	-29	-14	a c d unknown
2799	24	0	HB

Table 5.2.2.

HD no.	δc_1	δm_1	comments
2810	11	2	a normal
2859	11	4	a normal
2978	11	1	a d normal
3017	4	4	a normal
3085	-10	-3	c normal VAR?
3135	2	-8	Am
3180	3	6	iPII
3186	90*	-5	b d e sdFG?
3217	0	2	d normal
3300	13	5	a d normal
3604	6*	-5	unknown?/Am?
3621	9	6	d iPII
3735	6	7	iPII
3736	29	4	ePI
3762	61	3	d normal
3783	4	1	a normal
3864	17	2	a normal
3885	23*	-6	unknown
3999	-1	-8	Am
4011	32	3	ePI
4052	9	-3	a normal
4073	4	1	d normal
4157	26	5	a normal
4158	29	8	iPII
4289	15	2	a d normal
4397	2	9	PII
4417	9	1	a normal
4485	7	3	a normal
4689	12	2	a normal
4731B	8	0	d normal
4772	36	4	HB VAR
4876	17	-6	d Am?
4966	4	8	iPII
4983	-7	3	c d normal
5057	2	1	d normal
5061	33*	0	e HB
5250	24	3	ePI?
5251	12	2	a normal
5423	10	-1	a normal
5508	5	9	PII
5643	18	8	iPII
5737	72*	-1	unknown VAR
5865	9	2	d unknown
5868	5	6	iPII
6069	-4	0	d normal
6292	24	3	ePI
6340	14	0	a normal

Table 5.2.2.

HD no.	δc_1	δm_1	comments
6427	5	-1	a d normal
6451	3	-5	Am
6532	-9	-3	Am
6790	5	1	a normal
7487	-21	1	c d normal?
7607	9	6	iPII
7676	-12	-7	a c Am?
7739	11	2	a normal
7875	18	-6	d Am
7932	3	1	a normal
8033	1	-2	a normal
8351	16	-1	Am
8380	6	-10	Am
8415	-19	-1	a c d unknown
8932	-4	-9	Am
8976	5	-8	Am
9132	53*	-67	b d e AIV? VAR
9451B	-4	9	PII VAR
9793	9	9	PII
9918SE	-16	-5	a c Am/unknown?
10148	23	0	Am/ePI?
10178	7	0	a normal
10433	22	-1	a normal
11398	13	-1	a normal
223466	-3	-9	Am
225282	8	0	a normal

Key:

iPII : Intermediate Pop.II.
PII : Pop.II.
ePI : Evolved Pop.I.
Am : Am star.
HB : Horizontal Branch.
Normal : Apparently normal MS star.
VAR : Variable velocity.
a : $E(b-y)<-0.03$.
b : $E(b-y)>0.100$.
c : $\delta c_1<-0.05$.
d : Photometric Variable?
e : $\delta\beta>0.28$

Table 5.3.1.

Population as a Function of Height

SGP

Distance (pc.)	A Stars iPII/PI	PII/PI	Am/PI	F Stars iPII/PI	PII/PI
0-99	0.05	0.03	0.08	0.11	0.04
100-199	0.02	---	0.10	0.03	0.01
200-299	0.01	---	0.03	0.03	---
300-399	---	---	0.14	---	---

Distance (pc.)	Pop.I B/A	F/A
0-99	0.05	1.26
100-199	0.04	1.05
200-299	0.02	0.36
300-399	0.03	0.07

Combined SGP and NGP samples

Distance (pc.)	A Stars iPII/PI	PII/PI	F Stars iPII/PI	PII/PI
0-99	0.04	0.00	0.12	0.02
100-199	0.03	0.01	0.08	0.01
200-299	0.03	0.00	0.07	0.02
300-399	0.00	0.00	0.10	0.02
400-499	0.04	0.00	0.25	0.04
500-999	0.16	0.01	0.44	0.06

Table 5.3.2.

PI stars more than 500 pc. from the plane.

HD Number	MK Type	Distance (pc.)	V mag.
157	B9	886	10.68
1999	B9	817	8.29
2846	F0	571	10.52
4052	A8	509	10.59
4157	A0	705	9.59
4327	A4	556	9.51
4329	A2	593	10.12
4485	A2	531	10.52
5496	B9	914	10.57
5546	A5	636	10.23
6340	A2	508	8.99
7876	F6	510	10.05
10646	A9	534	10.34

Table 5.4.1.

Detection of Velocity Variables

	$\overline{\sigma}$	n	% probable	% possible
A0-F4	8	55	16%	31%
F5-G0	5	25	16%	32%

Table 5.4.2.

Velocity Variables

HD Numbers

Probable		Possible	
A0-F4	F5-G0	A0-F4	F5-G0
1101	5156	203	1000
6668	11379	256	1683
8351	224763	319	2477
9132	225120	1431	5057
9411		1856	5659S
9673		2037	6367
223561		2395	8350
224820		2696	11549
225132		2916	
		4691	
		6178	
		6493	
		8130	
		9061	
		10798	
		223884	
		225101	
		225200	
		225282	

Table 5.5.1.

Mean and rms Velocities

South Galactic Pole

A0-F4

distance (pc.)	no. stars	$\bar{W}$ (kms^{-1})	rms. (kms^{-1})	no.obs. per star
0-300	29	-6.2	10.4	3+
0-300	49	-6.7	10.2	2+
0-200	46	-6.2	9.6	2+
0-99	25	-7.7	9.3	2+
100-199	21	-4.5	9.4	2+

F5-F9

distance (pc.)	no. stars	$\bar{W}$ (kms^{-1})	rms (kms^{-1})	no.obs. per star
0-300	13	-2.8	10.0	3+
0-200	19	-4.2	12.1	2+
0-99	14	-6.9	10.06	2+

star type	distance (pc.)	no. stars	$\bar{W}$ (kms^{-1})	rms (kms^{-1})
A0-A5	0-300	13	-4.7	13.4
A6-F4	0-300	36	-7.5	8.1
	0-99	22	-8.4	8.2
	100-199	13	-6.6	7.5
F5-F6	0-300	14	-8.0	11.1

Table 5.5.1.

North Galactic Pole

(from Hill et al 1979)

distance (pc.)	no. stars	A0-F4 $\bar{W}$ (kms^{-1})	rms (kms^{-1})	no. stars	F5-F9 $\bar{W}$ (kms^{-1})	rms (kms^{-1})
0-199	84	-6.0	9.7	109	-4.1	10.5
200-299	24	-7.7	14.0	15	-7.1	12.6

(from published data)

distance (pc.)	no. stars	A0-F4 $\bar{W}$ (kms^{-1})	rms (kms^{-1})	no. stars	F5-F9 $\bar{W}$ (kms^{-1})	rms (kms^{-1})
0-199	41	-7.9	11.7	119	-4.1	10.7

Combined NGP and SGP Data

distance (pc.)	no. stars	A0-F4 $\bar{W}$ (kms^{-1})	rms (kms^{-1})	no. stars	F5-F9 $\bar{W}$ (kms^{-1})	rms (kms^{-1})
0-200	87	-6.4	11.0	138	-4.1	10.9

Table 5.5.2.

w-velocity distribution of PI stars within 200pc.

A0-F4			F5-F9		
no. stars	$\bar{w}$ (kms^{-1})	rms (kms^{-1})	no. stars	$\bar{w}$ (kms^{-1})	rms (kms^{-1})
87	0.6	11.1	138	-2.9	10.9

Figure 5.1.1.

Extent of SGP Photometric Data

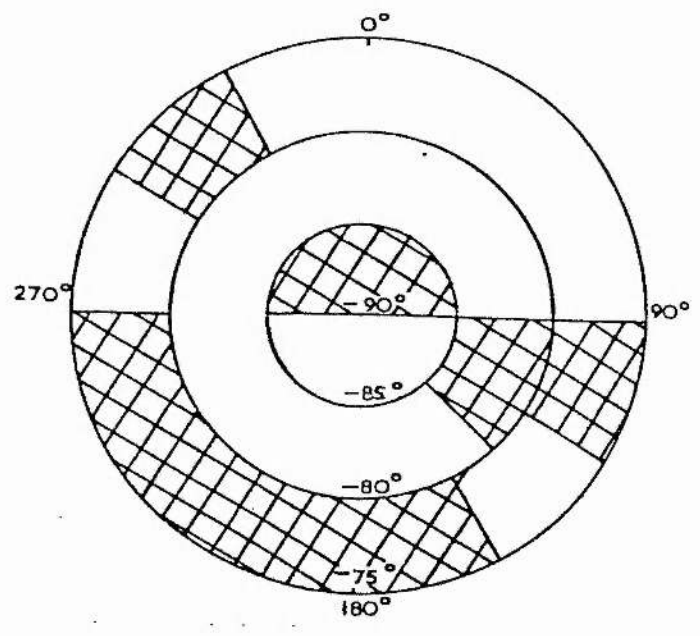

The cross-hatched areas are those for which no reddening data are available out to 400pc.

Figure 5.2.1.

c_1 - (b-y) diagram for SGP stars

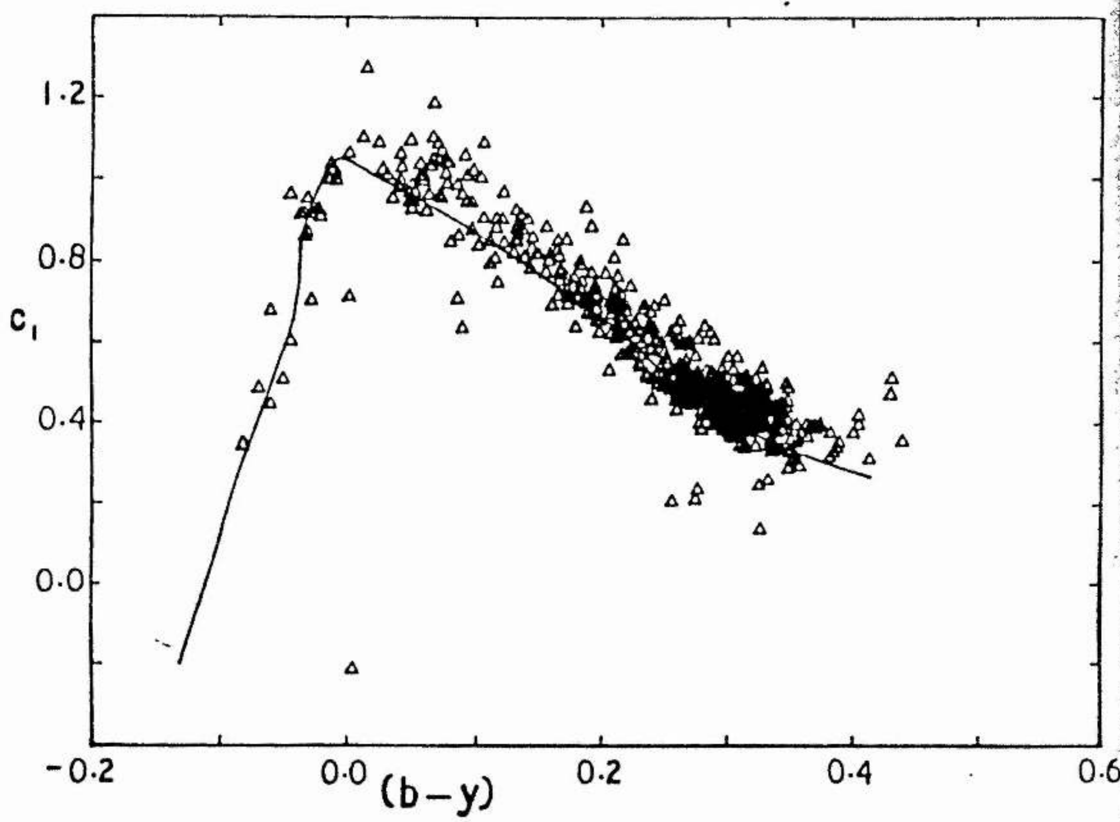

The solid line is the intrinsic colour line from Crawford (1975, 1978, 1979) and Hilditch et al (1983).

Figure 5.2.2.

m_1 - (b-y) diagram for SGP stars

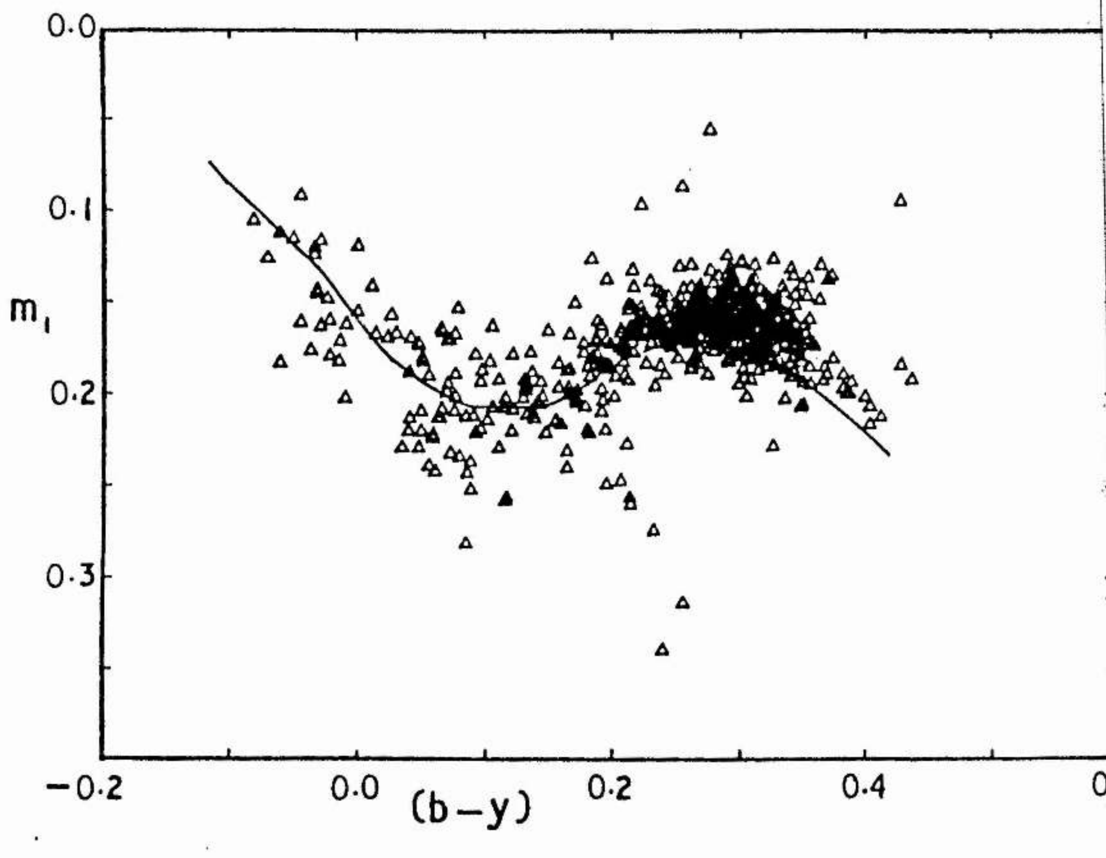

The solid line is the intrinsic colour line from Crawford (1975, 1978, 1979) and Hilditch et al (1983).

Figure 5.2.3.

β ~ (b-y) diagram for SGP stars

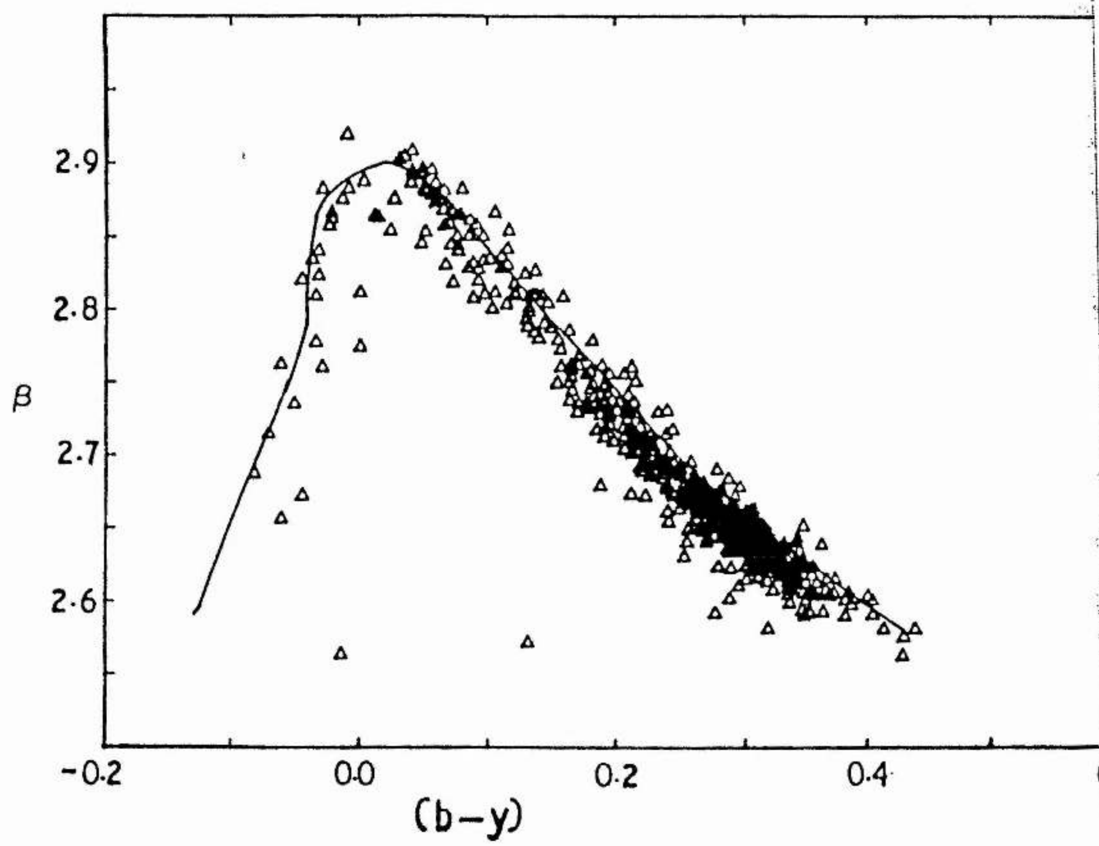

The solid line is the intrinsic colour line from Crawford (1975, 1978, 1979) and Hilditch et al (1983).

Figure 5.6.1.

δm_1 - W velocity for SGP PI and iPII stars

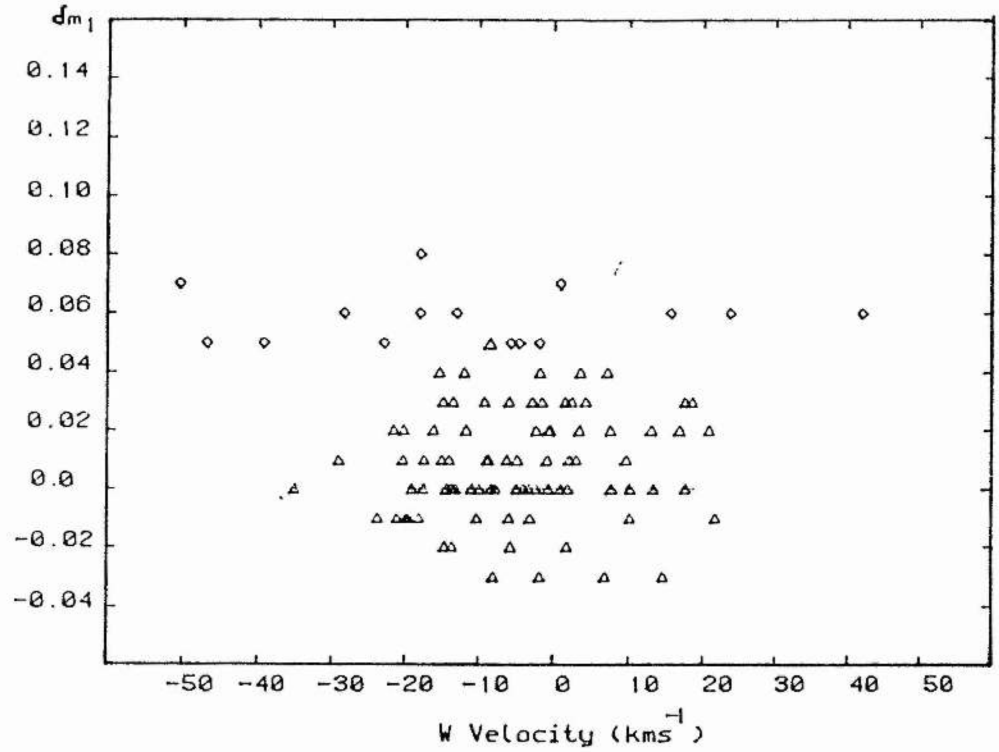

Diamonds represent iPII stars and triangles represent PI stars.

Figure 5.8.1.

Observed A Star Distributions

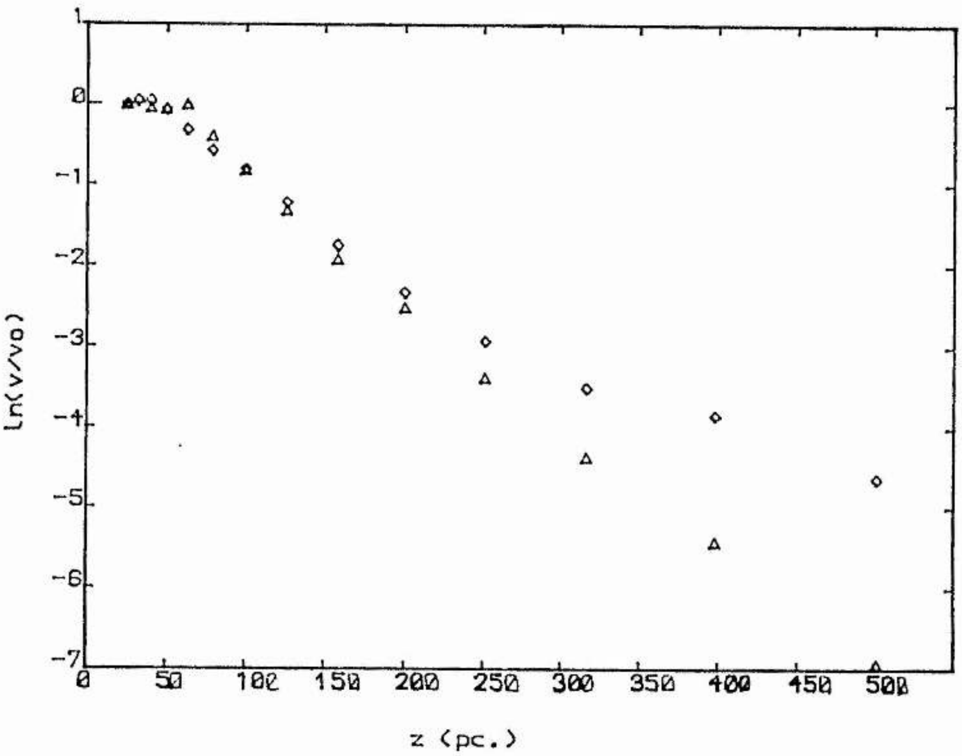

Triangles indicate distribution from galactic pole photometry. Diamonds indicate distribution given by Hill et al (1979)

Figure 5.8.2.

Observed F Star Distributions

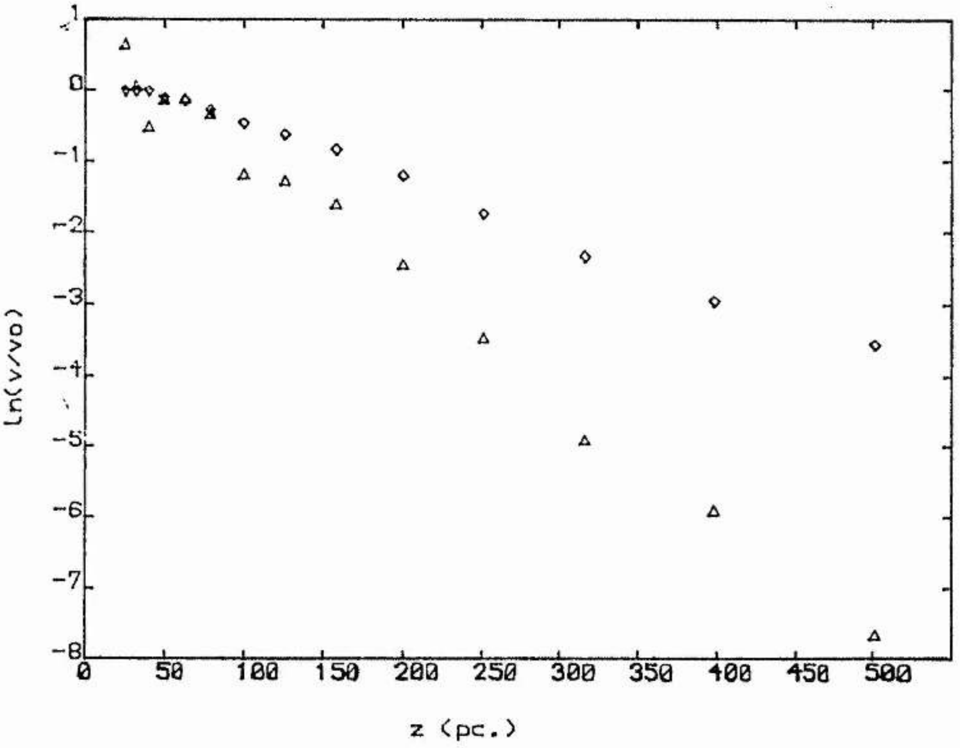

Triangles indicate distribution from galactic poles photometry. Diamonds indicate distribution given by Hill et al (1979).

Figure 5.8.3.

HHB Model: Predicted A Star Distributions

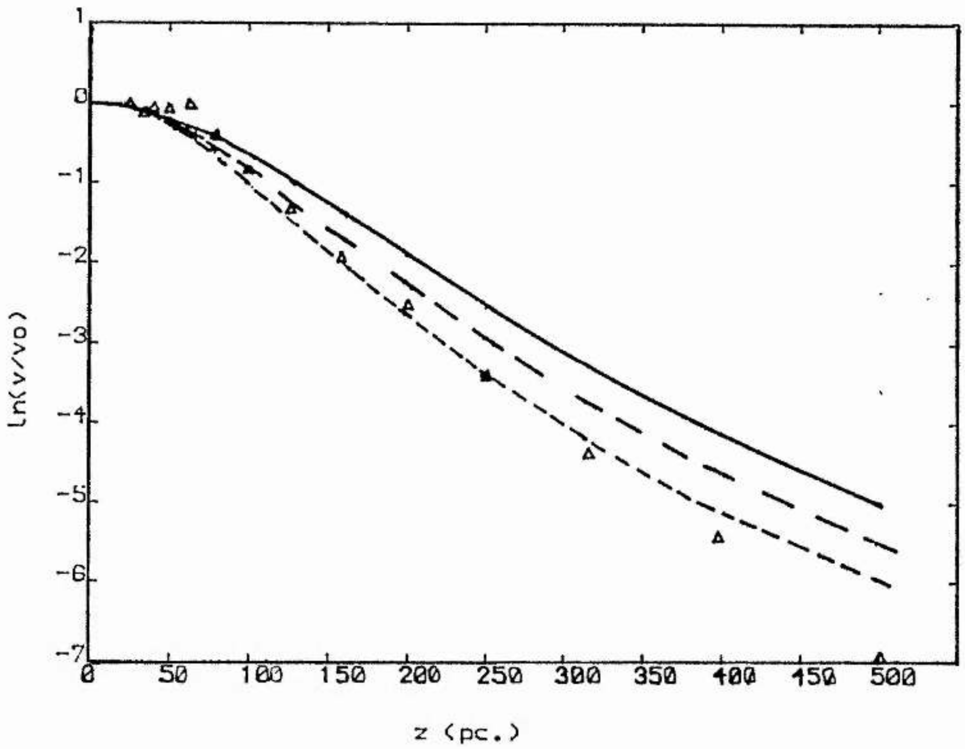

Solid line: model with ρ_0 of 0.1. Broken line: model with ρ_0 of 0.14. Dotted line: model with ρ_0 of 0.185. Triangles indicate observed distribution from galactic poles data.

Figure 5.8.4.

HHB Model: Predicted F Star Distributions

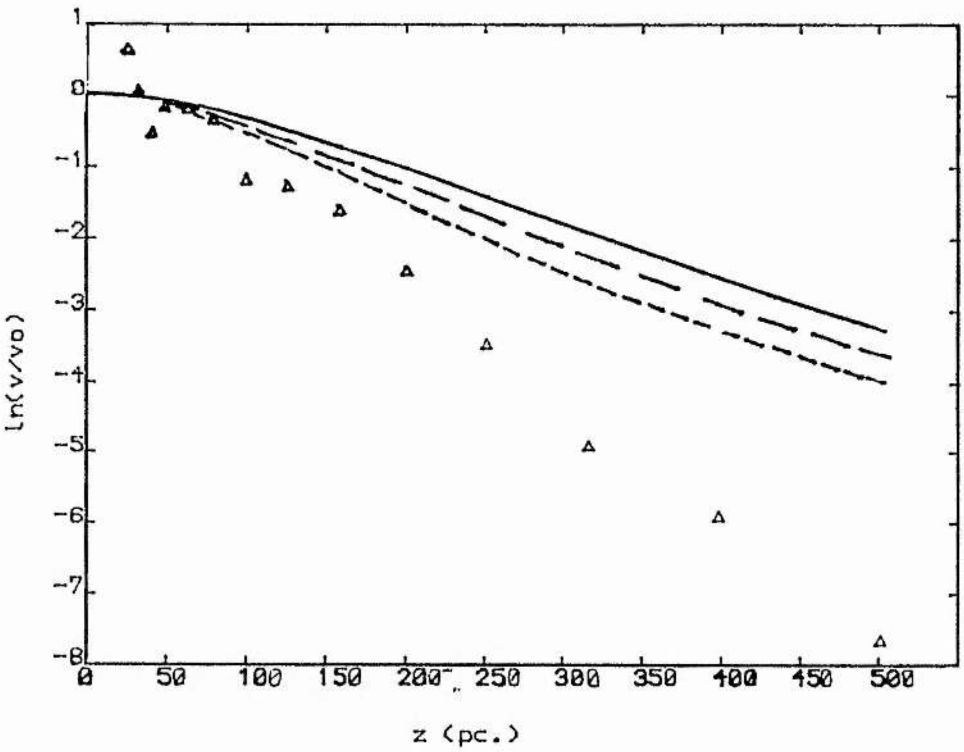

Solid line: model with ρ_o of 0.1. Broken line: model with ρ_o of 0.14. Dotted line: model with ρ_o of 0.185. Triangles indicate observed distribution from galactic poles data.

Figure 5.8.5a.

Bahcall Model: Predicted A Star Distributions for PI velocity Dispersion 7.3kms/s.

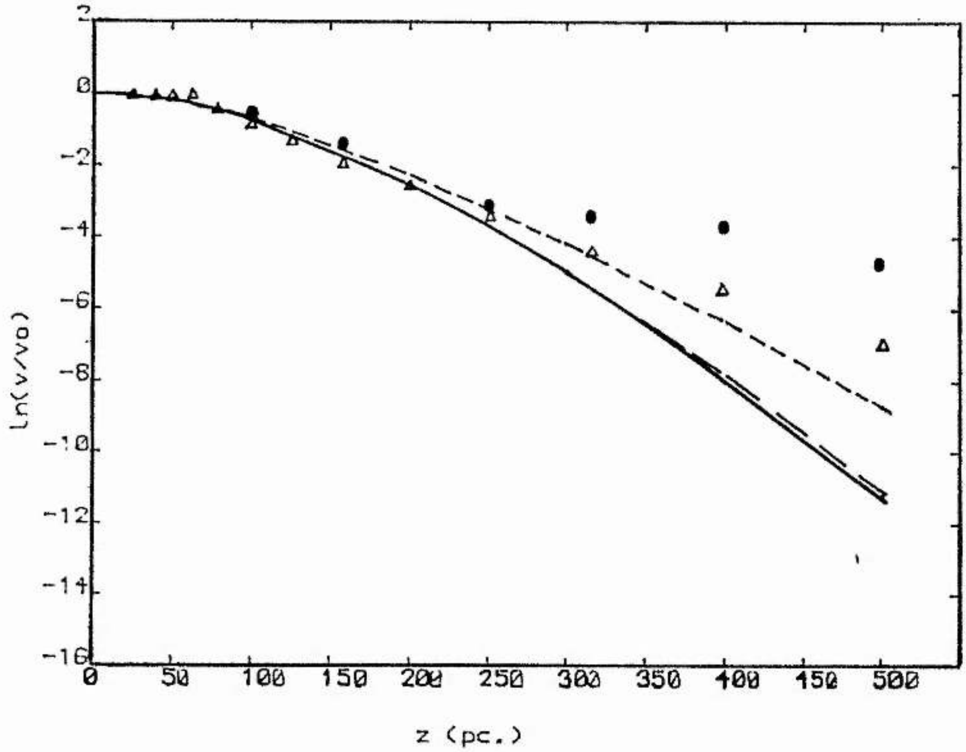

Solid line: model with ρ_0 of 0.185. Broken line: model with ρ_0 of 0.24. Dotted line: model with ρ_0 of 0.245. Triangles indicate observed distribution from galactic poles photometry. Ovals indicate observed distribution of Hill et al (1979).

Figure 5.8.5b.

Bahcall Model: Predicted A Star Distribution for PI Velocity Dispersion 11kms/1.

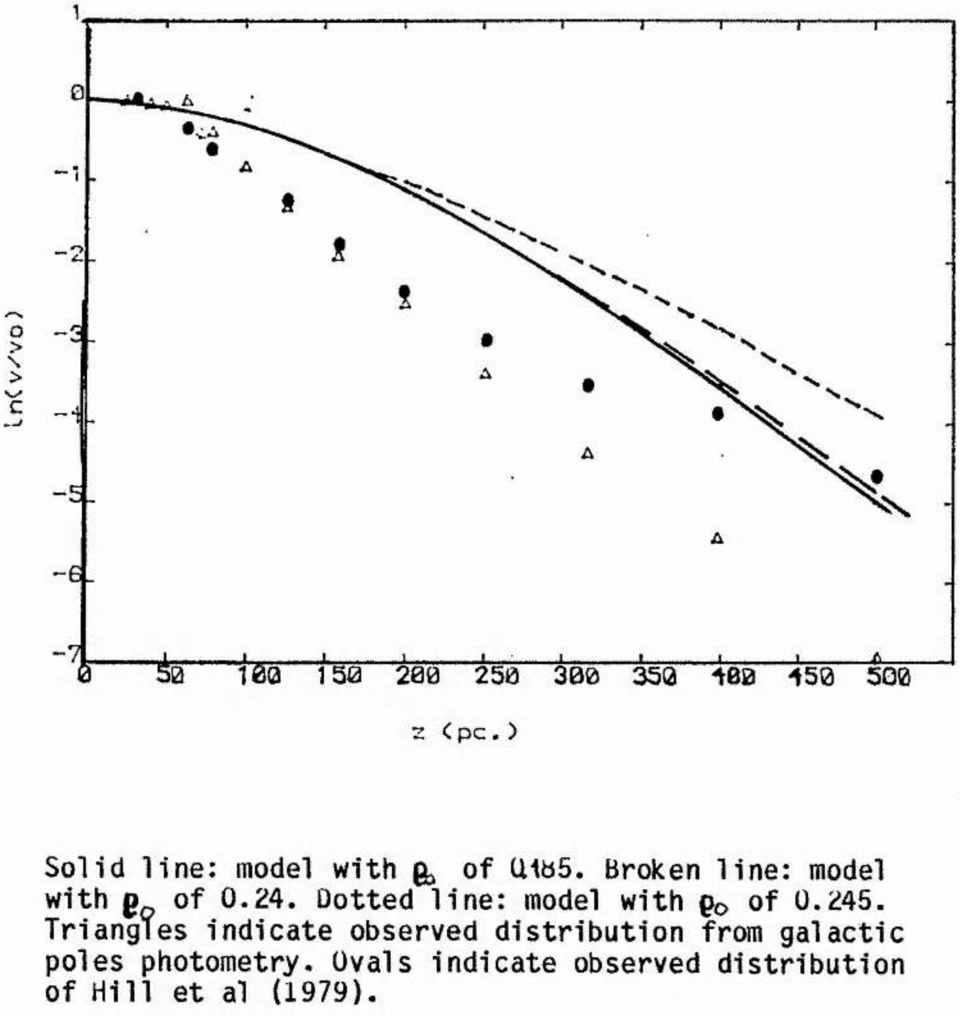

Solid line: model with ρ_0 of 0.185. Broken line: model with ρ_0 of 0.24. Dotted line: model with ρ_0 of 0.245. Triangles indicate observed distribution from galactic poles photometry. Ovals indicate observed distribution of Hill et al (1979).

Figure 5.8.6.

Bahcall Model: Predicted F Star Distributions

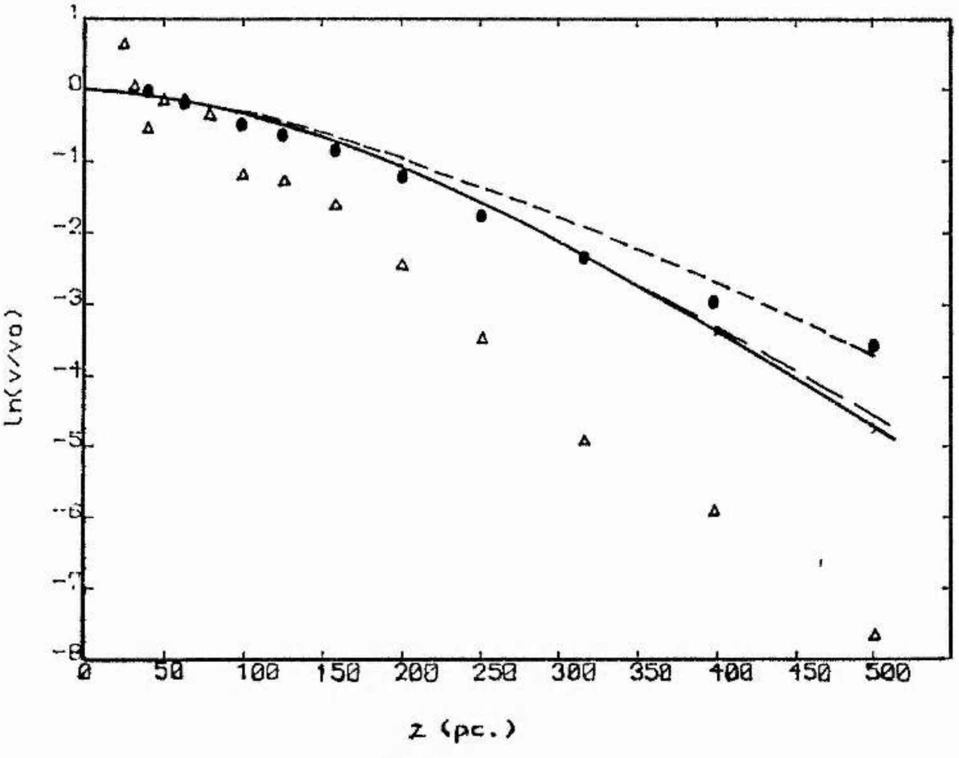

Solid line: model with $\rho_\odot$ of 0.185. Broken line: model with $\rho_\odot$ of 0.24. Dotted line: model with $\rho_\odot$ of 0.245. Triangles indicate observed distribution from galactic poles photometry. Ovals indicate observed distribution of Hill et al (1979).

Chapter 6

Conclusion

'I am too much a sceptic to deny the possibility of anything.'

T.H.Huxley

6: Conclusion

6.1 The North Galactic Pole Catalogue

The catalogue of faint blue stars presented in Appendix I has been compiled from all major post-1947 surveys of faint blue stars within 15° of the North Galactic Pole. It covers a nominal magnitude range of 13m-17m although it is not expected to give complete coverage of all blue objects in this region which fall within the required magnitude range because of:

i) the non-central position of the pole in the majority of the original surveys.

ii) mis-identifications and non-identifications of objects in the original surveys leading to the omission of faint blue objects from the surveys and the inclusion of non-existent objects.

iii) The vague nature of the colour classifications in many of these surveys, which leads to uncertainties in the assignment of 'faint blue' status to many of the stars. (Eg. many of the Luyten Blue stars were subsequently found to be of spectral type G.)

iv) the uncertainties in the magnitudes quoted in the original surveys which tend to 'blur' the upper and lower limits of the catalogue- stars which lie outwith the required magnitude range will be included and stars of the appropriate magnitude will be excluded.

In order to minimise errors in the catalogue due to iii) and iv) above the literature was searched for accurate photoelectric photometry and/or spectral classifications for the catalogue stars. Where available these provided more accurate magnitudes and spectral types. In addition all catalogue stars within 3° of the pole were assigned spectral types on the basis of objective prism and grism spectroscopy. Any objects not found on these prism and grism plates were indicated in the catalogue, reducing the errors due to misidentification. Any objects of spectral types later than G were also excluded.

The problems of non-central surveys and incomplete surveys can only be removed by a new survey centred on the pole, preferably making use of high quality objective prism plates to identify the true blue stars in the region.

6.2 South Galactic Pole Catalogue

The uvbyβ photometry of 572 O-F8 stars at the South

Galactic Pole, presented in Chapter 3, was combined with the radial velocity data on these stars presented in Chapter 4. The resulting catalogue of positions, photometric indices, reddenings, spectral types and velocities is given in Table 6.2.1. The columns give:

i) HD no.

ii) V magnitude

iii) $(b-y)_o$

iv) c_o

v) δc_1 or $\delta\beta$ if asterisked

vi) m_o

vii) δm_1

viii) Distance (pc.)

ix) Mv

x) E(b-y)

xi) Spectral Type from Michigan Spectral Catalogue

xii) Spectral Type from uvbyB photometry

xiii) Galactic Longitude

xiv) Galactic Latitude

xv) Velocity (kms^{-1})

xvl) Standard Error in Velocity (kms^{-1})

From the data contained in this catalogue the mean interstellar reddening towards the pole has been found to be $E(b-y)=-0.004\pm0.003$, in good agreement with the HI/GC method of Burstein and Heiles (1982) and the photometric findings of Perry and Johnston (1982). Equivalent MK spectral types assigned on the basis of uvbyβ photometry have been shown to agree extremely well with true MK classifications, and a number of non-PI stars in the sample have been identified from their photometric indices. In addition a list of photometrically normal PI stars more than 500pc. from the plane has been compiled. Detailed spectroscopic observation of these objects would be of interest in the light of the apparent dominance of such stars out to 1kpc. from the plane. Considering the evidence for a thick disk of iPII stars which should start to dominate just beyond this point, it is important to determine the correlation between photometrically defined population groups and those defined spectroscopically.

6.3 Space Distributions Perpendicular to the Plane

The relative proportions of various types of star have been determined from the SGP data presented in Table 6.2.1. The samples involved are small and possibly incomplete, but it is evident that PI F stars greatly outnumber PI A stars within 100pc. of the plane, yet by 200pc. the PI A stars are more numerous by a factor of three, and by a factor of fourteen at 400pc. If these variations are real then the space distribution of PI A stars must be radically different from that for the PI F stars, with a much slower decrease in number density with increasing distance from the plane.

From the combined NGP and SGP sample the increase in the numbers of iPII and PII stars beyond 400pc. is easily seen. This presumably reflects the scale height of the disk. Beyond 500pc. there are far more PI A stars relative to iPII A stars than is true for the corresponding F stars, the ratio of numbers of iPII/PI F stars being roughly consistent with the Gilmore and Reid (1983) "thick disk" of ipII stars. Compared to this "thick disk" view of the Galaxy there appear to be too many PI A stars beyond 500pc., relative to the numbers of iPII stars. There appears, therefore, to be some photometric evidence for an excess of apparent PI stars out to at least 1kpc., as reported by other authors (eg. Rodgers et al 1981). If these stars follow the same distribution law as those nearer the plane then, either the scale height of the PI A stars is much greater than 300pc., or the number of iPII A stars is much less than expected.

6.4 Velocity Distributions Perpendicular to the Plane

6.4.1 South Galactic Pole

It has been shown that all of the normal PI A stars within 200pc. of the Sun share a W-velocity distribution which is fitted by a gaussian with $W=-6.22kms^{-1}$ and rms dispersion of $\pm9.6kms^{-1}$ (from 46 stars), and the corresponding PI F stars share a distribution which is fitted by a gaussian with $W=-4.19kms^{-1}$ and rms dispersion of $\pm12.1kms^{-1}$ (from 19 stars). Although the samples involved are small and probably incomplete there is no evidence for any deviation from these gaussian distributions, either with spectral type or distance from the plane.

6.4.2 Combined Distribution of North and South Galactic Pole Stars

The mean and rms W velocities for SGP PI A and F stars agree remarkably well with those given by Hill et al (1979) for a larger sample of similar NGP stars, and also with those determined here from the published NGP velocities (Hill et al 1976). Combining the SGP sample with the published NGP data the distributions at both poles are shown to be equivalent for PI A stars within 200pc., and also for PI F stars within 200pc. In both the A and F star cases the velocity distributions within 200pc. are well fitted by gaussians and show no evidence of deviation from those gaussians. There is therefore no evidence from the available data to suggest the existence of non-gaussian velocity distributions within 200pc. of the plane, or of distributions composed of more than one gaussian. The existence of higher velocity dispersion 'contaminants' of the local W-velocity distribution is not supported by these data.

6.4.3 Implications

Taking the solar w-velocity to be 7 ± 1 kms^{-1} there is no suggestion of streaming of PI A stars throughthe galactic plane, and any apparent motion on the part of the PI F stars can be attributed to the errors (at least $\pm 2kms^{-1}$) in the net w-velocity of the F stars determined here.

Therefore, the normal PI A and F stars, lying within 200pc. of the galactic plane and less than 15° from the SGP follow similar gaussian velocity distributions. There is no evidence for non-gaussian behaviour in the present samples, and no strong evidence for any net motion of stars through the galactic plane.

6.5 Future Work

The obvious priorities are the completion of the SGP survey, to give uvbyβ photometry and radial velocities for all O-F8 stars brighter than 13m within 15° of the pole, and the completion of the NGP extension to 17m. The latter should provide data on objects beyond 2 kpc. from the plane, and should produce a substantial sample of iPII stars from the proposed thick disk. It should thus help to establish the true situation regarding the apparent excess of Pop.I stars at large z distances.

Both surveys should lead to a better knowledge of the space and velocity distributions of various population groups, establish whether or not the velocity dipsersion of a given population group does increase with z distance (and if it does, is the effect real or due to contamination of the sample), and finally lead to a redetermination of Kz and ρ_o using a truly homogeneous, high quality data sample.

Other areas briefly mentioned above which require attention are the correletion between photometrically and spectroscopically defined population groups, and the true nature of the relationship between kinematics and population. As more data becomes available on the perpendicular structure of the Galaxy and its apparent anomalies, it becomes increasingly likely that the whole definition of a stellar population will have to be reconsidered.

Table 6.2.1

HD No.	V	(b-y)o	co	dc1	mo	dm1	D pc	Mv	E(b-y)	MK Type	Phot.Type	Long.	Lat.	Vel.	Error
223466	6.43	0.077	0.974	-3	0.228	-9	100	1.43	-0.029		Am	31.62	-67.22		
223655	7.69	0.204	0.739	12	0.178	0	140	1.96	0.007	F2V	F1	13.03	-67.78	4.9	4.6
223884	6.23	0.112	1.028	22	0.186	2	127	0.71	-0.014		A5	34.91	-67.79	-3.5	9.5
223991	6.33	0.120	0.800	-4	0.191	2	47	2.99	-0.009	A2V(+F)	A5	27.54	-68.47	21.6	4.3
225282	8.31	0.067	1.006	8	0.201	0	227	1.53	-0.076	A0IV/V	A0	18.74	-68.70	11.0	8.5
19	9.90	0.377	0.365	6	0.201	1	160	3.88	-0.042		F8	61.70	-77.66		
20	8.82	0.377	0.469	20	0.130	11	182	2.53	0.051	F2V	sdFG iPII	29.46	-79.72		
30	9.82	0.307	0.477	11	0.138	5	243	2.89	-0.012		F5	61.76	-77.68		
31	8.35	-0.034	0.875	36*	0.145	-2	314	0.87	0.003		B9	59.42	-77.99		
50	9.67	0.150	0.696	-10	0.222	-1	158	3.67	0.010	A9V	A8/Am	12.81	-79.43		
90	9.65	0.329	0.540	20	0.163	3	323	2.10	-0.001		F8	54.34	-78.61		
91	9.86	0.205	0.572	-11	0.177	1	153	3.93	0.011	A9/F0V	F0	14.55	-79.53		
117	8.88	0.319	0.395	2	0.177	2	104	3.79	0.044	F2V	F9	12.45	-79.54		
140	9.82	0.269	0.528	8	0.153	2	256	2.79	-0.005		F3	49.77	-79.18		
141	7.90	-0.028	0.934	16*	0.149	-2	230	1.09	0.005	B9V	B9	18.78	-79.83	-1.8	5.6
156	7.28	0.236	0.695	15	0.192	-2	122	1.85	0.006		F2	71.84	-76.20	13.6	3.4
157	10.68	-0.030	0.921	37*	0.175	-4	886	0.94	-0.006		B9	64.98	-77.51		
171	9.35	0.274	0.489	3	0.167	0	171	3.19	-0.015		F3	59.36	-78.32		
189	8.50	0.323	0.469	10	0.180	1	127	2.99	0.012		F7	44.42	-79.59		
203	6.17	0.273	0.522	7	0.171	0	46	2.86	-0.030		F2	52.18	-79.13	14.4	9.1
225	8.24	0.326	0.471	13	0.155	4	119	2.87	0.001		F7	69.71	-76.84		
235	8.60	0.015	1.015	-1	0.176	0	221	1.87	0.016	A1V	A1	10.76	-79.70	8.4	20.0
241	10.25	0.339	0.345	0	0.175	1	159	4.25	-0.024		F7	57.44	-78.73		
243	8.41	0.275	0.496	5	1.156	1	117	3.07	-0.019	F3V	F3	340.89	-75.75		
256	6.20	0.100	1.079	26	0.169	4	147	0.37	-0.027		A4	74.34	-75.91	1.8	11.0
258	10.00	0.348	0.421	11	0.162	4	220	3.29	-0.053	F5V	F5	349.56	-77.58		
268	7.05	0.304	0.420	3	0.150	3	50	3.55	-0.004		F5	40.61	-79.97	14.9	2.4
306	9.46	0.090	0.953	9	0.171	4	342	1.79	-0.042	A0V	A1	338.52	-75.26		
319	5.92	0.082	1.047	19	0.166	4	100	0.92	-0.005		A4	55.57	-79.08	-7.2	13.9

Table 6.2.1

HD No.	V	(b-y)o	co	dc1	mo	dm1	D pc	Mv	E(b-y)	MK Type	Phot.Type	Long.	Lat.	Vel.	Error
343	9.76	0.260	0.680	21	0.177	-1	472	1.39	-0.071	A8/A9V	F0	13.35	-80.05		
392	7.59	0.322	0.515	15	0.176	1	105	2.48	-0.010		F6	47.96	-79.86	-3.0	3.6
394	9.49	0.298	0.467	5	0.187	-1	179	3.22	0.004	F8III/V+F	F6	13.04	-80.13		
427	7.87	0.297	0.499	11	0.151	3	105	2.76	0.001	F3V	F5	350.31	-78.08	-18.6	4.5
428	8.63	0.294	0.468	7	0.142	4	128	3.10	0.002	F3V	F4	343.48	-76.81		
464	9.23	0.322	0.440	6	0.200	-1	151	3.33	0.021	F6V	F7	23.20	-80.56		
465SE	10.23	0.292	0.533	14	0.141	4	368	2.40	-0.036	A9V	F3	5.97	-79.86		
466	7.74	0.253	0.160	12	0.163	1	128	2.20	0.009	F3IV/V	F3	348.99	-77.95		
484	9.37	0.314	0.388	1	0.156	3	126	3.86	-0.014		F5	72.42	-77.02		
493	5.38	0.278	0.605	17	0.178	-1	49	1.95	-0.011	F3V	F3	25.21	-80.64	5.9	4.1
506	9.79	0.272	0.500	5	0.153	2	223	3.05	-0.008	F2IV	F3	4.82	-79.87		
511	8.91	0.322	0.390	3	0.162	2	105	3.81	0.003		F6	61.79	-78.87		
535	9.81	0.190	0.777	10	0.166	2	362	2.01	-0.023	A5II/II	A8	344.44	-77.29		
536	8.35	0.288	0.509	9	0.156	2	130	2.78	-0.006	F3/5V	F4	341.13	-76.55		
562	7.65	0.090	0.966	10	0.193	1	157	1.66	-0.019	A2V	A3	38.28	-80.65	4.8	1.4
574	10.05	0.293	0.465	4	0.182	-1	226	3.28	-0.025		F3	71.87	-77.42		
575	9.46	0.360	0.435	15	0.163	5	192	3.05	-0.023		F7	67.88	-78.16		
590	9.92	0.285	0.498	7	0.164	1	247	2.96	-0.036		F2	71.94	-77.44		
605	10.31	0.319	0.427	6	0.171	1	237	3.44	-0.030		F4	66.41	-78.45		
704	8.41	0.062	1.048	14	0.175	3	282	1.16	0.009	A3V	A4	359.23	-79.83		
718	8.48	0.311	0.431	5	0.166	1	103	3.43	-0.014		F5	73.35	-77.54		
719	9.27	0.182	0.763	6	0.212	-1	243	2.35	0.031	A8IV(m)	F0/Am	36.22	-81.04		
732	7.80	0.337	0.491	14	0.190	0	106	2.68	0.012		F8	51.90	-80.35	-10.2	2.5
739	5.24	0.296	0.445	5	0.151	3	24	3.35	-0.007	F3/5V	F5	347.17	-78.32	-2.4	9.9
768	7.91	0.246	0.520	0	0.160	1	82	3.35	-0.010		F2	56.47	-80.08		
781	9.09	0.296	0.467	6	0.158	2	155	3.14	0.005	F5V	F5	35.22	-81.23		
798	8.22	0.274	0.459	0	0.170	0	88	3.49	0.008	F5V	F4	26.30	-81.29		
824	9.13	0.304	0.442	7	0.136	5	147	3.29	-0.008	F3V	F5	358.95	-80.09		
836	8.70	0.307	0.448	6	0.163	2	123	3.25	0.008	F8IV/V	F6	354.21	-79.61		

Table 6.2.1

HD No.	V	(b-y)o	co	dc1	mo	dm1	D pc	Mv	E(b-y)	MK Type	Phot.Type	Long.	Lat.	Vel.	Error
867	9.54	0.315	0.451	8	0.165	2	186	3.19	-0.006	F5V	F6	15.18	-81.22		
899	7.40	0.289	0.566	16	0.165	1	111	2.18	0.012		F5	67.62	-79.13	20.3	3.3
900	7.98	0.256	0.545	5	0.171	0	105	2.88	-0.025		F2	52.28	-80.75	17.5	4.3
923	8.50	0.072	1.060	17	0.224	-1	320	0.97	0.019	A5IV	A4	14.34	-81.32		
955	7.37	-0.077	0.349	17*	0.104	0	450	-0.89	-0.004		B4	78.87	-77.08	-7.7	2.9
1000	6.84	0.303	0.488	6	0.162	2	52	3.28	0.011		F6	66.03	-79.68	-13.1	5.4
1001	9.24	0.284	0.521	10	0.156	2	204	2.70	-0.008		F4	64.28	-79.90		
1017	9.29	0.195	0.713	4	0.184	0	218	2.60	-0.014		F0	74.36	-78.33		
1052	9.35	0.268	0.510	4	0.179	0	183	3.04	0.028		F5	80.69	-76.92		
1065	9.77	0.261	0.584	12	0.149	2	313	2.30	-0.022	F2V	F2	9.98	-81.42		
1078	8.01	0.279	0.495	6	0.155	2	99	3.02	0.000	F3V	F4	358.33	-80.62		
1086	9.80	0.108	0.952	12	0.220	-1	434	1.61	-0.015		A4/Am	73.22	-75.44		
1097	9.00	0.227	0.461	-17	0.348	-16	81	4.48	0.013	A3/F0m	F2/Am	19.69	-79.63		
1101	7.63	0.252	0.640	15	0.164	1	139	1.91	0.008		F3	74.78	-75.11	14.0	20.5
1104	9.40	0.310	0.420	5	0.148	3	150	3.52	-0.010	F3/5V	F5	9.55	-79.23		
1137	9.30	0.305	0.465	8	0.157	2	176	3.08	-0.007	F5IV/V	F5	2.20	-78.75		
1232	8.56	0.323	0.465	12	0.150	4	133	2.95	-0.018		F5	72.39	-76.14		
1234	9.18	0.289	0.502	10	0.147	3	190	2.79	0.004	F3V	F5	344.56	-76.45		
1244	9.73	0.326	0.447	9	0.163	2	205	3.17	-0.013		F6	59.26	-78.39		
1245	9.32	0.305	0.471	8	0.177	0	178	3.07	0.011		F6	59.05	-78.41		
1256	6.45	-0.059	0.510	7*	0.117	-1	195	0.00	0.009		B8	64.68	-77.67	10.3	26.5
1285	9.65	0.306	0.498	11	0.164	2	242	2.73	-0.020	F3IV/V	F4	21.10	-80.06		
1343	6.45	0.270	0.506	6	0.149	2	49	2.99	-0.018		F2	69.34	-77.10	0.7	5.8
1431	6.52	-0.042	0.711	19*	0.132	-1	162	0.47	0.043		A0?/HB?	62.00	-78.51	23.7	10.1
1432	8.69	0.314	0.434	6	0.155	3	116	3.36	-0.007	F5V	F6	353.00	-78.38		
1433	9.46	0.315	0.446	8	0.151	3	177	3.21	-0.029	F3V	F5	346.76	-77.37		
1463	9.65	0.284	0.484	7	0.143	3	208	3.05	0.002	F2IV/V	F5	4.17	-79.63		
1464	9.31	0.367	0.468	20	0.143	8	222	2.57	-0.048	F5V	F6 iPII	334.12	-74.14		
1473	9.61	0.222	0.604	3	0.182	0	223	2.86	0.022		F2	69.14	-77.51		

Table 6.2.1

HD No.	V	(b-y)o	co	dc1	mo	dm1	D pc	Mv	E(b-y)	MK Type	Phot.Type	Long.	Lat.	Vel.	Error
1482	9.26	0.290	0.471	6	0.150	2	167	3.14	-0.008	F3/5V	F4	335.41	-74.65		
1492	8.79	0.183	0.703	0	0.188	0	151	2.90	0.007	A8III	F0	356.29	-78.94		
1493	9.70	0.300	0.426	4	0.145	3	173	3.51	-0.017	F5/6V	F5	349.49	-78.00		
1498	9.16	0.295	0.494	8	0.169	1	178	2.91	-0.013		F5	46.31	-80.10		
1524	8.72	0.281	0.503	7	0.166	1	143	2.95	0.011	F5V	F5	353.52	-78.70		
1541	9.69	0.155	0.888	15	0.214	-2	433	1.51	0.001	A5III(m)	A8/Am	339.95	-76.20		
1557	9.15	0.321	0.468	11	0.156	3	174	2.95	-0.016	F3/5IV/V	F6	9.29	-80.23		
1580	9.73	0.300	0.479	9	0.157	2	225	2.97	-0.040	F0V	F3	27.24	-80.79		
1595	9.44	0.335	0.395	7	0.148	5	144	3.64	-0.006	F7V	F7	2.92	-79.88		
1597	9.79	0.244	0.574	5	0.159	1	249	2.81	-0.023	F0V	F1	348.19	-78.10		
1616	8.61	0.206	0.676	-2	0.247	-6	129	3.06	0.001		F0m	45.33	-80.46		
1619	8.65	0.205	0.691	0	0.248	-6	140	2.92	-0.009		A9/Am	45.33	-80.46		
1666	8.15	0.325	0.485	12	0.184	0	117	2.81	0.002		F7	68.58	-78.25		
1667	6.77	0.192	0.857	21	0.197	-2	135	1.11	-0.020		A9	51.62	-80.20	14.6	7.1
1683	7.10	0.317	0.486	13	0.155	3	74	2.76	0.008	F6V	F7	335.16	-75.25	2.8	5.9
1692	9.32	0.358	0.337	3	0.168	4	105	4.22	-0.022	G0V	F8	36.17	-80.97		
1738	9.28	0.311	0.434	6	0.153	3	152	3.37	-0.015	F3V	F5	338.48	-76.40		
1751	8.52	0.338	0.411	7	0.168	3	101	3.50	0.004	F7V	F8	346.36	-78.18		
1776	8.92	0.295	0.424	2	0.159	2	115	3.61	0.015		F6	53.57	-80.33		
1791	8.38	0.192	0.721	2	0.218	-3	138	2.68	-0.011	A9III	A9	336.62	-76.05		
1797	8.42	0.279	0.508	6	0.174	0	124	2.95	-0.011		F3	42.95	-81.01		
1856	6.72	0.211	0.667	5	0.180	0	66	2.61	0.006	F2IV	F1	334.03	-75.45	13.7	10.6
1857	9.48	0.320	0.470	10	0.173	1	200	2.97	-0.012	F7/G0	F6	331.72	-74.60		
1858	9.37	0.334	0.351	3	0.136	6	113	4.11	-0.023	F5V	F6 iPII	331.51	-74.52		
1909	6.50	-0.042	0.708	32*	0.019	0	172	0.32	0.014	B9IV	B9	5.46	-80.81	19.1	13.2
1938	9.99	0.324	0.440	9	0.155	3	224	3.24	-0.002	F6/7V	F7	331.06	-74.58		
1947	9.19	0.287	0.502	8	0.160	1	183	2.88	-0.002	F3V	F4	355.54	-80.01		
1980	7.41	0.337	0.418	9	0.152	5	64	3.38	-0.026		F6	78.16	-77.30	5.3	
1988	9.30	0.268	0.534	8	0.156	1	205	2.74	-0.009	F2V	F3	28.85	-81.69		

Table 6.2.1

HD No.	V	(b-y)o	co	dc1	mo	dm1	D pc	Mv	E(b-y)	MK Type	Phot.Type	Long.	Lat.	Vel.	Error
1999	8.28	-0.046	0.608	92*	0.091	2	817	-1.28	0.002	B8II	B9	338.01	-77.06	-20.9	3.8
2007	9.48	0.107	0.969	13	0.236	-3	394	1.50	-0.018		A4	81.36	-76.53		
2026	8.12	0.078	1.002	0	0.221	-8	244	1.18	-0.019	A1V	A2/Am	17.90	-81.63	-8.2	1.6
2037	8.35	0.196	0.796	15	0.125	6	224	1.61	-0.120	A5IV	F0? iPII	32.35	-81.79	13.0	6.8
2050	9.29	0.345	0.420	9	0.179	2	152	3.39	-0.004		F8	46.97	-81.40		
2062	9.14	0.288	0.448	4	0.138	4	143	3.37	0.005	F5V	F5	352.58	-79.94		
2068	8.46	0.282	0.505	8	0.152	2	131	2.87	-0.006		F4	54.85	-80.96		
2069	8.23	0.262	0.642	18	0.167	1	201	1.71	0.020		F4	49.89	-81.29		
2080	8.82	0.251	0.580	8	0.166	1	176	2.59	-0.030		F1	71.71	-78.99		
2131	8.85	0.344	0.350	4	0.143	6	90	4.08	-0.009	F7V	F7 iPII	351.99	-77.51		
2160	8.32	0.283	0.564	14	0.176	0	160	2.30	0.025		F6	68.89	-76.60		
2161	7.63	0.329	0.499	15	0.178	2	102	2.59	0.018		F8	65.03	-77.29		
2178	7.62	0.068	1.097	22	0.168	4	254	0.60	-0.044		A1	58.38	-78.25	32.0	
2200	10.22	0.282	0.508	9	0.140	3	304	2.80	-0.020	F0/2V	F2	17.45	-79.72		
2215	10.17	0.310	0.428	5	0.160	2	220	3.45	-0.006	F5V	F6	8.62	-79.33		
2240	10.13	0.283	0.591	17	0.166	1	424	1.99	-0.043	F0V	F2	334.51	-73.51		
2269	9.48	0.284	0.521	10	0.152	2	229	2.69	-0.012	F0V	F3	8.00	-79.40		
2279	9.05	0.327	0.419	6	0.174	1	129	3.50	0.002	F7V	F7	336.60	-74.35		
2288	10.08	0.253	0.603	11	0.173	0	353	2.34	-0.006		F2	65.43	-77.52		
2318	8.45	0.265	0.658	19	0.185	-2	235	1.59	-0.003		F3	63.07	-77.97		
2319	9.10	0.319	0.401	3	0.160	2	120	3.71	-0.029	F5V	F5	336.74	-74.51		
2320	8.93	0.202	0.708	5	0.180	0	193	2.51	-0.010	A9V	F0	335.99	-74.27		
2327	9.09	0.299	0.475	8	0.155	2	164	3.01	0.002		F6	51.43	-79.27		
2337	9.33	0.336	0.414	9	0.145	5	153	3.40	-0.035		F6	63.79	-77.92		
2348	8.69	0.359	0.251	-11	0.227	-4	48	5.28	-0.003	F6V	F6	8.30	-79.60		
2362	9.52	0.291	0.468	5	0.160	1	184	3.20	-0.014		F4	54.25	-79.10		
2381	7.73	0.251	0.503	0	0.154	2	74	3.38	-0.002	F2V	F2	4.09	-79.37	20.2	2.6
2395	6.77	0.144	0.863	10	0.201	0	95	1.89	0.001		A7	65.52	-77.80	13.2	7.3
2402	9.73	0.331	0.403	6	0.158	3	167	3.61	-0.017		F6	74.88	-75.94		

Table 6.2.1

HD No.	V	(b-y)o	co	dc1	mo	dm1	D pc	Mv	E(b-y)	MK Type	Phot.Type	Long.	Lat.	Vel.	Error
2415	11.07	-0.019	1.007	312*	0.183	-4			0.005	B9/A0V	Unknown	16.43	-80.13		
2425	8.31	0.309	0.413	4	0.156	4	88	3.60	0.033		F8	43.59	-79.98		
2450	9.32	0.344	0.310	-3	0.172	2	88	4.60	0.008		F8	41.79	-80.11		
2465	9.11	0.378	0.357	6	0.200	1	107	3.96	0.011	G3V	G2	8.04	-79.84		
2477	7.10	0.324	0.436	10	0.137	6	59	3.23	-0.016	F5V	F6 iPII	17.54	-80.30	-23.8	6.1
2527	7.09	0.182	0.935	29	0.174	1			0.006		F0/ePI	45.16	-80.14	-5.1	14.4
2528	9.90	0.331	0.478	14	0.161	3	265	2.78	-0.052	F0/2V	F4	14.79	-80.31		
2554	9.84	0.258	0.642	17	0.165	1	408	1.79	-0.018		F2	76.22	-76.09		
2557	9.06	0.273	0.502	5	0.157	1	161	3.03	-0.028	F0V	F2	4.36	-79.76		
2571	9.89	0.369	0.445	16	0.174	5	249	2.90	-0.002		F8	74.49	-76.55		
2574	10.11	0.322	0.487	12	0.176	1	292	2.78	-0.028	F5V	F5	16.07	-80.43		
2613A	10.74	0.268	0.553	12	0.129	4	453	2.46	-0.015		F2	53.26	-79.77		
2613B	11.19	0.115	0.745	-13	0.256	-5	317	3.69	0.002		A5/Am	53.26	-79.77		
2615	7.62	0.317	0.435	9	0.127	6	75	3.25	-0.016	F5V	F6 iPII	359.37	-79.44		
2640	9.27	0.302	0.492	11	0.156	2	196	2.80	0.001		F6	71.16	-77.50		
2641	9.52	0.069	0.993	-1	0.208	-7	448	1.26	-0.019	A0V	A2/Am	11.67	-80.40		
2696	5.14	0.065	1.044	14	0.161	5	62	1.17	0.014		A4	50.51	-80.18	8.5	10.2
2719	7.47	0.313	0.468	10	0.156	3	79	2.99	0.015		F6	73.07	-77.34	-4.3	1.2
2724	6.12	0.178	0.886	21	0.193	0	103	1.06	0.014	F0/2III	A9/Am	331.63	-73.83	-3.5	5.9
2783	8.40	0.254	0.652	16	0.183	-1	205	1.85	-0.016		F2	63.08	-79.18		
2797	9.65	0.297	0.211	-29	0.313	-14			-0.014		Unknown	71.80	-77.82		
2799	10.96	0.010	1.279	24	0.169	0	1191	0.6	0.005	B9/A0V	B9/HB?	346.13	-78.06		
2810	10.13	0.337	0.453	11	0.171	2	261	3.05	-0.036		F6	54.27	-80.15		
2846	10.52	0.229	0.711	16	0.165	1	571	1.74	-0.022		F0	55.75	-80.10		
2859	10.31	0.331	0.449	11	0.155	4	279	3.08	-0.042		F4	57.26	-79.98		
2860	9.97	0.243	0.628	11	0.163	1	346	2.28	0.002		F2	52.70	-80.37		
2862	9.35	0.329	0.410	7	0.151	4	147	3.52	-0.003	F6V	F7	9.86	-80.73		
2870	9.47	0.393	0.425	15	0.213	1	186	3.12	0.011	G3V	G2	39.93	-81.05		
2903	9.73	0.303	0.463	6	0.177	0	203	3.19	0.002	F6V	F6	32.90	-81.27		

Table 6.2.1

HD No.	V	(b-y)o	co	dc1	mo	dm1	D pc	Mv	E(b-y)	MK Type	Phot.Type	Long.	Lat.	Vel.	Error
2916	7.30	0.252	0.544	5	0.160	1	75	2.93	-0.005		F2	46.55	-80.87	-9.7	7.3
2978	9.63	0.295	0.514	11	0.163	1	246	2.67	-0.054		F2	60.80	-79.92		
2980	8.94	0.214	0.726	15	0.168	1	274	1.75	0.001	F0V	F1	350.14	-79.14		
2988	9.41	0.282	0.497	7	0.153	2	196	2.95	0.008		F4	47.16	-81.01		
2998	10.07	0.340	0.449	10	0.189	0	245	3.13	0.002		F8	53.72	-80.62		
3002	9.48	0.142	0.856	9	0.191	1	314	2.00	-0.011	A5IV/V	A6	351.72	-79.41		
3017	9.59	0.359	0.348	4	0.169	4	126	4.09	-0.036		F7	77.07	-77.35		
3019	8.88	0.327	0.473	12	0.176	1	156	2.90	-0.008		F6	62.28	-79.86		
3020	10.19	0.319	0.425	5	0.173	1	221	3.47	-0.016		F6	49.12	-80.97		
3033	9.04	0.390	0.400	11	0.225	-1	130	3.46	0.014		G1	330.42	-74.31		
3058	9.30	0.274	0.489	5	0.141	3	174	3.10	-0.005		F3	54.55	-80.71		
3061	7.86	0.225	0.639	7	0.153	2	119	2.49	-0.012	F0V	F1	334.88	-76.02		
3085	7.41	-0.030	0.921	-10*	0.163	-3	169	1.27	0.002	B9V	B9	331.85	-75.02	-6.9	20.5
3092	8.22	0.306	0.421	3	0.163	2	86	3.56	-0.015	F5V	F5	333.32	-75.60		
3109	10.39	0.265	0.438	-4	0.171	0	203	3.85	-0.005	F3/5V	F4	346.81	-78.96		
3118	10.60	0.279	0.470	2	0.181	-1	281	3.36	-0.016	F2V	F3	347.40	-79.09		
3132	9.34	0.316	0.492	12	0.167	2	209	2.74	0.005		F7	73.68	-78.50		
3135	9.67	0.225	0.670	2	0.261	-8	234	2.82	-0.011	Ap SiCr	F1/Am	340.09	-77.70		
3180	9.66	0.298	0.406	3	0.123	6	157	3.68	-0.008		F5 iPII	49.12	-81.36		
3186	7.62	-0.053	0.549	90*	0.160	-5	698	-1.60	0.330		sdFG?	49.61	-78.92		
3216	9.43	0.276	0.490	4	0.171	0	180	3.16	0.016		F5	70.66	-76.14		
3217	8.36	0.298	0.406	0	0.158	2	82	3.78	-0.020		F4	69.98	-76.28		
3244	8.23	0.200	0.773	15	0.149	3	203	1.69	-0.029		A8	39.85	-79.59	-1.6	3.0
3257	8.62	0.247	0.607	11	0.145	3	183	2.30	-0.003	F0V	F2	31.83	-79.81		
3299	9.65	0.147	0.883	13	0.187	1	403	1.62	-0.010		A6	75.48	-75.16		
3300	10.28	0.357	0.428	13	0.162	5	267	3.15	-0.069		F4	48.36	-79.23		
3311	9.01	0.077	0.926	0	0.241	-4	216	2.34	-0.016		A2	69.32	-76.64		
3314	9.80	0.345	0.351	2	0.161	4	137	4.12	-0.010	F6V	F7	23.78	-79.90		
3316	9.27	0.367	0.399	9	0.191	1	141	3.52	-0.001	GIII+G	F9	339.33	-75.02		

Table 6.2.1

HD No.	V	(b-y)o	co	dc1	mo	dm1	D pc	Mv	E(b-y)	MK Type	Phot.Type	Long.	Lat.	Vel.	Error
3326	6.05	0.170	0.723	-3	0.230	-3	39	3.08	-0.005		A8	53.15	-78.90	8.1	2.3
3338	8.48	0.233	0.645	10	0.156	2	172	2.31	-0.010	F0V	F1	32.46	-79.94		
3337	7.86	0.295	0.426	1	0.164	1	70	3.63	-0.010		F4	62.30	-77.88		
3354	9.26	0.325	0.383	1	0.190	-1	117	3.92	-0.022		F6	73.09	-75.91		
3391	10.07	0.296	0.468	6	0.168	1	240	3.17	-0.007	F5V	F4	357.69	-78.57		
3389	7.93	0.242	0.700	17	0.194	-2	178	1.68	-0.008	F3IV/V	F2	28.75	-80.08		
3387	10.05	0.320	0.382	3	0.141	5	172	3.87	-0.004		F6	69.52	-76.82		
3417	10.76	0.203	0.710	6	0.718	0	462	2.44	-0.018	A8V	A9	353.38	-78.08		
3423	10.24	0.268	0.494	3	0.160	1	258	3.18	-0.012		A3	63.66	-77.91		
3436	9.81	0.210	0.631	-3	0.182	0	210	3.20	-0.012	F0V	F0	4.93	-79.35		
3437	10.10	0.327	0.474	11	0.186	0	272	2.92	-0.013	F6V	F6	2.72	-79.17		
3479	8.52	0.262	0.598	14	0.144	3	191	2.12	0.007	F0V	F3	39.56	-80.08		
3506	8.38	0.285	0.537	12	0.157	2	148	2.52	-0.001		F4	76.87	-75.49		
3525	8.73	0.306	0.459	7	0.166	2	131	3.15	0.014	F6V	F6	333.10	-73.60		
3559	8.49	0.107	0.906	7	0.207	0	194	2.05	0.009		A6	44.88	-80.04		
3580	6.72	-0.061	0.490	23*	0.125	-2	258	-0.34	-0.009		B7	65.62	-78.08	5.7	6.2
3581	7.10	0.267	0.492	3	0.157	1	60	3.20	-0.002		F3	50.69	-79.72	8.7	4.5
3596	8.92	0.310	0.508	13	0.171	1	183	2.61	0.005		F6	62.75	-78.52		
3597	8.84	0.326	0.430	8	0.154	4	126	3.33	0.002	F6V	F7	339.77	-75.92		
3604	9.52	-0.029	0.929	6*	0.181	-5	471	1.16	0.008		Am odd	72.18	-76.94		
3621	8.20	0.346	0.393	9	0.153	6	84	3.59	0.027		G0 iPII	71.00	-77.22		
3622	7.76	0.139	0.812	2	0.206	0	110	2.55	-0.024	A5V	A5	39.71	-80.37	3.3	4.3
3696	10.03	0.282	0.494	6	0.165	1	251	3.03	-0.004	F2/3V	F4	346.73	-77.71		
3734	9.27	0.293	0.412	2	0.130	5	132	3.67	-0.001	F2V	F5	33.38	-80.77		
3735	6.65	0.335	0.381	6	0.134	7	38	3.75	0.005	F7V	F7 iPII	352.96	-78.80	-24.8	
3736	8.57	0.104	1.096	29	0.163	4			0.002	A6V	A5 ePI	340.65	-76.52		
3762	8.03	0.393	0.884	61	0.195	3			-0.261	A8V	A6 iPII	336.41	-75.40		
3772	10.00	0.249	0.655	17	0.158	1	437	1.79	-0.022	Ap SiCr	F1	344.67	-77.50		
3785	8.66	0.335	0.453	13	0.156	4	136	3.00	0.008	F8V	F8	339.92	-76.45		

Table 6.2.1

HD No.	V	(b-y)o	co	dc1	mo	dm1	D pc	Mv	E(b-y)	MK Type	Phot.Type	Long.	Lat.	Vel.	Error
3783	9.51	0.315	0.424	4	0.172	1	159	3.49	-0.031		F4	52.48	-80.04		
3813	10.18	0.308	0.432	5	0.163	2	244	3.43	-0.018	F3/5V	F5	346.52	-77.94		
3812	9.57	0.289	0.504	9	0.152	2	226	2.80	-0.026	F0V	F3	0.37	-79.77		
3835	8.30	0.330	0.402	6	0.153	4	87	3.61	0.013	F6/7V	F7	29.14	-80.99		
3850	9.32	0.259	0.508	3	0.156	1	171	3.15	0.002	F6/G	F3	330.88	-73.65		
3864	9.11	0.297	0.560	17	0.155	2	252	2.10	-0.030		F3	54.36	-80.06		
3865	9.84	0.285	0.472	3	0.179	-1	205	3.28	-0.021		F3	52.32	-80.22		
3867	8.25	0.036	0.972	-1	0.191	0	171	2.09	0.016	A1V	A2	332.18	-74.22		
3876	10.12	0.267	0.527	6	0.161	1	283	2.86	0.000		F3	57.88	-79.77		
3885	9.79	-0.043	0.685	23*	0.182	-6			-0.017		Unknown	69.20	-78.30		
3978	9.59	0.272	0.482	3	0.167	1	184	3.27	0.008		F4	55.79	-80.22		
3999	9.32	0.079	0.987	-1	0.219	-8	399	1.32	-0.039	A2V	A2Am	1.17	-80.27		
4010	9.84	0.295	0.434	3	0.150	3	187	3.48	-0.015	F3V	F4	36.98	-81.27		
4011	9.55	0.211	0.855	32	0.144	3			0.006	A9V	F1 ePI	351.18	-79.18		
4023	9.25	0.316	0.457	9	0.157	3	170	3.10	-0.010		F6	68.31	-78.84		
4035	8.72	0.331	0.417	7	0.161	3	113	3.46	-0.007		F7	73.17	-78.01		
4052	10.59	0.193	0.779	9	0.214	-3	509	2.06	-0.038	A5	A8	359.11	-80.18		
4065	6.00	-0.031	0.912	8*	0.162	-3	94	1.13	0.010	B9.5V	B9	335.94	-76.10	1.8	10.3
4072	10.22	0.292	0.550	16	0.148	3	394	2.24	-0.027		F3	73.00	-78.14		
4073	9.56	0.261	0.521	4	0.161	1	204	3.01	0.007	F2V	F3	34.22	-81.43		
4110	10.26	0.211	0.689	9	0.171	1	394	2.28	-0.002		F0	76.37	-77.55		
4124	8.94	0.320	0.438	6	0.185	0	131	3.34	0.001	F6V	F6	38.98	-81.44		
4148	8.90	0.307	0.381	1	0.131	5	99	3.92	0.004	F3V	F6	8.88	-81.13		
4157	9.59	0.107	1.071	26	0.154	5	705	0.34	-0.106		A0	69.72	-79.01		
4158	9.54	0.244	0.744	29	0.095	8			-0.021		F1 iPII	69.12	-79.11		
4169	7.61	0.303	0.429	3	0.163	2	66	3.50	0.005	F5V	F6	337.93	-77.01		
4189	9.03	0.349	0.342	1	0.174	2	91	4.23	-0.010	F8V	F8	8.80	-81.22		
4210	8.96	0.287	0.464	4	0.166	1	136	3.29	0.016	F5V	F6	350.39	-79.57		
4247	5.22	0.233	0.553	1	0.137	4	26	3.19	-0.003		F1	62.58	-80.24	12.0	4.9

Table 6.2.1

HD No.	V	(b-y)o	co	dc1	mo	dm1	D pc	Mv	E(b-y)	MK Type	Phot.Type	Long.	Lat.	Vel.	Error
4248	10.35	0.138	0.851	6	0.210	-1	433	2.17	-0.005		A6	53.60	-81.05		
4259	8.93	0.238	0.632	11	0.151	2	210	2.32	-0.015		F1	70.20	-79.24		
4260	9.08	0.263	0.516	5	0.153	2	164	3.00	-0.023		F2	65.59	-79.91		
4274	8.71	0.353	0.402	10	0.160	5	111	3.47	0.002		F8	66.88	-76.80		
4288	9.85	0.320	0.449	10	0.140	5	222	3.12	-0.012		F6	42.44	-79.41		
4289	8.93	0.324	0.508	15	0.166	2	193	2.51	-0.071	F3V	F2	26.75	-79.75		
4291	8.92	0.270	0.509	6	0.144	3	157	2.94	0.009	F0V	F4	342.72	-75.68		
4327	9.51	0.083	1.059	21	0.188	2	556	0.78	-0.006		A4	61.34	-77.85		
4329	10.12	0.065	1.038	13	0.212	-1	593	1.25	0.000	A0V	A2	21.57	-79.78		
4338	6.47	0.185	0.806	12	0.189	0	86	1.80	-0.002		A9	76.00	-74.95	4.0	6.6
4339	9.80	0.292	0.474	7	0.149	3	220	3.08	-0.006		F4	60.12	-78.04		
4375	7.26	0.293	0.527	13	0.150	3	90	2.49	-0.003		F5	75.64	-75.16	13.5	3.4
4397	9.01	0.361	0.292	2	0.139	9	74	4.65	-0.012		F8 PII	55.97	-78.65		
4399	9.65	0.165	0.806	8	0.195	0	318	2.14	-0.007	A9V	A8	20.64	-79.90		
4414	9.06	0.206	0.703	6	0.168	1	214	2.41	-0.018	F0V	A9	39.42	-79.79		
4417	9.86	0.346	0.423	9	0.180	1	200	3.35	-0.036	F6/7V	F6	357.90	-78.50		
4426	9.48	0.326	0.469	12	0.158	3	206	2.91	-0.001		F7	50.16	-79.22		
4455	8.96	0.311	0.431	6	0.151	3	129	3.40	-0.011	F5V	F5	358.41	-78.63		
4470	9.31	0.281	0.541	1	0.156	2	227	2.52	-0.019		F3	65.67	-77.51		
4485	10.52	0.084	0.952	7	0.179	3	531	1.89	-0.033	A0IV	A2	357.06	-78.52		
4507	7.50	0.121	0.907	9	0.219	-1	131	1.90	0.000		A5	46.76	-79.60	-10.2	2.3
4530	9.06	0.337	0.405	7	0.166	3	125	3.57	-0.006	F7V	F7	18.76	-80.07		
4586	9.18	0.253	0.616	13	0.158	1	258	2.12	-0.016	F0V	F2	31.43	-80.28		
4596	9.12	0.303	0.539	16	0.152	3	233	2.28	-0.007	F3V	F5	0.86	-79.16		
4622	5.56	-0.025	0.960	33*	0.142	-1	82	0.98	-0.006		B9	59.38	-78.75	19.5	4.0
4623	7.57	0.209	0.736	15	0.169	1	146	1.74	-0.013	F0IV	F0	17.34	-80.20	0.8	0.0
4642	9.25	0.376	0.316	2	0.913	2	92	4.43	-0.020	F7V	F8	9.29	-79.91		
4679	8.64	0.302	0.426	4	0.152	3	106	3.50	0.007		F6	71.95	-76.95		
4689	9.42	0.313	0.489	12	0.165	2	212	2.79	-0.058		F3	53.51	-79.55		

Table 6.2.1

HD No.	V	(b-y)o	co	dc1	mo	dm1	D pc	Mv	E(b-y)	MK Type	Phot.Type	Long.	Lat.	Vel.	Error
4691	6.76	0.243	0.580	6	0.155	2	63	2.75	-0.019	F0V	F1	22.21	-80.50	0.4	7.3
4731A	8.85	0.291	0.437	0	0.181	-1	112	3.60	0.000		F5	61.66	-78.83		
4731B	9.99	0.381	0.378	8	0.214	0	179	3.73	0.019		G3?	61.66	-78.83		
4735	8.97	0.340	0.417	10	0.151	5	132	3.36	-0.022	F5V	F6	338.59	-75.78		
4763	8.53	0.295	0.451	6	0.133	5	114	3.24	-0.005	F6V	F5	27.56	-80.70		
4772	6.27	0.078	1.193	36	0.165	4	136	0.6	-0.011		A2 HB?	52.40	-79.84	-3.4	5.1
4792	9.46	0.362	0.416	11	0.178	3	169	3.31	-0.014	F7V	F8	2.90	-79.81		
4876	9.43	0.284	0.618	17	0.226	-6	321	1.90	-0.072	APIII/IV	F1/Am	28.82	-80.96		
4966	9.51	0.361	0.319	4	0.145	8	108	4.35	-0.008		F8 iPII	74.13	-77.41		
4974	9.47	0.215	0.683	10	0.163	2	285	2.19	0.004	F0V	F0	348.57	-78.56		
4975	7.09	0.357	0.393	7	0.191	1	49	3.65	0.010	G1V	F8	336.63	-75.90	17.4	3.9
4983	9.18	0.350	0.263	-7	0.166	3	65	5.10	-0.017	F8/G0 V	F7	6.64	-80.52		
4999	9.82	0.269	0.518	6	0.158	1	241	2.91	-0.012	F5IV	F3	34.71	-81.18		
5024	9.21	0.241	0.700	19	0.162	1	344	1.53	-0.022	A9V	F0	6.63	-80.61		
5057	7.54	0.286	0.448	2	0.165	1	65	3.46	0.019		F6	64.96	-79.24	8.9	7.2
5060	9.49	0.326	0.396	3	0.179	0	140	3.76	-0.001	F8/G0V	F7	0.01	-80.15		
5061	8.52	-0.014	1.104	33*	0.156	0	404	0.6	0.026	A0V	A0 HB?	344.53	-78.02		
5132	7.57	0.173	0.738	0	0.227	-3	88	2.84	0.010		F0	78.06	-77.03	6.8	
5134	9.07	0.354	0.381	6	0.176	3	116	3.76	0.005	G0V	F8	356.92	-80.04		
5145	9.30	0.295	0.517	12	0.147	3	221	2.57	-0.010		F4	45.10	-81.16		
5156	6.44	0.289	0.522	12	0.143	3	59	2.57	-0.001		F4	46.28	-81.12	-17.6	13.1
5173	8.33	0.226	0.619	5	0.183	-1	134	2.69	0.001	F0V	F1	334.93	-75.97		
5204	9.69	0.331	0.414	6	0.174	1	170	3.53	-0.013	F8V	F6	18.42	-81.49		
5205	8.58	0.233	0.648	10	0.164	1	180	2.30	-0.006	F0IV/V	F1	333.94	-75.71		
5228	8.98	0.293	0.471	6	0.156	2	148	3.13	-0.013	F2/3V	F4	10.38	-81.23		
5250	8.81	0.301	0.609	24	0.149	3			-0.031		F3 ePI	44.94	-81.37		
5251	8.96	0.307	0.500	12	0.159	2	179	2.70	-0.036		F3	44.94	-81.37		
5265	8.53	0.265	0.500	4	0.146	3	122	3.10	0.003	F3V	F3	338.92	-77.32		
5270	10.05	0.330	0.454	11	0.162	3	251	3.05	0.003	G2/3V	F7	6.12	-81.08		

Table 6.2.1

HD No.	V	(b-y)o	co	dc1	mo	dm1	D pc	Mv	E(b-y)	MK Type	Phot.Type	Long.	Lat.	Vel.	Error
5271	8.02	0.242	0.708	20	0.169	0	206	1.45	0.008	F2III/IV	F2	357.84	-80.42		
5288	9.27	0.292	0.462	7	0.132	5	169	3.13	0.009	F3V	F5	344.19	-78.60		
5321	8.44	0.277	0.515	8	0.145	3	134	2.81	-0.003	F3V	F4	349.75	-79.61		
5339	8.19	0.319	0.448	7	0.188	0	98	3.23	0.023		F8	72.86	-75.57		
5423	9.95	0.330	0.468	10	0.193	-1	247	2.99	-0.031		F5	61.79	-77.87		
5444	8.18	0.344	0.359	4	0.153	5	68	4.01	-0.009		F8	62.44	-77.83		
5454	9.76	0.309	0.488	11	0.164	2	244	2.82	-0.028		F4	54.91	-78.76		
5466	8.96	0.310	0.456	9	0.148	3	147	3.13	-0.007	F5V	F5	338.27	-74.80		
5487	7.96	0.026	1.098	10	0.187	0	257	0.91	0.023		A2	67.40	-77.15	34.9	4.4
5496	10.57	-0.030	0.922	63*	0.123	1	914	0.77	-0.003	B9V	B9	7.84	-79.44		
5497	9.05	0.111	0.842	0	0.213	-1	189	2.67	-0.009	A4V	A5	348.52	-77.24		
5508	8.88	0.355	0.331	5	0.135	9	86	4.20	-0.001		F8 iPII	49.54	-79.34		
5524	7.16	0.046	1.041	8	0.195	0	148	1.30	0.010		A2	40.59	-79.88	7.8	2.2
5531	8.75	0.333	0.417	8	0.156	4	116	3.43	-0.015	F5V	F5	351.88	-77.89		
5546	10.21	0.118	0.973	17	0.180	3	636	1.19	0.004	A5IV/V	A5	15.29	-79.93		
5590	9.15	0.249	0.511	-1	0.171	0	141	3.41	0.009		F3	55.92	-78.99		
5617	6.82	0.020	1.033	2	0.182	0	109	1.63	0.022		A2	69.76	-77.08	-4.2	
5618	8.85	0.066	1.094	20	0.201	1	434	0.66	0.004	A3V	A2	336.38	-74.64		
5630	9.99	0.212	0.704	7	0.200	-2	339	2.34	-0.010	F2V	F0	35.88	-80.25		
5643	7.71	0.247	0.630	18	0.090	8	154	1.77	0.008		F3 iPII	63.85	-78.17		
5669	8.87	0.287	0.491	7	0.166	1	148	3.02	-0.001		F4	61.87	-78.50		
5698	9.34	0.315	0.422	6	0.142	4	150	3.46	-0.006	F5V	F6	342.06	-76.43		
5737	4.28	-0.065	0.450	72*	0.113	-1			0.005	B7IIIp	Unknown	17.15	-80.37	-24.3	
5745	9.03	0.318	0.455	10	0.148	4	155	3.08	0.005		F6	75.36	-76.24		
5768	9.95	0.294	0.613	21	0.174	0	459	1.64	-0.004	F2IV/V	F5	34.30	-80.58		
5769	9.20	0.081	0.904	0	0.223	-1	224	2.45	0.025	A4V	A5	16.75	-80.45		
5815	9.38	0.313	0.521	16	0.149	4	250	2.40	-0.025	F2V	F4	9.80	-80.23		
5816	9.30	0.181	0.818	13	0.199	-1	324	1.75	-0.015	F0V	A8	347.21	-77.80		
5824	9.64	0.207	0.716	10	0.159	2	317	2.13	-0.018	A9V	A9	2.44	-79.75		

Table 6.2.1

HD No.	V	(b-y)o	co	dc1	mo	dm1	D pc	Mv	E(b-y)	MK Type	Phot.Type	Long.	Lat.	Vel.	Error
5836	9.46	0.318	0.497	13	0.172	2	227	2.68	0.013	F5/6V	F7	332.00	-73.72		
5868	8.46	0.312	0.410	5	0.135	6	95	3.58	0.014		F7 iPII	38.51	-80.66		
5865	9.62	0.408	0.357	9	0.212	2			0.030		Unknown	58.41	-79.40		
5866	8.99	0.310	0.477	9	0.182	0	160	2.97	0.011		F7	46.82	-80.31		
5910	8.35	0.279	0.469	4	0.151	2	108	3.18	-0.018		F3	77.72	-76.19		
5912	9.50	0.332	0.396	6	0.154	4	147	3.67	0.001		F7	43.16	-80.61		
5921	9.01	0.286	0.505	9	0.161	2	171	2.85	0.009		F5	77.75	-76.21		
5922	10.03	0.391	0.323	5	0.195	3	141	4.29	-0.009	G3/5V	G1	32.09	-80.92		
5932	7.87	0.226	0.658	10	0.157	2	130	2.30	0.001		F2	74.79	-76.99	11.7	2.6
5961	8.82	0.292	0.452	3	0.163	1	123	3.37	-0.020		F4	48.16	-80.45		
6002	9.92	0.235	0.681	16	0.146	3	416	1.83	0.004	A9V	F2	346.68	-78.13		
6056	9.61	0.274	0.502	6	0.152	2	209	3.01	-0.023	F2V	F2	330.82	-73.87		
6068	9.66	0.311	0.492	13	0.143	4	245	2.72	-0.019	F2V	F5	6.97	-80.56		
6069	8.91	0.224	0.535	-4	0.173	0	121	3.50	-0.018	F0V	F0	332.06	-74.40		
6088	9.75	0.236	0.630	9	0.165	1	291	2.43	-0.023	F0V	F0	38.91	-81.11		
6139	8.80	0.334	0.444	10	0.163	3	135	3.15	-0.012	F6/7V	F6	2.77	-80.40		
6140	8.44	0.225	0.622	6	0.131	4	146	2.61	-0.009	F0V	F0	332.17	-74.64		
6178	5.49	0.039	1.069	9	0.188	0	75	1.12	0.002	A1/2IV	A2	2.97	-80.49	-17.7	9.4
6196	10.07	0.333	0.385	5	0.152	4	181	3.78	-0.020	F5V	F6	31.75	-81.44		
6219	9.13	0.334	0.449	12	0.149	5	166	3.03	-0.005	F5V	F7	332.15	-74.87		
6234	8.52	0.365	0.299	0	0.170	4	60	4.62	-0.007	G5V	F8	338.95	-77.03		
6244	8.68	0.294	0.433	4	0.134	4	112	3.44	-0.011		F4	55.58	-80.52		
6270	9.56	0.283	0.495	6	0.169	0	203	3.02	-0.026	F2V	F3	356.34	-80.07		
6292	10.05	0.404	0.513	24	0.201	3			0.025		G ePI	79.91	-76.80		
6307	8.77	0.323	0.424	7	0.155	3	118	3.41	-0.014	F5/6V	F6	9.14	-81.17		
6322	9.23	-0.024	0.971	53*	0.160	-2	475	0.84	-0.020		B9	76.03	-77.87		
6339	9.83	0.306	0.509	12	0.182	0	272	2.66	0.010	F5V	F5	15.48	-81.54		
6340	8.99	0.099	1.004	14	0.212	0	508	0.46	-0.058	A2V	A2	347.20	-79.05		
6352	10.48	0.132	0.835	3	0.200	1	405	2.44	0.012		A6	78.12	-77.49		

Table 6.2.1

HD No.	V	(b-y)o	co	dc1	mo	dm1	D pc	Mv	E(b-y)	MK Type	Phot.Type	Long.	Lat.	Vel.	Error
6353	8.94	0.305	0.468	8	0.163	2	150	3.06	-0.003		F6	49.88	-81.20		
6354	7.03	0.080	1.021	15	0.208	0	144	1.24	-0.004	A3III/IV	A4	330.09	-74.49	-13.4	3.1
6363	9.96	0.243	0.602	8	0.163	1	304	2.55	-0.011		F1	60.09	-80.42		
6364	9.62	0.178	0.734	2	0.203	-1	241	2.71	-0.006	A5/7III	A8	30.72	-81.80		
6365	9.81	0.151	0.822	6	0.164	4	329	2.22	-0.001	A3III/IV	A7	11.28	-81.41		
6366	9.25	0.318	0.494	13	0.175	1	203	2.72	0.014	F5V	F7	348.00	-79.24		
6367	7.24	0.283	0.475	5	0.150	3	65	3.18	0.009	F5V	F5	330.26	-74.60	14.8	5.2
6390	8.69	0.300	0.521	12	0.183	0	166	2.59	0.016	F5/6V	F6	12.59	-81.52		
6402	8.14	0.312	0.430	6	0.154	4	89	3.41	0.021	F6V	F7	8.09	-81.32		
6411	9.38	0.343	0.387	5	0.168	3	135	3.74	-0.024		F6	80.05	-77.17		
6412	7.48	0.310	0.536	17	0.146	4	111	2.25	-0.005		F5	68.61	-79.49	-3.6	2.5
6427	10.44	0.355	0.389	5	0.200	-1	220	3.73	-0.050		F5	142.10	-80.18		
6451	8.55	0.113	0.884	3	0.259	-5	173	2.36	0.003		A5/Am	147.08	-82.07		
6492	9.18	0.178	0.855	17	0.186	0	363	1.37	-0.013	A9V	A8	289.76	-77.95		
6493	7.17	0.275	0.486	5	0.146	3	64	3.14	-0.011	F3V	F3	291.41	-76.55	9.2	6.7
6491	8.04	0.222	0.636	7	0.171	1	126	2.54	0.017	F2IV/V	F2	210.46	-86.84	-2.1	2.7
6504	8.22	0.301	0.446	4	0.172	1	94	3.36	0.013		F6	166.20	-85.21		
6515	8.49	0.228	0.583	2	0.167	1	125	3.01	-0.005		F1	154.21	-83.52		
6516	9.22	0.244	0.527	1	0.142	3	158	3.23	-0.008	A9V	F2	186.68	-86.38		
6531	8.98	0.299	0.451	5	0.164	1	136	3.31	-0.007		F5	147.57	-81.75		
6532	8.43	0.080	0.851	-9	0.233	-3	120	3.04	0.000	Ap SrCrEu	A4/Am	206.74	-86.75	-7.7	7.9
6533	9.31	0.342	0.338	1	0.156	4	102	4.27	-0.005	F8V	F7	292.23	-75.47		
6547	9.06	0.185	0.719	1	0.201	-1	183	2.75	-0.013		A8	145.82	-81.04		
6548	9.79	0.307	0.459	8	0.151	3	216	3.12	-0.011	F3V	F5	222.03	-86.73		
6594	8.03	0.355	0.402	8	0.192	1	79	3.55	0.019	G2V	G0	281.32	-81.70		
6593	9.29	0.297	0.448	4	0.170	1	152	3.38	0.006		F6	149.69	-82.13		
6619	6.61	0.067	1.013	8	0.238	-4	102	1.55	-0.011	A1V	A2	283.29	-80.88	13.7	
6640	8.16	0.317	0.513	15	0.164	2	136	2.49	0.006		F7	159.63	-84.02		
6653	10.02	0.365	0.347	4	0.182	2	153	4.10	-0.026		F8	147.65	-84.94		

Table 6.2.1

HD No.	V	(b-y)o	co	dc1	mo	dm1	D pc	Mv	E(b-y)	MK Type	Phot.Type	Long.	Lat.	Vel.	Error
6668	6.31	0.121	0.824	-1	0.207	0	52	2.73	0.009		A6	172.33	-85.27	-0.9	18.9
6670	9.38	0.220	0.652	8	0.150	3	246	2.42	-0.007	A9V	F0	249.73	-85.76		
6723	9.08	0.199	0.746	10	0.171	1	248	2.11	-0.021	A8V	A9	237.64	-86.10	-2.5	
6724	9.30	0.254	0.619	15	0.145	3	285	2.03	-0.001	F0V	F2	245.09	-85.84		
6740	9.96	0.329	0.419	6	0.170	2	198	3.48	-0.019		F6	145.61	-79.77		
6790	9.35	0.384	0.340	5	0.204	1	110	4.14	-0.034	G0V	F8	286.03	-78.68		
6807	9.86	0.299	0.462	8	0.133	5	226	3.09	-0.005	F3V	F5	269.16	-83.58		
6806	8.21	0.357	0.366	6	0.161	5	74	3.87	-0.006		F8	176.93	-85.21		
6855	9.44	0.250	0.572	7	0.164	1	223	2.69	-0.019	F0V	F2	276.73	-81.91		
6868	8.19	0.314	0.431	6	0.154	3	91	3.39	-0.001	F5V	F6	246.95	-85.43		
6957	9.66	0.305	0.407	3	0.135	5	159	3.66	-0.009		F5	210.53	-85.93		
6958	8.41	0.068	0.933	-1	0.219	-2	167	2.30	-0.018	A2IV/V	A2	288.07	-76.45		
6993	9.91	0.292	0.471	6	0.153	2	227	3.13	-0.011		F4	191.83	-85.51		
7037	9.58	0.336	0.428	8	0.175	2	177	3.34	0.009	F6V	F8	217.04	-85.78		
7038	9.38	0.268	0.565	10	0.179	-1	238	2.50	-0.016	F2V	F2	275.37	-81.59		
7058	10.16	0.338	0.437	10	0.167	3	245	3.21	0.002		F7	183.97	-85.02		
7059	8.87	0.281	0.539	12	0.149	2	187	2.52	-0.013	F2V	F3	222.59	-85.71		
7079	10.21	0.278	0.599	17	0.157	2	452	1.94	-0.015		F3	183.91	-84.96		
7092	10.45	0.415	0.319	5	0.211	2	168	4.32	-0.002		G3	148.87	-79.27		
7135	9.71	0.283	0.548	13	0.153	2	288	2.41	-0.020		F3	155.21	-81.18		
7184	9.87	0.112	0.854	1	0.228	-2	286	2.58	-0.001	A2III/IV	A5	204.39	-85.39		
7209	9.66	0.269	0.462	0	0.154	2	172	3.48	0.002		F4	175.77	-84.04		
7257	7.63	0.310	0.404	3	0.147	3	61	3.69	-0.007		F6	159.94	-81.76	5.9	3.3
7259	6.44	0.289	0.509	9	0.166	1	54	2.79	0.016	F5IV	F6	252.86	-84.12	15.0	3.3
7269	9.06	0.301	0.438	4	0.159	2	136	3.40	0.004	F7V	F6	282.69	-78.04		
7281	9.57	0.327	0.454	11	0.157	3	200	3.06	-0.017	F5V	F6	262.99	-83.03		
7312	5.94	0.173	0.816	11	0.195	-1	64	1.89	-0.007	A9IV+F/G	A8	281.55	-78.37	18.1	5.6
7323	7.80	0.070	1.055	17	0.163	4	229	1.01	-0.004	A0V	A2	276.30	-80.24	9.0	
7382	7.25	0.275	0.454	-1	0.174	0	55	3.56	-0.006	F3/5V	F3	284.14	-76.78	10.0	[illegible]

Table 6.2.1

HD No.	V	(b-y)o	co	dc1	mo	dm1	D pc	Mv	E(b-y)	MK Type	Phot.Type	Long.	Lat.	Vel.	Error
7399	8.85	0.314	0.428	5	0.167	1	120	3.45	-0.015		F5	161.92	-81.64		
7400	9.72	0.205	0.710	7	0.178	0	298	2.35	0.004		F0	184.47	-84.20		
7413	9.49	0.303	0.470	7	0.181	0	188	3.12	0.007	F7/8V	F6	268.25	-81.83		
7488	8:21	0.298	0.445	5	0.145	3	95	3.31	0.002	F5V	F5	278.19	-79.00		
7488	8.15	0:285	0.442	2	0.154	2	85	3.52	0.015	F5V	F5	278.19	-79.00		
7487	8.79	0.352	0.141	-21	0.183	1	29	6.46	-0.025	F7V	F7	254.23	-83.44		
7496	8.50	0.137	0.787	-2	0.208	0	133	2.87	0.006		A7	152.77	-78.73		
7553	9.57	0.227	0.658	10	0.171	0	283	2.31	-0.028		F0	160.50	-84.74		
7594	8.46	0.375	0.381	9	0.193	2	90	3.68	0.007		G0	144.34	-80.69		
7606	8.69	0.301	0.390	-2	0.175	0	87	3.98	-0.021		F4	142.50	-79.70		
7607	9.75	0.348	0.388	9	0.152	6	167	3.63	0.022	F8/G0V	F9 iPII	269.18	-84.55		
7629	7.13	0.195	0.755	9	0.179	0	99	2.15	-0.011		A9	169.70	-85.45	-6.5	0.1
7631	9.81	0.325	0.430	6	0.176	1	192	3.39	-0.002	F7/8 V	F7	274.34	-83.66		
7642	8.86	0.297	0.453	6	0.148	3	133	3.25	-0.011		F4	148.33	-81.94		
7643	8.22	0.262	0.596	13	0.163	1			0.008	F3V	Unknown	290.73	-76.85		
7676	8.38	0.146	0.715	-12	0.280	-7	84	3.76	-0.061	Ap SrCrEu	A4/Am	279.51	-82.30	6.6	2.6
7704	8.92	0.337	0.444	9	0.185	0	140	3.18	-0.002	F7V	F7	273.68	-83.54		
7729	8.70	0.330	0.385	4	0.153	4	96	3.79	0.014		F8	150.31	-82.14		
7739	8.88	0.300	0.501	11	0.161	2	169	2.74	-0.030		F3	157.22	-83.63		
7751	8.29	0.252	0.580	9	0.153	2	143	2.52	-0.002		F3	143.47	-79.33	-4.9	0.8
7786	8.74	0.314	0.417	3	0.178	0	108	3.58	-0.004	F5V	F6	261.67	-84.89		
7817	8.19	0.346	0.342	2	0.160	4	62	4.21	-0.003	F8V	F8	279.47	-81.74		
7826	9.74	0.214	0.677	3	0.208	-3	255	2.71	-0.022		F0	147.84	-80.82		
7827	10.01	0.286	0.495	8	0.147	3	261	2.92	0.003		F4	174.77	-85.30		
7867	8.63	0.302	0.423	4	0.146	3	105	3.52	-0.006	F5V	F5	283.61	-79.99		
7875	9.71	0.204	0.832	18	0.239	-6	462	1.39	-0.039		A8/Am	171.85	-84.93		
7876	10.04	0.083	0.992	12	0.212	0	510	1.50	0.002		A4	179.21	-85.43		
7898	7.73	0.172	0.821	12	0.182	1	152	1.82	-0.014	A9IV	A8	276.75	-82,13	6.5	
7908	7.29	0.213	0.660	4	0.136	4	85	2.64	-0.017		F0	166.87	-84.35	15.3	1.5

Table 6.2.1

HD No.	V	(b-y)o	co	dc1	mo	dm1	D pc	Mv	E(b-y)	MK Type	Phot.Type	Long.	Lat.	Vel.	Error
7932	9.89	0.331	0.390	3	0.177	1	166	3.80	-0.034	F3/5V	F5	243.47	-85.66		
7951	9.80	0.384	0.345	6	0.200	2	140	4.06	0.003	G3V	FG1	199.68	-86.02		
7954	8.71	0.198	0.776	12	0.192	-1	234	1.87	0.005	F2IV/V	F0	282.27	-80.18		
7971	9.10	0.283	0.471	3	0.168	0	146	3.28	-0.014	F3/5V	F3	278.35	-81,47		
8033	9.19	0.218	0.645	1	0.205	-2	181	2.90	-0.039		A9	169.25	-84.27		
8040	7.80	0.296	0.417	1	0.159	2	67	3.69	0.007	F5V	F6	276.41	-81.70	21.0	
8072	9.27	0.353	0.402	7	0.186	1	139	3.57	0.002		F8	160.39	-82.94		
8076	7.61	0.377	0.331	2	0.204	0	46	4.27	0.008	G2V	G0	286.89	-77.21	-2.9	
8104	9.45	0.335	0.446	11	0.161	3	186	3.11	-0.002		F7	178.86	-84.85		
8130	7.34	0.004	1.026	-2	0.171	0	124	1.86	0.023	A0V	A1	280.42	-80.06	0.7	10.2
8145	8.43	0.189	0.778	10	0.198	-1	188	2.05	0.003	F0V	F0	244.47	-85.15		
8164	9.17	0.316	0.424	5	0.171	1	137	3.49	-0.028	F5V	F4	246.56	-85.00		
8279	9.51	0.319	0.413	5	0.160	2	154	3.57	-0.020		F5	153.89	-80.57		
8282	9.03	0.319	0.369	1	0.148	4	100	4.03	-0.012	F5V	F6	208.30	-85.44		
8304	9.77	0.342	0.408	9	0.157	4	182	3.47	0.000	F7V	F8	208.78	-85.40		
8350	6.31	0.293	0.490	9	0.159	2	48	2.92	0.009		F5	155.12	-80.59	-7.6	4.7
8351	6.70	0.149	0.907	16	0.203	-1	118	1.35	-0.008	A9V	A7/Am	280.33	-79.16	4.0	16.7
8380	8.09	0.234	0.683	6	0.286	-10	131	2.50	-0.001		F2/Am	164.46	-82.51		
8408	8.27	0.287	0.458	3	0.160	1	97	3.35	0.004		F5	161.64	-81.94		
8415	8.86	0.319	0.215	-19	0.188	-1			-0.004	F3V	Unknown	250.79	-84.14		
8460	9.37	0.310	0.435	5	0.173	1	156	3.40	-0.010		F6	157.92	-80.92		
8461	9.81	0.257	0.550	8	0.132	4	270	2.65	0.005		F3	160.60	-81.53		
8471	9.45	0.320	0.421	5	0.170	1	155	3.50	-0.005		F6	154.58	-79.95		
8487	6.58	0.122	0.812	-2	0.220	-1	55	2.87	0.016		A6	184.95	-84.28	-15.3	
8603	8.77	0.071	0.994	9	0.204	0	270	1.62	0.006		A4	195.03	-84.50		
8604	8.78	0.278	0.510	8	0.154	2	152	2.87	-0.001	F3V	F4	282.25	-77.29		
8616	9.26	0.295	0.468	7	0.148	3	170	3.10	-0.022		F4	165.53	-81.95		
8715	8.06	0.306	0.451	8	0.144	4	94	3.20	-0.003		F5	176.45	-85.99		
8716	8.92	0.139	0.929	17	0.197	0	339	1.27	-0.007	A8V	A6	201.31	-86.76		

Table 6.2.1

HD No.	V	(b-y)o	co	dc1	mo	dm1	D pc	Mv	E(b-y)	MK Type	Phot.Type	Long.	Lat.	Vel.	Error
8717	8.35	0.259	0.894	-11	0.233	-9	297	0.99	-0.174	F4V	F3	241.39	-86.47		
8743	8.82	0.087	0.948	7	0.199	1	242	1.90	0.010	A3V	A4	288.61	-78.56		
8795	9.74	0.296	0.529	13	0.156	2	286	2.46	-0.018		F4	141.94	-78.83		
8806	8.84	0.311	0.383	1	0.144	4	97	3.91	-0.009	F5V	F5	288.46	-78.26		
8868	8.92	0.067	1.013	9	0.233	-2	302	1.52	-0.008	A5IV/V	A2	284.27	-80.19		
8886	9.77	0.220	0.669	10	0.150	3	319	2.25	-0.004		F0	146.53	-80.50		
8895	6.89	0.287	0.533	12	0.151	2	75	2.51	0.001		F4	152.16	-82.28	16.1	3.4
8899	9.59	0.284	0.469	5	0.153	2	195	3.14	0.000	F2/3V	F4	278.56	-82.05		
8924	10.01	0.182	0.765	7	0.176	1	356	2.25	-0.004		A9	144.29	-79.26		
8932	9.10	0.066	0.960	-4	0.228	-9	323	1.56	-0.031		A1/Am	173.28	-85.16		
8933	8.44	0.256	0.515	1	0.186	-1	109	3.24	0.022		F4	187.45	-85.92		
8976	8.55	0.224	0.699	5	0.267	-8	157	2.57	-0.009	Fm	F0/Am	285.70	-78.92		
8983	8.70	0.079	0.961	5	0.231	-3	225	1.94	-0.006		A4	146.96	-80.11		
8985	7.65	0.315	0.404	3	0.165	2	62	3.70	0.017	F6/7V	F7	227.59	-86.18	29.1	0.9
9019	8.75	0.285	0.533	12	0.152	2	175	2.54	-0.008		F4	170.29	-84.66		
9026	8.05	0.199	0.733	6	0.196	-1	137	2.37	0.011	F2III/IV	F1	263.40	-84.27	19.9	3.0
9027	9.33	0.067	0.967	4	0.212	-1	300	1.94	-0.004	A3V	A2	271.81	-83.07		
9061	6.65	0.292	0.519	12	0.144	3	66	2.56	-0.001		F5	147.59	-79.94	1.5	9.7
9063	7.03	0.137	0.869	9	0.194	1	103	1.96	-0.004		A6	183.08	-85.42	6.2	1.8
9065	6.58	0.211	0.775	21	0.161	1	114	1.29	-0.019	A9/F0V	F0	274.54	-82.40	-33.4	
9084	8.79	0.342	0.355	1	0.178	2	86	4.12	-0.013	F8/G0V	F8	265.97	-83.80		
9113	9.07	0.319	0.454	6	0.225	-4	145	3.25	0.029		F8	153.00	-81.50		
9131	9.15	0.321	0.374	1	0.162	2	108	3.99	-0.018		F6	153.60	-81.56		
9132	4.38	-0.169	0.243	53*	0.865	-67	2	7.99	0.173		A0/DA?	160.80	-83.09	-5.4	20.6
9133	8.88	0.127	0.893	9	0.196	1	248	1.90	0.006	A7V	A6	271.75	-82.70		
9134	9.05	0.334	0.353	0	0.178	1	94	4.19	-0.019	F7V	F6	279.06	-80.89		
9159	8.29	0.274	0.571	13	0.159	1	158	2.29	0.001	F3V	F4	249.73	-85.02		
9205	9.32	0.242	0.605	8	0.160	1	226	2.55	-0.010		F1	190.64	-85.39		
9206	8.73	0.245	0.644	14	0.168	0	216	2.06	-0.003	F2IV	F2	280.97	-79.90		

Table 6.2.1

HD No.	V	(b-y)o	co	dc1	mo	dm1	D pc	Mv	E(b-y)	MK Type	Phot.Type	Long.	Lat.	Vel.	Error
9245	9.15	0.369	0.403	10	0.188	2	138	3.45	0.000		F9	191.92	-85.36		
9291	9.53	0.267	0.464	-1	0.163	1	159	3.52	-0.008	F2/3V	F3	278.18	-80.50		
9292	8.03	0.222	0.691	13	0.162	1	159	2.03	-0.008	F2IV	F1	283.09	-78.60		
9301	9.02	0.278	0.474	3	0.156	2	142	3.26	-0.007		F3	160.87	-82.47		
9310	9.33	0.316	0.458	9	0.157	3	177	3.09	-0.010		F6	184.41	-84.86		
9316	9.22	0.277	0.487	5	0.153	2	165	3.13	-0.018		F3	156.01	-81.34		
9317	8.48	0.307	0.467	9	0.155	3	123	3.04	-0.018	F3V	F4	226.30	-85.48		
9336	6.82	0.135	0.815	1	0.215	-1	69	2.63	0.004		A7	153.79	-80.64	-4.0	0.5
9400	9.41	0.106	1.014	19	0.177	3	488	0.97	-0.013		A5	149.03	-78.64		
9401	8.48	0.206	0.724	10	0.182	0	186	2.13	-0.010		F0	150.52	-79.26		
9411	7.24	0.181	0.759	6	0.195	-1	95	2.36	-0.015		A8	177.30	-84.14	-21.8	22.3
9413	8.89	0.365	0.335	2	0.192	1	84	4.27	-0.015	F8V	F8	273.18	-81.42		
9422	9.84	0.324	0.435	7	0.178	1	199	3.34	-0.025		F5	160.62	-81.98		
9436	9.11	0.327	0.479	12	0.182	0	179	2.85	0.003	F6V	F7	209.72	-85.32		
9451A	7.99	0.110	0.881	4	0.218	-1	137	2.31	-0.013	A5V	A4	206.73	-85.27	21.1	4.0
9451B	9.00	0.357	0.241	-4	0.131	-9	56	5.24	-0.080	A5V	F4 PII	206.83	-85.27		
9475	8.72	0.214	0.748	13	0.218	-4	236	1.85	-0.019	F0/2IV	F0	242.93	-84.68		
9487	8.62	0.142	0.820	3	0.224	-2	168	2.50	0.006		A7	169.78	-83.21		
9515	9.87	0.343	0.409	6	0.189	0	184	3.55	-0.003	F7V	F8	224.13	-85.13		
9553	9.20	0.178	0.784	8	0.185	0	260	2.12	-0.011		A8	159.71	-81.34		
9577	8.26	0.295	0.427	2	0.159	2	86	3.59	0.004	F5V	F5	279.78	-78.84		
9607	7.94	0.328	0.403	4	0.179	1	71	3.68	0.017		F8	164.12	-82.01		
9651	9.57	0.252	0.625	14	0.165	2	321	2.04	0.035	F3V	F4	237.35	-84.49		
9673	7.83	0.123	0.916	11	0.185	2	167	1.72	0.013	A5V	A6	216.59	-84.88	-16.9	34
9693	9.56	0.273	0.470	2	0.154	2	175	3.35	-0.005	F2V	F3	238.07	-84.44		
9769	8.50	0.337	0.399	6	0.164	3	94	3.63	-0.009		F7	163.76	-85.15		
9793	9.66	0.351	0.369	9	0.137	9	150	3.77	0.013		F9 PII	141.13	-79.13		
9857	9.73	0.223	0.628	6	0.163	1	265	2.61	-0.016	A9V	F0	258.22	-85.57		
9906	5.67	0.208	0.696	7	0.181	0	45	2.38	0.001	F2V	F0	253.82	-85.72	-1.9	16.1

Table 6.2.1

HD No.	V	(b-y)o	co	dc1	mo	dm1	D pc	Mv	E(b-y)	MK Type	Phot.Type	Long.	Lat.	Vel.	Error
9918SE	9.69	0.164	0.642	-16	0.251	-5	128	4.14	-0.075	A2/7/F0m	Unknown	286.58	-79.40		
10001	8.23	0.299	0.537	15	0.151	3	152	2.32	-0.003		F5	182.80	-85.84		
10138	9.95	0.339	0.493	15	0.180	1	294	2.61	-0.020		F7	185.68	-85.57		
10148	5.54	0.204	0.812	23	0.174	0			0.006		F0 ePI Am	158.08	-82.89	18.2	2.1
10161	6.66	-0.035	0.867	78*	0.120	1	170	0.50	0.002		B9	185.59	-85.51	29.0	4.0
10177	8.88	0.344	0.363	2	0.181	2	93	4.03	0.013		F9	168.92	-84.30		
10178	8.98	0.344	0.415	7	0.191	0	126	3.48	-0.036		F5	187.18	-85.53		
10186	7.62	0.180	0.702	-2	0.196	0	84	3.00	-0.007		A9	147.75	-79.76	2.4	7.9
10209	7.43	0.209	0.719	11	0.185	-1	118	2.08	-0.013	F0III	F0	239.19	-85.61	3.1	6.1
10255	10.21	0.296	0.495	9	0.161	1	296	2.85	-0.028	F2V	F3	229.30	-85.75		
10412	8.41	0.230	0.638	8	0.166	1	156	2.45	0.000		F2	163.64	-82.93		
10433	9.24	0.098	1.105	22	0.219	-1	450	0.97	-0.032	A3IV/V	A2	274.41	-81.43		
10510	7.72	0.279	0.603	17	0.169	0	144	1.93	-0.013		F3	154.87	-80.71		
10538	5.68	-0.016	1.045	3*	0.171	-3	78	1.22	0.003	A0V	A0	279.78	-79.37	-14.7	29.0
10646	10.34	0.217	0.735	16	0.202	-3	534	1.70	-0.024	A9V	A9	239.21	-84.66		
10691	8.63	0.121	1.011	23	0.181	2	383	0.71	-0.017	A3V	A5	250.04	-83.91		
11231	8.54	0.288	0.489	6	0.181	-1	124	3.07	0.003	F5V	F5	275.57	-81.71		
10412	8.41	0.230	0.638	8	0.166	1	156	2.45	0.000		F5	163.64	-82.93		
10433	9.24	0.098	1.105	22	0.219	-1	450	0.97	-0.032	A3IV	A2	274.41	-81.43		
10510	7.72	0.279	0.603	17	0.169	0	144	1.93	-0.013		F3	154.87	-80.71		
10538	5.68	-0.016	1.045	3*	0.171	-3	78	1.22	0.003	A0V	A0	279.78	-79.37		
10646	10.34	0.217	0.735	16	0.202	-3	534	1.70	-0.024	A9V	A9	239.21	-84.66		
10691	8.63	0.121	1.011	23	0.181	2	383	0.71	-0.017	A3V	A5	250.04	-83.91		
11231	8.54	0.288	0.489	6	0.181	-1	124	3.07	0.003	F5V	F5	275.57	-81.71		
11369	8.97	0.300	0.523	14	0.155	2	199	2.48	-0.009		F5	182.66	-84.73		
11398	8.77	0.216	0.710	13	0.184	-1	236	1.91	-0.030		A9	166.77	-83.20		
11573	8.02	0.129	0.850	4	0.207	0	137	2.33	-0.007	A5III/IV	A5	264.22	-82.68	-13.0	0.8
11597	8.15	0.303	0.415	2	0.161	2	80	3.64	-0.009	F5V	F5	264.15	-82.63	2.3	2.9
11808	8.52	0.095	0.867	-3	0.242	-4	144	2.73	-0.009		A4	184.10	-86.36		

'Just to stir things up seemed a great reward in itself'

Sallust c86-c35B.C.

References

Aitken, R.G. 1935, 'The Binary Stars', McGraw-Hill, New York.

Albrecht, R. and Maitzen, H.M. 1980, Astr.and Ap. Supple., 42, 29.

Bahcall, J.N. 1984, Ap.J. 276, 169.

Bahcall, J.N. and Soniera, R.M. 1980, Ap.J. Supple., 44, 73.

Bahcall, J.N., Schmidt, M. and Soniera, R.M. 1983, Ap.J., 265, 730.

Becker, W. 1970, Astr.and Ap., 9, 204.

Becker, W. 1980, Astr. and Ap., 87, 80.

Bernat, J.S. and Piersol, A.G. 1971, 'Random Data: Analysis and Measurement Procedures', Wiley-Interscience, New York.

Blaauw, A. 1978, 'Astronomical Papers Dedicated to B. Stromgren'.

Bok, B.J. 1983, Ap.J., 273, 411.

Brault, J.W. and White, O.R. 1971, Astr.and Ap., 13, 169.

Burstein, D. 1979, Ap.J., 234, 829.

Burstein, D. and Heiles, C. 1982, Astr.J., 87, 1165.

Camm, G.L. 1950, M.N.R.A.S., 110, 305.

Camm, G.L. 1952, M.N.R.A.S., 112, 155.

Chiu, L-T.G., 1980a, Ap.J.Supple., 44, 31.

Chiu, L-T.G., 1980b, Astr.J., 85, 812.

Conover, W.J. 1971, 'Practical Non-parametric Statistics', Wiley, New York.

Crawford, D.L. 1973, I.A.U. Symposium #54, p93.

Crawford, D.L. 1975, Astr.J., 80, 955.

Crawford, D.L. 1978, Astr.J., 83, 48.

Crawford, D.L. 1979, Astr.J., 84, 1858.

Crawford, D.L. and Mander, J.V. 1966, Astr.J., 71, 114.

Crawford, D.L. and Barnes, J.V. 1970, Astr.J., 75, 978.

Crawford, D.L., Mavridis, L.N. and Stromgren, B. 1979, Abh.der Hamburger Sternwarte, 10, 82.

Eelsalu, H. 1958, Tartu Astr.Obs.Pub., 33, 153.

Eggen, O.J. 1961, R.Obs.Bull., #5.

Gilmore, G. 1984, M.N.R.A.S., 207, 223.

Gilmore, G. and Reid, I.N. 1983, M.N.R.A.S., 202, 1025.

Gould, E. and Vandervoort, P.O. 1972, Ap.J., 77, 360.

Gray, D.F. 1976, 'The Observation and Analysis of Stellar Photospheres', Wiley, New York.

Griesen, E.W. and Harten, R.H. 1981, Astr.and Ap.Supple., 44, 371.

Gronbech, B. and Olsen, E.H. 1976, Astr.and Ap.Supple, 25, 213.

Gronbech, B. and Olsen, E.H. 1977, Astr.and Ap.Supple, 27, 443.

Harding, G.A., Fahim, F. and Haslam, C.M. 1971, R.Obs.Bull., #165.

Hartkopf, W.I. and Yoss, K.M. 1982, Astr.J., 87, 1679.

Hauck, B. and Mermilliod, M. 1980, Astr.and Ap. Supple., 40,1.

Heiles, C. 1976, Ap.J., 204, 379.

Hilditch, R.W., Hill, G. and Barnes, J.V. 1976, M.N.R.A.S., 176, 175.

Hilditch, R.W., Hill, G. and Barnes, J.V. 1983, M.N.R.A.S., 204, 241.

Hilditch, R.W., McFadzean, A.D., Hill, G. and Barnes, J.V. 1984, I.A.U. Symposium #106, D.Reidel, Dordrecht.

Hill, E.R. 1960, B.A.N., 15, 1.

Hill, G. 1982a, Pub.D.A.O., 16, 59.

Hill, G. 1982b, Pub.D.A.O., 16, 67.

Hill, G. 1982c, REDUCE Users Manual, D.A.O.

Hill, G. 1982d, Private Communication

Hill, G., Allison, A., Odgers, G.J., Pfannenschmidt, E.L., Younger, P.F. and Hilditch, R.W. 1976, Mem.R.A.S., 82, 69.

Hill, G., Hilditch, R.W. and Barnes, J.V. 1979, M.N.R.A.S., 186, 813.

Hill, G., Ramsden, D., Fisher, W.A. and Morris, S.C. 1982a, Pub.D.A.O., 16, 11.

Hill, G., Fisher, W.A. and Poeckert, R. 1982b, Pub.D.A.O., 16, 27.

Hill, G., Fisher, W.A. and Poeckert, R. 1982c, Pub.D.A.O., 16, 43.

Hill, G., Barnes J.V. and Hilditch, R.W. 1982d, Pub.D.A.O., 16, 111.

Hoffleit, D. 1964, Catalogue of Bright Stars, Yale University Observatory.

Houk, N. and Cowley, A.P. 1982. 'University of Michigan Catalogue of Two-Dimensional Spectral Types', 3, University of Michigan.

House, F. and Kilkenny, D. 1978, Astr.and Ap., 67, 421.

Humason, M.L., and Zwicky, F. 1947, Ap.J., 105, 85.

Ichikawa, T., 1981, Pub.A.S.Jap., 33, 107.

Iriarte, B., Johnson, H.L., Mitchell, R.I. and Wisniewski, W.Z. 1965, Sky.Telesc., 30, 21.

Joeveer, M. and Einasto, J. 1976, Tartu Astr.Obs.Teated, 54,77.

Johnson, H.L. and Morgan, W.W. 1953, Ap.J., 117, 313.

Johnson, H.L., Mitchell, R.I., Iriarte, B. and Wisniewski, W.Z. 1966, Comm.Lunar.Planet,Obs., 4, 99.

Jones, D.H.P. 1962, R.Obs.Bull., #52.

Jones, D.H.P. 1972, Ap.J., 178, 467.

Kapteyn, J.C. 1922, Ap.J., 55, 302.

Keenan, F.P. and Dufton, P.L. 1983, M.N.R.A.S., 205, 435.

Kelly, B.D., Cooke, J.A. and Emerson, D. 1982, M.N.R.A.S., 199, 239.

Kilkenny, D. and Hill, P.W. 1975, M.N.R.A.S., 173, 625.

King, I.R. 1965, Astr.J., 70, 296.

Knude, J. 1977, Ap.Let., 18, 115.

Knude, J. 1982a, (private communication).

Knude, J. 1982b, preprint (unpublished).

Kron, R.G. 1978, Ph.D. Thesis, University of California, Berkeley.

Krug, P.A., Morton, D.C. and Tritton, K.P. 1980, M.N.R.A.S., 190, 237.

Kukarkin, B.V., Kholopov, P.N., Federovich, V.P., Frolov, M.S., Kukarkina, N.P., Kurochkin, N.E., Medvedeva, G.I., Perova, N.B. and Pskovsky, Yu.P. 1976, 'Third Supplement to the Third Edition of the General Catalogue of Variable Stars.', Academy of Sciences of the U.S.S.R., Moscow.

Kuzmin, G.G. 1952, Tartu Astr.Obs.Pub., 32, 55.

Kuzmin, G.G. 1955, Tartu Astr.Obs.Pub., 33, 3.

Luyten, W. 1968, M.N.R.A.S., 139, 221.

McCuskey, S.W. 1966, Vistas in Astronomy, 7, 141.

Mihalas, D. and Binney, J. 1981, 'Galactic Astronomy', 2nd. Ed., W.H.Freeman, San Francisco.

Mikami, T. and Ishida, K. 1981, Pub.A.S.Jap., 33, 135.

Nahon, F. 1957, Bull.Astr.Paris 21, 55.

Nandy, K., Reddish, V.C., Tritton, K.P., Cooke, J.A. and Emerson, D. 1977, M.N.R.A.S., 178, 63p.

Nicolet, B. 1982, Astr.and Ap.Supple., 47, 199.

Oort, J.H. 1932, B.A.N., 6, 249.

Oort, J.H. 1958, Ric.Astr.Specola Vaticana, 5, 415.

Oort, J.H. 1960, B.A.N., 15, 45.

Oort, J.H. 1965, 'Galactic Structure', ed.A.Blaauw and M.Schmidt, University of Chicago.

Peir, J.R. 1983, Ap.J.Supple., 53, 791.

Perry, C.L. 1969, Astr.J., 74, 139.

Perry, C.L. and Johnston, L. 1982, Ap.J.Supple., 50, 451.

Peterson, B.A., Ellis, R.S., Kibblewhite, E.J., Bridgeland, M.T., Hooley, T. and Herne, D. 1979, Ap.J., (Letters), 233, L109.

Phillip, A.G.D. 1972, Pub.A.S.Pac., 84, 677.

Pritchett, C. 1983, Astr.J., 88, 1476.

Reid, I.N. 1982, M.N.R.A.S., 201, 51.

Reid, I.N. and Gilmore, G. 1982, M.N.R.A.S., 201, 73.

Rodgers, A.W., Harding, P. and Sadler, E. 1981, Ap.J., 244, 992.

Schmidt, M. 1975, Ap.J., 202, 22.

Simkin, S.M. 1974, Astr.and Ap., 31, 129.

Stetson, P.B. 1983, Astr.J., 88, 1349.

Stokes, N.R. 1972, M.N.R.A.S., 160, 155.

Stromgren, B. 1956, Astr.J., 61, 45.

Stromgren, B. 1963, 'Basic Astronomical Data', ed.K.Aa.Strand, University of Chicago, p123.

Stromgren, B. 1966, Ann.Rev.Astr.and Ap. 4, 433.

Stromgren, B. 1976, ESO 'Messenger', #7, 12.

Tobin, W. and Kilkenny, D. 1981, M.N.R.A.S., 194, 937.

Tobin, W. and Kaufmann, J.P. 1984, M.N.R.A.S., 207, 369.

Turon-Lacarrieu, C. 1971, Astr.and Ap., 14, 95.

Tyson, J.A. and Jarvis, J.F., 1979, Ap.J. (Letters), 230, L153.

Upgren, A.R. 1962, Astr.J., 67, 37.

Upgren, A.R. 1963, Astr.J., 68, 194.

Van der Kruit, P.C. and Searle, L. 1982, Astr.and Ap., 110, 79.

Wayman, P.A. 1961, R.Obs.Bull., #36.

Wells, D.C., Greisen, E.W. and Harten, R.H. 1981, Astr.and Ap.Supple., 44, 363.

Wielen, R. 1974, 'Highlights of Astronomy', D.Reidel, Dordrecht, 3, 395.

Woolley, R.v.d.R. and Stewart, J.M. 1967, M.N.R.A.S., 136, 329.

Yoshii, Y. 1982, Pub.A.S.Jap., 34, 365.

'You will find it a very good practice always to verify your references, sir!'

Dr.Routh 1755-1854

Appendix I

The North Galactic Pole Blue Star Catalogue

Appendix I: NGP Blue Star Catalogue

Columns give:
- i) name
- ii) RA (1950) in format hhmm
- iii) DEC (1950) in format ddmm
- iv) Galactic latitude
- v) V magnitude (or equivalent)
- vi) (B-V) if available (original survey values taken unless otherwise noted)
- vii) Spectral type if known
- viii) Comments, including other names, sources of photometry and spectral types.

Key

Names

TON	:	Chavira and Iriarte (1957) Chavira (1958)
LB	:	Luyten (1970)
ZL	:	Zwicky and Luyten (see above)
K	:	Noguchi et al (1980)
HZ	:	Humason and Zwicky (1947)
EG	:	Eggen and Greenstein (1965)
B	:	Steppe (1978)
FB	:	Greenstein and Sargent
II	:	Sletteback and Stock (1959) second list
BU	:	Burbidge and Hewitt (1980)
BF	:	Berger and Fringent (1977)

Comments

N.B. "P" denotes photometry, "S" denotes spectral type

G1 : Greenstein (1966)
Ir2 : Iriarte (1959)
ES1 : Eggen and Sandage (1965)
St : Steppe (1978)
NMK : Noguchi et al (1980)
SS : Slettebak and Stock (1959)
EG : Eggen and Greenstein (1965)
GS : Greenstein and Sargent (1974)
HZ : Humason and Zwicky (1947)

Non-attributed spectral types are from U.K.S.T. prism/ St.Andrews grism plates.

'NB' denotes no blue object within 2 arcminutes of position on U.K.S.T. prism plate.

'NF' indicates no stars found within 2 arcminutes of position on U.K.S.T. plate.

References

Berger, J. and Fringent, A.M. 1977,
Astr. and Ap. Supple, 28, 123.

Burbidge,G. and Hewitt, A. 1980,
Ap.J. Supple, 43, 57.

Chavira, E. 1958,
Bol.Observ.Tonantzintla y Tacubaya, 17, 15.

Chavira, E. and Iriarte, B. 1957,
Bol.Observ.Tonantzintla y Tacubaya, 16, 3.

Eggen, O.J. and Greenstein, J. 1965, Ap.J., 141, 83.

Eggen, O.J. ans Sandage, A. 1965, Ap.J., 141, 821.

Greenstein, J. 1966, Ap.J., 144, 496.

Greenstein, J. and Sargent, A. 1974,
Ap.J. Supple., 28, 157.

Humason, M.L. and Zwicky, F. 1947, Ap.J., 105, 85.

Iriarte, B. 1965, Lowell Obs.Bull., #101.

Luyten, W.J., 1970,
'A Search for Faint Blue Stars I-L',
University of Minnesota, Minneapolis, Minnesota.

Noguchi, T., Maehava, H. and Kondo, M. 1980,
Ann.Tokyo Astr.Obs., 28, 55.

Steppe, H. 1978, Astr. and Ap. Supple., 31, 209.

Slettebak, A. and Stock, J. 1959,
Hamburger Sternwarte V no.5.

No.	Name	RA (1950)	Dec	Lat.	V	(B-V)	Type	Comments
1	TON 660	1249.00	2720.00	89.9	16.53		F	
2	TON 663	1249.40	2728.00	89.8	16.78		A	
3	TON 659	1249.00	2713.00	89.8	14.27		A-F	
4	TON 658	1248.90	2732.00	89.8	14.20		A	
5	TON 657	1248.50	2734.00	89.8	15.08		A	
6	LB 11395	1249.90	2744.00	89.6	13.23	-1.00	LTE A	
7	LB 11416	1251.10	2711.00	89.5	14.52	1.00	G	
8	TON 654	1247.70	2703.00	89.5	15.52			NF
9	LB 18	1246.60	2704.00	89.4	12.70	-0.10	A0	II212 PSS SSS
10	LB 11414	1251.10	2754.00	89.3	13.05	-2.00	F	
11	LB 11413	1251.10	2758.00	89.3	14.52	1.00	LTE F	
12	LB 20	1249.40	2641.00	89.3	18.28	0.10	LTE A	
13	LB 19	1247.70	2647.00	89.3	15.60	-0.20		NF
14	LB 11373	1247.60	2647.00	89.3	14.23	-1.00	EMISS	ODD : QSO ?
15	LB 11363	1246.80	2658.00	89.3	15.02	2.00	F	
16	TON 650	1246.30	2740.00	89.3	16.66		G?	
17	TON 649	1246.20	2739.00	89.3	17.03		F	
18	LB 11361	1246.10	2710.00	89.3	16.59	-1.00	LTE A	
19	LB 11433	1252.30	2734.00	89.2	13.88	0.00	A	
20	LB 7368	1252.00	2755.00	89.2	16.47	-0.20		NF
21	TON 668	1250.90	2646.00	89.2	15.77		A-F	
22	LB 11410	1250.80	2644.00	89.2	13.73	-1.00	G	
23	TON 665	1249.90	2808.00	89.2	16.53		ELY F	
24	LB 7396	1252.80	2642.00	89.1	16.78	0.10	G	
25	LB 11436	1252.50	2703.00	89.1	14.69	0.00	F	
26	TON 136	1251.20	2642.00	89.1	14.00		A	
27	K 12506	1250.60	2812.20	89.1	16.00		F	PNMK
28	LB 11532	1252.20	2642.00	89.0	13.42	-1.00	LTE A	
29	LB 11429	1251.90	2636.00	89.0	16.00	0.00		NF
30	LB 11406	1250.60	2817.00	89.0	13.30	-1.00	ELY F	

No.	Name	RA (1950)	Dec	Lat.	V	(B-V)	Type	Comments
31	LB 11391	1249.70	2626.00	89.0	14.27	1.00	A	
32	K 12485	1248.50	2824.90	89.0	16.50		LTE A	PNMK
33	TON 648	1245.80	2803.00	89.0	17.03		ELY F	
34	LB 11360	1245.70	2808.00	89.0	13.25	0.00	A	
35	TON 647	1245.60	2804.00	89.0	16.53		ELY F	
36	LB 11356	1244.90	2754.00	89.0	13.19	0.00	G	
37	LB 11351	1244.50	2713.00	89.0	16.00	0.00	A	
38	K 12531	1253.10	2756.20	88.9	16.00		ELY F	PNMK
39	LB 7357	1251.80	2632.00	88.9	16.78	0.20	LTE F	
40	LB 11401	1250.10	2620.00	88.9	14.42	-1.00	LTE F	
41	K 12486	1248.60	2827.70	88.9	16.50		LTE A	PNMK
42	K 12481	1248.10	2826.30	88.9	15.50		F	PNMK
43	LB 21	1251.00	2619.00	88.8	17.47	-0.10		NB
44	LB 11357	1245.20	2637.00	88.8	13.05	-3.00	F	
45	TON 642	1243.80	2734.00	88.8	14.12	-0.23	AO	II208 PIr2 SSS
46	TON 675	1254.50	2708.00	88.7	15.52		F	
47	ZL 108	1254.20	2652.50	88.7	15.80	-0.20	LTE A	
48	TON 140	1254.00	2758.70	88.7	15.50		A	K 12540 PNMK
49	TON 672	1253.60	2633.00	88.7	16.66		LTE F	
50	TON 671	1253.20	2891.30	88.7	15.50		ELY F	K 12532 PNMK
51	TON 667	1249.90	2840.00	88.7	17.03		LTE A	
52	TON 666	1249.90	2838.00	88.7	13.89		LTE A	
53	TON 645	1245.20	2826.00	88.7	15.52		G	
54	TON 673	1253.70	2823.50	88.6	13.50		Fp	TON 139 K12537 II232 PG1
55	TON 670	1252.20	2838.00	88.6	15.02		A-F	
56	LB 11350	1244.40	2625.00	88.6	13.70	1.00	LTE F	
57	LB 7028	1243.50	2809.00	88.6	17.00	0.00		NB
58	TON 678	1255.40	2700.00	88.5	14.89		LTE A	
59	LB 11332	1242.60	2753.00	88.5	13.77	1.00	LTE F	
60	LB 22	1254.60	2823.00	88.4	15.75	0.00	LTE F	

No.	Name	RA (1950)	Dec	Lat.	V	(B-V)	Type	Comments
61	TON 660	1251.90	2901.00	88.3	15.02		A-F	
62	LB 11384	1249.20	2906.00	88.3	16.09	-1.00	F	
63	LB 11341	1243.30	2828.00	88.3	13.70	1.00	F	
64	LB 24	1257.20	2740.00	88.20	16.0	0.00	G?	
65	HZ 47	1257.02	2737.50	88.20	15.3	-0.13	B5	K12570 B286 FB117 PG1 SHZ
66	HZ 38	1256.95	2750.00	88.2	14.20	-0.27	sdO	K12569 B362 PG1 SG1
67	TON 682	1256.80	2655.00	88.2	14.70		MID F	
68	TON 681	1256.70	2653.00	88.2	14.89		MID F	
69	TON 680	1256.60	2652.00	88.2	15.52		LTE F	
70	TON 679	1256.50	2806.00	88.2	15.52		LTE F	
71	TON 651	1246.80	2907.00	88.2	15.08		ELY F	
72	EG 94	1257.50	2750.00	88.1	15.40	0.28	A DAs	K12574 PEG SEG
73	ZL 117	1256.80	2818.30	88.1	17.20	-0.10	ELY F	
74	TON 683	1256.80	2812.00	88.1	16.53		LTE F	
75	TON 684	1256.80	2816.00	88.1	15.52		LTE F	
76	TON 677	1255.00	2844.00	88.1	14.89		LTE F	
77	K 12505	1250.50	2913.90	88.1	16.00		LTE F	PNMK
78	LB 11359	1250.60	2909.00	88.1	15.52	3.00		NF
79	LB 11348	1244.40	2903.00	88.1	13.77	1.00	LTE F	
80	TON 690	1258.10	2735.00	88.0	17.03		LTE A	
81	TON 688	1257.90	2736.00	88.0	15.52		LTE F	
82	ZL 123	1257.35	2813.10	88.0	16.38	0.00		NF
83	TON 687	1257.30	2643.00	88.0	14.77		LTE A	
84	TON 686	1257.20	2811.00	88.0	16.80		A	K12572 BP3191 PNMK
85	K 12562	1256.20	2838.95	88.0	16.00		LTE F	PNMK
86	LB 11423	1251.70	2918.00	88.0	13.77	2.00		NB
87	ZL 103	1240.20	2760.00	88.0	16.16	0.10		NF
88	LB 11314	1238.90	2744.00	88.0	14.55	-3.00	A ODD	
89	TON 692	1258.50	2720.00	87.9	15.39		A	
90	LB 11394	1249.90	2929.00	87.9	16.13	0.00	A2	K12500 SII2

No.	Name	RA (1950)	Dec	Lat.	V	(B-V)	Type	Comments
91	TON 121	1241.90	2602.00	87.9	15.40		ELY F	
92	LB 11428	1251.90	2933.00	87.8	14.02	1.00	A	
93	TON 661	1249.10	2934.00	87.8	15.52		LTE A	K12491
94	TON 653	1247.60	2933.00	87.8	15.27		LTE A	
95	LB 11370	1247.50	2936.00	87.8	13.56	0.00	LTE A	
96	LB 11322	1240.60	2840.00	87.8	15.00	0.00		NB
97	LB 11319	1240.40	2836.00	87.8	13.50	0.00		NB
98	TON 636	1239.90	2812 00	87.8	14.70		A?	
99	LB 11306	1239.20	2751.00	87.8	14.52	1.00	LTE A	
100	TON 693	1259.30	2744.00	87.8	15.58		A-F	K12593
101	TON 664	1249.50	2941.00	87.7	15.58		LTE A	
102	TON 662	1249.10	2940.00	87.7	17.03		A	
103	TON 643	1244.10	2923.00	87.7	15.39		ELY F	
104	TON 118	1241.50	2900.00	87.7	14.70		A	
105	LB 11312	1239.70	2832.00	87.7	16.41	2.00		NB
106	K 12586	1258.60	2835.90	87.6	16.50		A?	PNMK
107	K 12581	1258.10	2846.30	87.6	17.53		QSO	BU1258+287 PNMK
108	LB 11374	1247.80	2948.00	87.6	13.30	-2.00	AO	II217 PSS SSS
109	LB 11355	1244.80	2938.00	87.6	13.05	-2.00	A	
110	TON 106	1238.40	2803.00	87.6	14.80			NB
111	TON 685	1256.90	2910.00	87.5	14.58		LTE A	
112	LB 11369	1247.40	2950.00	87.5	14.39	1.00		NB
113	LB 7178	1247.10	2950.00	87.5	17.03	0.10		NB
114	LB 11367	1247.10	2952.00	87.5	14.52	1.00		NB
115	LB 11300	1238.30	2814.00	87.5	16.22	-1.00		NB DIFFUSE
116	K 13005	1300.50	2745.90	87.4	15.50		LTE F	PNMK
117	LB 27	1300.30	2756.82	87.4	14.30	0.00	sdB	B 282 K13003 FB 121 PGS SGS
118	TON 674	1253.80	2944.00	87.4	16.66		LTE A	
119	LB 11421	1251.50	2954.00	87.4	13.23	-2.00	A	
120	LB 11411	1251.00	2956.00	87.4	13.00	0.00	LTE F	

No.	Name	RA (1950)	Dec	Lat.	V	(B-V)	Type	Comments
121	K 12479	1247.90	2959.93	87.4	15.00		LTE A	PNMK
122	TON 634	1238.60	2835.00	87.4	15.38	0.33	ELY A	PIr2
123	TON 633	1238.60	2831.00	87.4	15.78	0.04	LTE A	PIr2
124	TON 691	1258.30	2910.00	87.3	15.39		A	K12583
125	B 154	1257.03	2924.91	87.3	17.26	1.30		PSt DIFFUSE: NON-STELLAR
126	LB 11354	1234.80	2955.00	87.3	16.78	1.00	A	
127	TON 641	1243.00	2943.00	87.3	14.77		LTE F	
128	TON 122	1241.90	2939.00	87.3	15.50			NF
129	LB 11301	1238.70	2849.00	87.3	16.03	2.00		NB
130	K 13016A	1301.60	2733.30	87.2	16.50			NF
131	TON 143	1301.40	2703.00	87.2	15.10		B	K13014
132	TON 694	1300.80	2827.00	87.2	16.66		B-A	K13008
133	TON 689	1257.90	2920.00	87.2	14.39		LTE A	
134	TON 635	1239.00	2910.00	87.2	12.85	-0.18	A	PIr2 mag. doubtful
135	TON 629	1236.80	2755.00	87.2	15.52		LTE A	
136	LB 11286	1236.60	2648.00	87.2	14.39	1.00	LTE A	
137	TON 695	1302.10	2716.00	87L1	15.70		ELY F	
138	LB 11404	1250.40	3019.00	87.1	14.69	0.00		
139	LB 11342	1243.50	3004.00	87.1	17.41	2.00	G?	
140	LB 6911	1240.60	2940.00	87.1	16.88	0.00		NB
141	TON 141	1300.80	2858.00	87.0	15.11	0.02	A	PIr2
142	LB 11440	1253.00	3017.00	87.0	13.73	-1.00		
143	K 12509	1250.90	3022.78	87.0	15.50			PNMK
144	HZ 35	1250.90	3023.56	87.0	15.80	-0.22	B2	PG1 SHZ
145	LB 11409	1250.80	3023.00	87.0	14.55	-2.00		
146	LB 11340	1243.30	3006.00	87.0	13.77	1.00	LTE F	
147	LB 11327	1242.40	2959.00	87.0	17.03	2.00	A	
148	TON 117	1241.10	2949.00	87.0	14.00		A	
149	LB 11302	1238.80	2925.00	87.0	14.00	0.00	A0	II191 PSS SSS
150	TON 631	1238.00	2912.00	87.0	14.77		LTE F	

No.	Name	RA (1950)	Dec	Lat.	V	(B-V)	Type	Comments
151	LB 11292	1237.10	2845.00	87.0	14.70	1.00	LTE F	
152	K 13030	1303.00	2734.30	86.9	15.50		A	PNMK
153	HZ 39	1302.40	2823.60	86.9	15.40	-0.32	sdB?	EG97 K13024 B303 FB122 PEG SEG
154	K 13016B	1301.60	2847.70	86.9	16.00		A	PNMK
155	LB 7174	1247.00	3031.00	86.9	17.03	0.20		
156	LB 11307	1239.40	2937.00	86.9	14.52	2.00	LTE F	
157	LB 11296	1237.50	2911.00	86.9	14.27	1.00	LTE F	
158	LB 11279	1236.10	2831.00	86.9	14.52	3.00	G	
159	LB 11275	1235.60	2813.00	86.9	15.52	2.00		NB
160	LB 14	1235.30	2653.00	86.9	17.53	0.10	F	
161	TON 696	1303.00	2655.00	86.9	15.52		LTE F	
162	LB 26	1259.50	2510.00	86.8	17.91	0.10	G	
163	LB 11385	1249.30	3036.00	86.8	14.38	0.00		
164	LB 11375	1247.90	3033.00	86.8	16.91	2.00		
165	TON 627	1235.30	2635.00	86.8	14.70			NF
166	TON 144	1303.70	2752.00	86.7	15.50			K13037 m=16? (NMK)
167	TON 697	1303.70	2723.00	86.7	15.52			K13036B m=16?
168	K 13036A	1303.60	2706.70	86.7	13.50			PNMK
169	TON 142	1300.90	2526.00	86.7	15.40		A	
170	LB 11431	1252.20	3036.00	86.7	14.02	1.00		
171	TON 637	1241.70	3020.00	86.7	15.27			
172	LB 11274	1235.60	2856.00	86.7	13.23	-1.00	LTE A	
173	LB 11273	1235.40	2839.00	86.7	16.03	2.00	LTE F	
174	LB 11270	1235.00	2622.00	86.7	13.27	1.00		
175	LB 11403	1250.40	3047.00	86.6	14.02	1.00		
176	LB 11397	1250.10	3048.00	86.6	13.19	0.00		
177	LB 11382	1248.90	3046.00	86.6	17.28	2.00		
178	TON 133	1248.50	3045.00	86.6	16.20			
179	TON 640	1242.80	2416.00	86.6	14.52			
180	TON 628	1236.60	2530.00	86.6	14.52			

No.	Name	RA (1950)	Dec	Lat.	V	(B-V)	Type	Comments
181	LB 11267	1234.50	2626.00	86.6	16.78	1.00		
182	LB 11262	1233.90	2733.00	86.6	13.00	-1.00	AO	II179 PSS SSS
183	LB 31	1304.80	2719.00	86.5	15.70	0.10		
184	K 13016C	1301.60	2932.20	86.5	15.50		A	PNMK
185	LB 11439	1253.00	3049.00	86.5	14.30	-1.00		
186	LB 11396	1250.00	3055.00	86.5	13.50	0.00		
187	TON 664	1245.10	3046.00	86.5	15.39			
188	LB 11345	1243.90	3043.00	86.5	16.78	2.00		
189	LB 11308	1239.50	3012.00	86.5	16.53	2.00		
190	LB 12`	1235.20	2543.00	86.5	16.53	0.10		
191	LB 11259	1233.60	2658.00	86.5	16.03	1.00		
192	LB 23	1256.20	3036.00	86.4	17.00	0.00		
193	TON 655	1247.90	3057.00	86.4	16.03			
194	LB 11372	1247.60	3102.00	86.4	14.19	0.00		
195	LB 11337	1243.10	3047.00	86.4	13.05	-1.00		
196	LB 11304	1239.00	3012.00	86.4	14.56	0.00		
197	LB 15	1235.40	2527.00	86.4	16.16	0.10		
198	TON 624	1234.40	2856.00	86.4	15.64	0.17		
199	LB 11	1234.00	2607.00	86.4	16.41	0.10		
200	LB 11258	1233.60	2827.00	86.4	16.73	-1.00		
201	LB 11256	1233.40	2822.00	86.4	13.00	-1.00		
202	LB 262	1304.30	2849.40	86.3	15.00	0.00		
203	K 12568	1256.80	3042.65	86.3	17.00			PNMK
204	K 12560	1256.00	3045.20	86.3	17.50			PNMK
205	LB 11368	1247.40	3105.00	86.3	16.53	2.00		
206	TON 630	1237.70	2443.00	86.3	15.39			
207	TON 626	1235.20	2927.00	86.3	16.66			
208	LB 6931	1241.20	3045.00	86.2	16.63	0.00		
209	TON 632	1238.00	3019.00	86.2	15.61	0.43		PIr2
210	LB 11283	1236.40	3001.00	86.2	17.00	0.00		

No.	Name	RA (1950)	Dec	Lat.	V	(B-V)	Type	Comments
211	K 13066	1306.60	2800.30	86.1	16.50			PNMK
212	K 13065	1306.50	2739.10	86.1	16.50			PNMK
213	TON 639	1242.40	2348.00	86.1	16.03			
214	LB 11285	1236.60	3008.00	86.1	14.70	2.00		
215	LB 11280	1236.30	3006.00	86.1	17.03	2.00		
216	LB 10	1233.80	2533.00	86.1	17.78	0.10		
217	LB 6591	1231.90	2646.00	86.1	17.09	-0.40		
218	LB 11251	1231.40	2723.00	86.1	14.00	0.00		
219	B 134	1257.56	3058.57	86.0	16.26	0.60		PSt
220	LB 11444	1253.60	3119.00	86.0	13.42	-1.00		
221	LB 11408	1250.80	3122.00	86.0	15.77	1.00		
222	LB 11326	1242.40	3106.00	86.0	17.03	1.00		
223	LB 11317	1240.40	3054.00	86.0	14.20	1.00		
224	LB 11298	1237.80	3034.00	86.0	14.89	1.00		
225	K 13074	1307.40	2705.90	85.9	16.00			PNMK
226	TON 638	1241.80	3114.00	85.9	14.89			
227	LB 11290	1237.00	3032.00	85.9	13.25	0.00		
228	LB 11291	1237.00	3030.00	85.9	14.77	1.00		
229	K 13009	1300.90	3042.50	85.8	16.00			PNMK
230	LB 11434	1252.40	3133.00	85.8	14.00	0.00		
231	LB 11390	1249.50	3135.00	85.8	14.52	1.00		
232	LB 11386	1249.40	3134.00	85.8	14.20	1.00		
233	TON 652	1246.90	3135.00	85.8	15.27			
234	LB 16	1241.80	2331.00	85.8	15.23	-0.50		
235	LB 13	1235.20	2438.00	85.8	14.69	0.00		
236	LB 11269	1234.90	3017.00	85.8	14.73	-1.00		
237	LB 6616	1232.80	2940.00	85.8	17.00	0.00		
238	LB 11248	1230.50	2825.00	85.8	13.00	0.00		
239	LB 11243	1230.00	2746.00	85.8	13.58	1.00		
240	K 13015	1301.50	3042.60	85.7	17.50			St114 PNMK

No.	Name	RA (1950)	Dec	Lat.	V	(B-V)	Type	Comments
241	LB 11427	1251.90	3140.00	85.7	14.05	-1.00		
242	LB 11407	1250.80	3140.00	85.7	13.00	0.00		
243	LB 11377	1248.40	3142.00	85.7	16.03	1.00		
244	LB 11339	1243.20	3130.00	85.7	16.53	3.00		
245	LB 11311	1239.70	3112.00	85.7	13.19	0.01	A0	II193 PES1 SSS
246	LB 11288	1236.90	3046.00	85.7	14.80	-1.00		
247	LB 11246	1230.40	2621.00	85.7	14.23	-2.00		
248	LB 11241	1229.70	2715.00	85.7	16.50	0.00		
249	B 108	1302.93	3032.67	85.6	16.04	0.69		Pst non-stellar ?
250	TON 676	1254.60	3137.00	85.6	15.70			
251	LB 17	1246.10	2302.00	85.6	14.05	-0.30		
252	LB 11277	1235.80	3040.00	85.6	16.53	3.00		
253	LB 11266	1234.20	3021.00	85.6	15.39	1.00		
254	TON 621	1231.40	2926.00	85.6	16.03			
255	LB 6521	1229.80	2628.00	85.6	16.59	-0.20		
256	TON 698	1309.10	2718.00	85.5	16.80	0.00		K13090
257	K 13027	1302.70	3043.30	85.5	16.50			PNMK
258	LB 11437	1252.60	3147.00	85.5	13.70	1.00		
259	LB 11425	1251.90	3149.00	85.5	14.30	-1.00		
260	LB 11309	1239.60	3124.00	85.5	14.77	2.00		
261	LB 11294	1237.30	3107.00	85.5	17.91	1.00		
262	LB 11284	1236.50	3059.50	85.5	15.77	2.00		
263	TON 85	1231.80	2507.00	85.5	15.60			
264	LB 11240	1229.30	2623.00	85.5	13.42	-1.00		
265	B 326	1309.59	2758.41	85.4	16.95	0.49		Pst
266	TON 146	1308.80	2853.00	85.4	15.30	0.18		K13088A PIr2
267	LB 7411	1253.40	3156.00	85.4	17.09	-0.10		
268	LB 7291	1250.10	3159.00	85.4	16.72	-0.10		
269	K 13035	1303.50	3048.90	85.3	17.50		QSO	BU 1303+308 PNMK
270	LB 11424	1251.80	3205.00	85.3	13.23	-2.00		

No.	Name	RA (1950)	Dec	Lat.	V	(B-V)	Type	Comments
271	LB 11343	1243.60	3155.00	85.3	13.20	1.00		
272	LB 11313	1239.90	3142.00	85.3	14.70	2.00		
273	TON 101	1238.00	2323.00	85.3	14.30			
274	TON 700	1310.50	2642.00	85.2	16.20	0.00		
275	LB 264	1309.40	2903.70	85.2	15.20	0.20		
276	K 13061	1306.10	3021.60	85.2	16.65	0.40	QSO	B182BU1306+303 PSt
277	LB 11352	1244.70	3209.00	85.2	13.70	1.00		
278	LB 11299	1238.30	3137.00	85.2	13.06	0.00		
279	LB 11249	1231.10	3012.00	85.2	13.69	0.00		
280	LB 11224	1227.50	2710.00	85.2	14.89	1.00		
281	TON 699	1309.40	2929.00	85.1	16.60	0.00		
282	LB 11443	1253.40	3215.00	85.1	13.30	-1.00		
283	LB 11261	1233.70	3058.00	85.1	16.47	-1.00		
284	LB 35	1311.60	2803.00	85.0	17.20	0.20		
285	LB 11346	1244.30	3215.00	85.0	15.20	3.00		
286	LB 11321	1240.60	3205.00	85.0	14.52	2.00		
287	LB 11289	1237.00	3139.00	85.0	14.39	1.00		
288	LB 11219	1227.20	2854.00	85.0	13.23	-1.00		
289	LB 11217	1226.70	2803.00	85.0	16.88	0.00		
290	K 13011	1301.10	3143.40	84.9	17.50			PNMK
291	TON 656	1248.30	3229.00	84.9	16.03			
292	LB 6942	1241.40	3212.00	84.9	16.66	0.10		
293	LB 11239	1229.30	3003.00	84.9	13.61	-1.00		
294	TON 619	1227.70	2537.00	84.9	15.77			
295	LB 11225	1227.60	2920.00	84.9	15.56	0.00		

Appendix II

The St.Andrews Grism

'In two words: im possible'

Samuel Goldwyn

Appendix II: The St.Andrews Grism

II.1 Introduction

II.1.1 Description of the Grism

A grating-prism ('grism') consists of a blazed transmission grating used in conjunction with a thin, low angle prism. The device is placed in the converging beam of a telescope, near the focal plane. The grating diffracts the incident light and the prism corrects the coma, astigmatism and field curvature which result from the use of a diffraction grating with a non-collimated light beam. The incident light from a point source is thus dispersed into a first order spectrum plus a point-like zero order spectrum and other spectra of order greater than one. By far the greatest percentage of the incident light is diffracted into the first order spectrum. The grism is used in place of a large, expensive objective prism for intermediate field ($0^{\circ}.5$ - $2^{\circ}.5$) slitless spectroscopy and produces a similar result.

II.1.2 Grism Development

Hoag and Schroeder (1970) tried to obtain low dispersion spectra (~1000Å/mm) in the wavelength range 3200Å to 5000Å , over a field of 30 minutes of arc using a prism and, independently, a blazed transmission grating in the converging beam close to the focal plane of a telescope. The prism was rejected for this purpose due to the excessive aberrations (notably coma) produced by a prism in a converging beam. The aberrations of a grating used in this way are much smaller, but are still significant, especially at higher dispersions. Hoag and Schroeder found that a grating used in the converging beam near the focal plane produced both a first order image, the stellar spectrum, and an almost point-like zero order image. The zero order image provided a useful reference point for wavelength measurements as its position relative to the first order image was a constant for the particular grating/telescope combination used.

Bowen and Vaughan (1973) showed that the aberrations which limit the use of a grating in a converging beam could be significantly reduced if the grating is preceded by a low angle prism, orientated such that it deflects the incident light in the opposite direction to the deflection produced by the grating, with the upper surface of the prism perpendicular to the optical axis of the telescope. The prism is aligned relative to the grating in such a way that i) the point of zero coma in the first order images lies at the centre of the image, thus minimising the coma, and ii) the field curvature and astigmatism are zero for the two ends of the spectral range considered, and as small as possible in between. Any residual astigmatism will spread out the spectrum perpendicular to the direction of dispersion and will thus tend to widen the spectra. This residual astigmatism and any residual field curvature may be reduced by using a coarse grating at a large distance from the focal plane. The use of the prism produces a new focal plane which is not perpendicular to the optical axis of the telescope. Thus the detector system (usually a photographic plate) must be tilted to compensate for this. The dispersion obtained is linearly proportional to the distance between the grating and the focal plane. Different dispersions may thus be obtained by moving the instrument along the optical axis of the telescope. In order to prevent extra reflections within the system, Bowen and Vaughan suggested that the grating be replicated directly to the prism, or at least cemented to it.

Buchroeder (1974) has designed two similar grating-prism instruments for the K.P.N.O. 4.2m Mayall telescope. Both designs give dispersion of 1500 and 3000Å/mm, with a flat unvignetted field of 30 minutes of arc, one design being for the blue wavelength region (3200-5200Å) the other for the red (6000-7000Å). In these designs residual astigmatism is corrected by separating the grating from the prism and adjusting their relative positions to obtain minimum aberration. Buchroeder's design report also includes a wealth of detail on the behaviour and properties of gratings and prisms in converging beams, and provides a description of the fundamentals of grism design.

Hoag (1976) has used a grism similar to those designed by Buchroeder to obtain spectra at about 2300Å/mm over the spectral range 4500-6900Å with the Mayall telescope, giving a field of 30 minutes of arc. He describes a major problem with the technique of grating slitless spectroscopy, namely the crowding of the field caused by the overlapping of zero and first order spectra. For example, zero order images of objects too faint to produce recordable first order spectra can be mistaken for emission features when superimposed on the first order spectrum of other objects. This confusion can generally be avoided by taking two or more grism plates, with different orientations of the direction of dispersion, and referring to a direct plate of the field for identification purposes. Hoag also discusses the establishment of a wavelength scale based on the positions of the zero order images and the emulsion cut-off of the photographic plate (IIIaJ emulsions for example have a sharp cut-off at about 5380Å).

Buchroeder (1977) has presented two grism designs for use with the 3.8m A.A.T., one giving a dispersion of 1350Å /mm, the other a dispersion of 560Å /mm. Both designs give a useable field of 1° diameter and are designed for the spectral range 3400-6900Å. The second design is for an anastigmatic grism (this is achieved by seperating the grating and prism). For the lower dispersion design astigmatism is not as much of a problem and the grating is cemented to the prism. Both designs require gratings of 280mm diameter which are difficult (and expensive) to make. It is not known if either design was ever used.

Finally, Greyer (1979) has given a tantalisingly brief description of a grism used with a collimated beam. The principle is the same: the blazed transmission grating produces the dispersion and the thin prism corrects the aberrations and prevents deviation of the spectra from the optical axis. Unfortunately no details of its performance are given.

II.1.3 The St.Andrews Grism

The St.Andrews Grism was designed by E.H.Richardson at the Dominion Astrophsical Observatory, Victoria, (D.A.O.) specifically for the St.Andrews James Gregory Telescope and manufactured by Bausch and Lomb. The grating was made from a 44 groove/mm master (originally made for the C.F.H.T.), and is blazed for 4000Å. The prism is made from a 160mm diameter blank of Schott UBK7 glass, with a wedge angle of $1^{\circ}.2$, being 25mm thick at its widest. The two are cemented together, the orientation being such that the dispersions are additive, with the grating being on the sloping face of the prism and nearest the focal plane. This introduces a focal plane tilt of about $0^{\circ}.415$ in the same sense as the wedge (see Figure II.1). The grism produces useable spectra over a field of about $2^{\circ}.5$. The completed grism was delivered in April 1981 and immediately installed on the telescope for testing.

II.2 Installation and Tests

II.2.1 The James Gregory Telescope

The James Gregory Telescope (JGT) is a Cassegrian-Schmidt with a 0.9m spherical primary and an 0.45m spherical secondary, having a theoretical field diameter of 4°. In practice this is not attainable due to the position of the focal plane (inside the telescope tube) and the non-availability of circular photographic plates. As a result the effective field has a diameter of about $2^{\circ}.5$, with a minimal amount of field curvature being present as well as some coma and astigmatism. In order to reduce these the primary is generally stopped down to about 0.85m. Under perfect observing cconditions the best attainable image diameter for a point source is about 3 arcseconds. For typical conditions at St.Andrews this is increased to about 4 arcseconds. The telescope in its current configuration has been described by Van Breda (1970). In preparation for the grism's installation the plate holder was adjusted to compensate for a focal plane tilt of about $0^{\circ}.4$.

II.2.2 Grism Adjustment and Preliminary Tests

The grism was installed in the JGT at a distance of 207mm from the focal plane giving a dispersion of about $1100A^{\circ}$/mm. The orientation was such that spectra were aligned along the north-south axis, with the red end to the south. A visual estimate of the telescope focus was made using a ground glass screen in place of the plate holder, after which a normal focus plate was taken to establish an accurate focus. Minor problems due to paint flakes from the telescope's focal plane shutter, and a bent plate holder (producing a variation in focus towards the north-west corner of the plate) were isolated and corrected.

A number of test plates were taken at various exposures, on unbaked IIIaJ plates to check the orientation and general performance of the instrument. For exposures longer than about 100 minutes the sky background becomes very pronounced and starts to swamp the spectra. From plate #8 (100 minute exposure) the faintest spectra which could be classified directly from the plate were those of objects estimated to be about 14th magnitude. For classification from microdensitometer scans this limit is estimated to be about 14th.5 magnitude. The faintest detectable stellar images for direct photography with this telescope (100 minutes on unbaked IIIaJ) were estimated to be about 16th.5 magnitude.

Little in the way of fine structure was apparent in any of the spectra, although gross spectral features such as the Balmer jump were easily identified. Due to the relatively bright plate limits on most of these test plates overcrowding of the field was not a problem. Contamination of the plates by non-first order spectra, which can cause problems by obscuring, overlapping or in some cases mimicking the first order spectra, was overcome by reference to a direct plate of the same field.

Careful examination of the plates indicated that the quality of the spectra is essentially constant over the entire field of $2^{\circ}.5$. Consequently the effective grism field was taken to be $2^{\circ}.25$, a slightly conservative estimate. On some plates it was noticed that the plate background was quite high and varied substantially with position in an unusual manner. This was at first attributed to unidentified smears on the upper surface of the prism, but removal of these did not reduce the problem. Possibly this is a result of scattering, of both starlight and the high sky background, within the system. It has little effect on direct classification from the plate but does have an adverse effect on the automated microdensitometer search/scan routines mentioned in chapter 2 as these may identify large background fluctuations as real images.

<u>II.2.3 The Dispersion of the Grism</u>

Parker (1982) has discussed the determination of the dispersion curve for the grism configuration described above (grism at 207mm from focal plane). From measurements of known spectral features in stellar spectra whose positions were found relative to their zero order images in microdensitometer scans he found the dispersion to be about 1150A°/mm at 4000A°. The resultant dispersion curve for the grism is reproduced in Figure II.2.

II.3 The Grism in Research

II.3.1 Spectral Classification

Plate #8 from the 1980/81 observing season was used to assess the grism's performance for the purposes of spectral classification. Much use was made of microdensitometer scans, the spectra being sampled every 15μm, giving 250 data points per spectrum. (For a more detailed discussion see chapter 2.) A number of spectra visible on this plate were classified directly from the plate using a x10 magnifying eyepiece, from microdensitometer scans using the computer controlled Joyce-Loebl and directly from an unwidened U.K.S.T. plate of the region (dispersion about 2400A°/mm at $H\gamma$). The classifications were based on the criteria given by Krug et al (1980) and Kelly et al (1982). The resulting classifications are given in Table II.1 from which it can be seen that the agreement is satisfactory.

However in every case classification was found to be easiest when working from the U.K.S.T. plates since more of the shape and structure of the spectra could be discerned on these lower dispersion plates. Of the two techniques applied to the grism plates, classification from microdensitometer scan was faster and simpler, making fuller use of the spectral information available. It seems initially surprising that the lower dispersion U.K.S.T. objective prism plate spectra show more detail (and are thus more readily classified) than the grism spectra at almost twice the dispersion. However, given the poor quality of the St.Andrews site and the resolution of the JGT optics it is not surprising that the details in the spectra are smeared out and lost.

In the spring of 1982 a number of survey plates of the North Galactic Pole region were obtained on hyper-sensitised IIIaJ plates, baked in a nitrogen atmosphere at 65°C for 4 hours. The longest exposures obtained were 50 minutes (equivalent to 100 minutes on unbaked plates), the plate limit for direct classification being about 14th magnitude. These were used in conjunction with an U.K.S.T. prism plate of the

North Pole region to provide classifications for known blue stars (chapter 2).

In September 1982 the grism's position in the telescope was adjusted to a distance of 315mm from the focal plane, to give a dispersion of about 750A° /mm. A number of test plates were taken to assess the performance at this higher dispersion. The results were extremely disappointing. There was no apparent increase in the amount of visible detail and structure compared with the lower dispersion plates. An U.K.S.T. objective prism plate with a dispersion of 1200A° /mm was available by this time and this showed a substantial amount of detail in the individual spectra- hydrogen lines in early type stars being clearly visible. None of this structure was visible in grism spectra at either 1150A° /mm or 750A° /mm.

II.3.2 Galaxy Redshifts

Parker (1982) studied the grism's application to the determination of galaxy redshifts using the method described by Cooke (1980). Essentially the redshift is found from low dispersion spectra by measuring the displacements of gross spectral features, such as the 4000A° feature, relative to their rest positions. The inaccuracies of the method are large (about $\pm$25,00kms^{-1})

and it is really only suitable for galaxies with redshifts in excess of 15,000kms^{-1}.

The JGT grism has a limiting magnitude for microdensitometer scans of about 14m.5, which for a typical galaxy means a recession velocity of less than 10,000 kms^{-1}.. It therefore seemed unlikely that redshifts could be determined with any accuracy. Parker found his velocities for a sample of galaxies in the Coma cluster to be in remarkable agreement with published results, but in most cases the formal error in his velocities was about half the measured velocity. This error is mostly due to the difficulty in accurately measuring the separation between two points in a spectrum. Given the blurring of spectral features caused by the site and telescope such large errors are to be expected.

II.3.3 Conclusion

i) JGT grism spectra show little in the way of spectral structure when compared with U.K.S.T. objective prism spectra at the same or lower dispersions. This is attributed to the combined effect of the telescope optics and poor seeing which smear out a point source into an image of 4 arcseconds diameter, thus destroying any intrinsic spectral details. There is no advantage to be gained by using a dispersion higher than 1150Å/mm as no more structure is apparent. The only important effect of a higher dispersion is to spread out the spectrum and thus lower the plate limit.

ii) Exposure times at St.Andrews are limited mainly by the night sky brightness arising from the lights of the town. The longest practical exposure for hyper-sensitised IIIaJ plates is about 50 minutes. For non-sensitised plates it is about 100 minutes. At a dispersion of about 1150Å/mm this results in a plate limit for classifiable spectra of about 14th magnitude, or 14th.5 magnitude if microdensitometer scans are used. The plate limit for direct photography is 16th- 16th.5 magnitude.

iii) Spectral classification is possible from plates taken with the grism mounted on the JGT. The technique of classification from microdensitometer scans is to be preferred to direct visual classification, and results in an accuracy of about half a spectral class at best, with a plate limit of about 14th.5.

vi) The role of the grism in determining galaxy redshifts is limited due to the large errors involved and the inadequate magnitude limit attainable.

v) In principle, for a telescope with a small effective field of up to $2^\circ.5$ diameter a grism is an excellent device for low dispersion slitless spectroscopy over the whole of that field. It has all the attributes of an objective prism, but is smaller and cheaper. The zero order images provide an extremely useful fixed reference point for wavelength calibrations. Being mounted internally it is less susceptible to dust and damage than an objective prism. The dispersion achieved can be easily altered by moving the grism relative to the focal plane of the telescope. In practice the site and telescope must be carefully matched to the instrument, as is true for objective prisms . The resolution attained at St.Andrews is insufficient for the grism to perform properly.

References

Bowen, I.S. and Vaughan, A.H. 1973, Pub.A.S.Pac., 85, 174.

Buchroeder, R.A. 1974, 'A Raytrace Study of Prime Focus Grisms', Optical Sciences Centre, University of Arizona.

Buchroeder, R.A. 1977, 'Two Low Dispersion Grisms-Optical Design Report', Optical Sciences Centre, University of Arizona.

Cooke, J.A. 1980, PhD. Thesis, University of Edinburgh.

Greyer, E.H. 1979, I.A.U. Colloquium #47, 271.

Hoag, A.A. 1976, Pub.A.S.Pac., 88, 860.

Hoag, A.A. and Schroeder, D.J. 1970, Pub.A.S.Pac., 82, 1141.

Kelly, B.D., Cooke, J.A. and Emerson, D. 1982, M.N.R.A.S., 199, 239.

Krug, P.A., Morton, D.C. and Tritton K.P. 1980, M.N.R.A.S., 190, 237.

Parker, Q.A. 1981, Honours Project, University of St.Andrews.

Van Breda, I.G. 1970, Physics Bulletin, 21, 207.

Table II.2.

Classification: Grism vs U.K.S.T. prism.

object	Grism direct	Grism scan	U.K.S.T. direct
1	F	F	F
2	A	early F	A
3	A	A	A
4	A-F	F	F
5	B	B	B
6	G	G	G
7	B	B	B
8	F	early F	F
9	A-F	late A	late A
10	A	A	early A
11	mid-F	late F	F
12	F	F	F
13	late A-F	early F	F
14	late F	late F	late F
15	A-F	early F	A-F
16	early F	early F	F
17	early F	late A	F
18	F	late F	F
19	A	A	late A
20	A	A	A
21	late B-A	A	A
22	early F	mid F	F
23	mid F	mid F	F
24	early F	mid F	F
25	mid-late F	G	G
26	A	mid A	A
27	late F	G	F
28	B	A	A
29	A	A-early F	A
30	F	late F	F
31	B-A	A	A

Figure II.1.

Grism Configuration

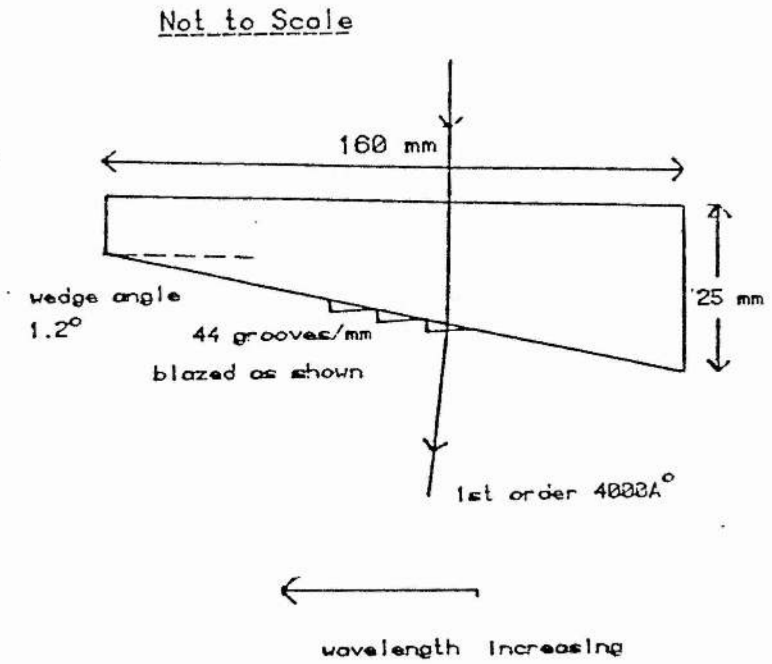

Figure II.2.

Grism Dispersion Curve for 1100A°/mm Configuration

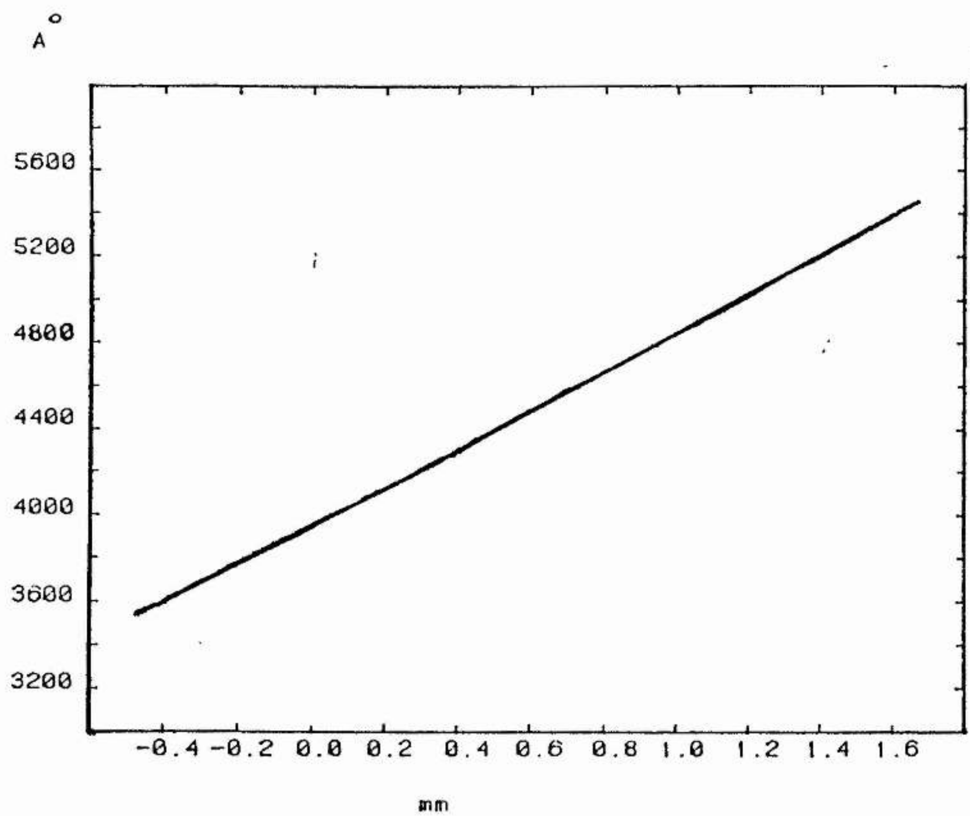

'But it does move...'

Galileo Galilei